

University of Strathclyde

Department of Naval Architecture, Ocean and Marine Engineering



**Development of a Semi-empirical Ship Operational  
Performance Model for Voyage Optimization**

By

**Ruihua Lu**

A thesis presented in fulfilment of the requirements for the degree of

Doctor of Philosophy

2016

*This thesis is the result of the author's original research. It has been composed by the author and has not been previously submitted for examination which has led to the award of a degree.*

*The copyright of this thesis belongs to the author under the terms of the United Kingdom Copyright Acts as qualified by University of Strathclyde Regulation 3.50. Due acknowledgement must always be made of the use of any material contained in, or derived from, this thesis.*

Signed: Ruihua Lu

Date:

# ACKNOWLEDGEMENTS

---

I would firstly like to thank my academic supervisors Professor Osman Turan and Dr. Evangelos Boulougouris for their insightful guidance, powerful support, and valuable advice throughout my PhD journey.

Secondly, I would like to express my appreciation to my colleagues and friends in Glasgow who assisted me in my work: Dr. Charlotte Banks, Dr. Paula Kellett, Dr. Gerasimos Theotokatos, Dr. Mahdi Khorasanchi, Dr. Rafet Kurt.

I would also like to thank Mrs Thelma Will and all the administrative personnel of the Department of NAOME for assisting me with my student business.

Last but certainly not least, I would like to thank my father Zhichen Lu, my mother Fengmin Yang. They gave me life, brought me up and taught me the philosophy of life. And finally, I would like to thank my family and friends, especially Mr. Yaojun Yu and Dr. Wei Jin for seeing me through this undertaking.

# ABSTRACT

---

Voyage optimization is the endeavour to select the optimum route and optimum speed along the voyage in order to maximise the ship performance in energy efficiency and the reduction of the Green House Gas emission footprint within fixed voyage duration. For achieving these goals, it is essential to develop an easy-to-use and accurate enough ship operational performance prediction model, which is the main aim of this study. A detailed critical review of the literature regarding the prediction of ship's added resistance in waves and its operational performance modelling has been carried out. The existing research gap has been identified and addressed herein.

The empirical added resistance prediction formulae have been improved based on the actual ship operational performance data and developed as a semi-empirical added resistance prediction method, which estimates the speed loss due to added resistance. Together with the calm water resistance model, propulsion efficiency model, main engine Specific Fuel Oil Consumption (SFOC) diagram, correction factor indicating fouling effect on fuel consumption, and actual ship operational performance data, the novel semi-empirical ship operational performance prediction model for oil tanker and container ship have been developed and validated.

The easy-to-use and practical semi-empirical model is able to accurately predict main engine fuel consumption rate at varying speeds and wave angle encountered. This has been tested successfully on an oil tanker and a container ship. A GRIDS system has been developed to indicate the combination of potential routes and the corresponding weather forecast along each route between departure port and destination. By integrating the GRIDS system with the proposed semi-empirical ship operational performance prediction model, a weather routing

model and a speed optimization model have been developed for voyage optimization. In this study, weather routing is achieved by optimum route selection. Its objectives include minimum passage time and minimum fuel consumption under fixed main engine output. Speed optimization is achieved by evaluating the predicted main engine fuel consumption with different speed combinations along the voyage, while a fixed Estimated Time of Arrival (ETA) is set as the constraint.

Finally, the main findings are discussed and conclusions are drawn with some recommendations for future research.

# CONTENTS

---

ACKNOWLEDGEMENTS .....	I
ABSTRACT.....	II
LIST OF FIGURES .....	IX
LIST OF TABLES.....	XIV
Chapter 1 – INTRODUCTION.....	1
1.1 Chapter Overview .....	1
1.2 Background .....	1
1.3 Problem Definition.....	2
1.4 Aims and Objectives .....	6
1.5 Contributions to the Field of Study.....	7
1.6 Structure of thesis .....	8
1.7 Chapter Summary .....	10
Chapter 2 – CRITICAL REVIEW .....	11
2.1 Chapter Overview .....	11
2.2 Ship Routing .....	11
2.3 Algorithm Applied for Weather Routing.....	20
2.3.1 Calculus of Variations.....	20
2.3.2 Isochrone Method .....	21
2.3.3 Isopone Method .....	23

2.3.4	Dynamic Programming .....	25
2.3.5	Evolutionary Method .....	27
2.3.6	Dijkstra's Method .....	28
2.4	Speed Optimization.....	29
2.5	Ship Added Resistance Prediction .....	31
2.5.1	Causes of Added Resistance .....	32
2.5.2	Approach to Determine Added Resistance .....	32
2.5.2.1	The strip theory method and radiated energy method .....	32
2.5.2.2	The Rankine panel method .....	34
2.5.2.3	The Cartesian grid method and CFD method .....	34
2.5.2.4	The semi-empirical method .....	35
2.5.2.5	The experimental method .....	37
2.5.2.6	The empirical method .....	37
2.6	Ship Operational Performance Modelling .....	40
2.6.1	Overview of Ship Performance Monitoring and Analysis Systems on the Market 41	
2.6.2	Methods of Ship Performance Modelling.....	42
2.7	Effect of Fouling on Ship Operational Performance .....	48
2.8	Research Gaps.....	50
2.9	Chapter Summary .....	54
Chapter 3 – METHODOLOGY FOR VOYAGE OPTIMIZATION .....		55
3.1	Chapter Overview .....	55

3.2 Practical Questions Regarding Voyage Optimization.....	55
3.3 Overview of the Methodology for Voyage Optimization .....	56
3.4 Chapter Summary.....	61
Chapter 4 – DATA DESCRIPTION.....	62
4.1 Chapter Overview .....	62
4.2 Actual Operational Data .....	62
4.3 Sea Trial Data .....	66
4.4 Main Engine Performance Report .....	68
4.5 Chapter Summary .....	70
Chapter 5 – SEMI-EMPIRICAL SHIP OPERATIONAL PERFORMANCE PREDICTION MODEL .....	71
5.1 Chapter Overview .....	71
5.2 Overview of the Semi-empirical Ship Operational Performance Prediction Model....	71
5.3 Calm water Resistance Prediction.....	74
5.4 Speed Loss Prediction .....	75
5.5 Ship Operational Performance Prediction.....	81
5.6 Development of Semi-empirical Ship Operational Performance Model for Oil Tanker .....	83
5.6.1 Development of semi-empirical added resistance prediction method for oil tanker .....	84
5.6.2 Integrating the time-dependent correction for oil tanker.....	95
5.7 Validation of Semi-empirical Ship Operational Performance Model for Oil Tanker..	98



5.8	Development of Semi-empirical Ship Operational Performance Model for Container Ship.....	102
5.8.1	Development of semi-empirical ship operational performance model for container ship.....	103
5.8.2	Integrating the time-dependent correction for container ship .....	113
5.9	Validation of Semi-empirical Ship Operational Performance Model for Container Ship .....	116
5.10	Discussion on Time-dependent Correction for Oil Tanker and Container Ship .....	121
5.11	Chapter Summary.....	123
Chapter 6 –WEATHER FORECAST AND GRIDS SYSTEM .....		125
6.1	Chapter Overview .....	125
6.2	Weather Forecast.....	125
6.3	GRIDS System .....	129
6.4	Integration of Weather forecast and GRIDS System .....	132
6.4	Chapter Summary.....	134
Chapter 7 – WEATHER ROUTING AND SPEED OPTIMIZATION FOR VOYAGE OPTIMIZATION.....		135
7.1	Chapter Overview .....	135
7.2	Integration of the Semi-empirical Ship Operational Performance Modelling with GRIDS system.....	135
7.2.1	Statement of Parameters .....	136
7.2.2	Fuel Consumption Modelling between Two Stages.....	139

7.3 Best Route Selection for Weather Routing .....	140
7.3.1 Constraints for Route Selection .....	141
7.3.2 Case Study of Best Route Selection .....	142
7.4 Optimal Speed Set Selection for Speed Optimization .....	146
7.4.1 Case Study of Aframax Oil Tanker .....	148
7.4.2 Case Study of Post-panamax Container Ship .....	150
7.5 Chapter Summary.....	153
Chapter 8 – DISCUSSION .....	154
8.1 Chapter Overview .....	154
8.2 Achievement of Research Aims and Objectives .....	154
8.3 Novelties and Contributions to the Field.....	157
8.4 Shortcomings.....	159
8.5 Chapter Summary.....	160
Chapter 9 – CONCLUSIONS AND RECOMMENDATIONS FOR FUTURE RESEARCH .....	161
9.1 Chapter Overview .....	161
9.2 Concluding Remarks .....	161
9.3 Recommendations for Future Research .....	162
9.4 Chapter Summary.....	164
REFERENCE.....	165

# LIST OF FIGURES

---

Figure 1: Four Alternative Routes between Ports A and B (Journ é and Meijers, 1980) .....	13
Figure 2: Marine Weather Forecast displayed by SPOS (Spaans and Stoter, 2000) .....	18
Figure 3: VVOS screen showing route optimization for trans-Pacific passage (Jeppesen, accessed 2014) .....	19
Figure 4: Least time track (dashed line) (Bijlsma, 1975) .....	21
Figure 5: All minimum time routes of the sail-assisted motor vessel reaching each isochrone (eastbound voyage) (Hagiwara, 1989) .....	22
Figure 6: Isopones in three-dimensional state space (Klompstra et al., 1992) .....	24
Figure 7: The last few isopones in a two-dimensional state space (Klompstra et al., 1992) ...	24
Figure 8: Example of a grid track from A (Quessant) to B (Nantucket L. V.) (De Wit, 1990) .....	26
Figure 9: Estimate of fuel consumption between two stages (Shao and Zhou, 2012) .....	27
Figure 10: Different possible directions (Korving, 2011) .....	29
Figure 11: The ship performance modelling diagram (Hansen, 2011) .....	47
Figure 12 Power Increase due to Fouling (Journ é and Meijers, 1980) .....	49
Figure 13: Flowchart of the Proposed Method for Voyage Optimization .....	56
Figure 14: Relation between required main engine power and ship speed under varying sea state .....	58
Figure 15: Encountered angle .....	65
Figure 16: Sample Expected Specific Fuel Oil Consumption Rate at ISO Reference Conditions (MAN Diesel & Turbo, accessed 2014) .....	69
Figure 17: Flowchart of the Development of Semi-empirical Ship Operational Performance Prediction Model .....	73
Figure 18: Validation Case Study for the H&B Resistance Prediction Model .....	75

Figure 19: Overview of the comparison between the predicted EEO using original Kwon’s method and recorded EEO .....	84
Figure 20: Time-dependent error between recorded EEO and predicted EEO using sea trial	85
Figure 21: Comparison between the predicted EEO using original Kwon’s method and recorded EEO during the first 5 months since launching .....	86
Figure 22: Comparison between the predicted EEO using original Kwon’s method and recorded EEO during the first 5 months since launching under $BN = 2$ .....	87
Figure 23: Comparison between the predicted EEO using original Kwon’s method and recorded EEO during the first 5 months since launching under $BN = 3$ .....	87
Figure 24: Comparison between the predicted EEO using original Kwon’s method and recorded EEO during the first 5 months since launching under $BN = 4$ .....	88
Figure 25: Comparison between the predicted EEO using original Kwon’s method and recorded EEO during the first 5 months since launching in Head Sea .....	89
Figure 26: Comparison between the predicted EEO using original Kwon’s method and recorded EEO during the first 5 months since launching in Bow Sea.....	89
Figure 27: Comparison between the predicted EEO using original Kwon’s method and recorded EEO during the first 5 months since launching in Beam Sea .....	90
Figure 28: Comparison between the predicted EEO using original Kwon’s method and recorded EEO during the first 5 months since launching in Following Sea.....	90
Figure 29: Comparison between the predicted EEO using the proposed semi-empirical method and recorded EEO .....	93
Figure 30: Overview of the comparison between the predicted EEO using the semi-empirical added resistance prediction method and recorded EEO .....	94
Figure 31: Error between predicted EEO and recorded one since ship launch date for Suezmax Oil Tanker A.....	95

Figure 32: Overview of the comparison between the predicted EEO using the semi-empirical added resistance prediction method after time-dependent correction and recorded EEO .....	96
Figure 33: Overview of the comparison between the predicted EEO using original Kwon’s method and recorded EEO .....	98
Figure 34: Overview of the comparison between the predicted EEO using the semi-empirical added resistance prediction method, the predicted EEO using original Kwon’s method and recorded EEO .....	99
Figure 35: Error between predicted EEO and recorded one since ship launch date for Aframax Oil Tanker B .....	100
Figure 36: Overview of the comparison between the predicted EEO using the semi-empirical added resistance prediction method after time-dependent correction and recorded EEO .....	101
Figure 37: Overview of the comparison between the predicted FCR using original Kwon’s method and recorded FCR .....	103
Figure 38: Time-dependent error between recorded EEO and predicted EEO using sea trial .....	104
Figure 39: Comparison between the predicted FCR and recorded FCR for Container Ship A .....	105
Figure 40: Comparison between the predicted FCR using original Kwon’s method and recorded FCR under $BN = 2$ .....	106
Figure 41: Comparison between the predicted FCR using original Kwon’s method and recorded FCR under $BN = 3$ .....	106
Figure 42: Comparison between the predicted FCR using original Kwon’s method and recorded FCR under $BN = 4$ .....	106
Figure 43: Comparison between the predicted FCR using original Kwon’s method and recorded FCR in Head Sea.....	107

Figure 44: Comparison between the predicted FCR using original Kwon’s method and recorded FCR in Bow Sea.....	107
Figure 45: Comparison between the predicted FCR using original Kwon’s method and recorded FCR in Beam Sea.....	108
Figure 46: Comparison between the predicted FCR using original Kwon’s method and recorded FCR in Following Sea.....	108
Figure 47: Comparison between the predicted FCR using the proposed semi-empirical method and recorded FCR during first 5 months since launching.....	112
Figure 48: Overview of the comparison between the predicted FCR using the semi-empirical added resistance prediction method and recorded FCR.....	113
Figure 49: Error between predicted FCR and recorded one since launch date for Container Ship A .....	114
Figure 50: Overview of the comparison between the predicted FCR using the semi-empirical added resistance prediction method after time-dependent correction and recorded FCR .....	114
Figure 51: Overview of the comparison between the predicted FCR using original Kwon’s method and recorded FCR .....	117
Figure 52: Overview of the comparison between the predicted FCR using the semi-empirical added resistance prediction method and recorded FCR.....	117
Figure 53: Error between predicted FCR and recorded one since ship launch date for Container Ship B.....	118
Figure 54: Overview of the comparison between the predicted FCR using the semi-empirical added resistance prediction method after time-dependent correction and recorded FCR .....	120
Figure 55: Daily Four Updated GRIB2 Files (Corresponding to the update frequency of weather forecast).....	126

Figure 56: Screenshot of Global Ocean Wind Speed (Based on the program written in Matlab)	127
Figure 57: Screenshot of Global Sea Direction (Based on the program written in Matlab)..	128
Figure 58: Screenshot of Global Significant Wave Height (Based on the program written in Matlab).....	128
Figure 59: Grids example for the route between Los Angeles Offshore, United States and Chiba, Japan.....	130
Figure 60: Grids example for the route between Lagos, Nigeria and Barcelona, Spain.....	130
Figure 61: Optimum route selection for weather routing (Los Angeles Offshore, United States and Chiba, Japan).....	143
Figure 62: Flowchart of the optimal speed set selection for speed optimization.....	147
Figure 63: Selected commercial trade route (Lagos, Nigeria – Barcelona, Spain) for an Aframax oil tanker (Google map API, 2015) .....	149
Figure 64: Selected commercial trade route (Penang, Malaysia – Port Louis, Mauritius) for a Post-panamax container ship (Google map API, 2015).....	151

# LIST OF TABLES

---

Table 1: Exemplary compilation of routing service or decision support systems (Hinnenthal, 2008) .....	16
Table 2: Characteristics of test cases for speed optimization (Norstad et al., 2011) .....	30
Table 3: Speed optimization – profit and fuel cost differences (in percent) from fixed service speed (Norstad et al., 2011) .....	30
Table 4: Exemplary compilation of ship performance monitoring and analysis systems (Hasselaar, 2010) .....	41
Table 5: Sample Expected Fuel Consumption at ISO Reference Conditions (MAN Diesel & Turbo, accessed 2014) .....	68
Table 6: Direction reduction coefficient $C\beta$ due to weather direction (Kwon, 2008).....	77
Table 7: Speed reduction coefficient $CU$ due to Block coefficient $Cb$ (Kwon, 2008).....	77
Table 8: Ship form coefficient $C_{form}$ due to ship categories and loading condition (Kwon, 2008).....	77
Table 9: Modifications of the formula to calculate ship form coefficient .....	91
Table 10: Ship form coefficient $C_{form}$ due to ship categories and loading condition for Suezmax oil tanker.....	91
Table 11: Modifications of the formulae to calculate direction reduction coefficient .....	92
Table 12: Direction reduction coefficient $C\beta$ due to weather direction for Suezmax oil tanker .....	93
Table 13: Statistical analysis of the error between recorded EEO and predicted EEO for Oil Tanker A .....	96
Table 14: Increasing energy consumption rate for Oil Tanker A and Oil Tanker B .....	100
Table 15: Statistical analysis of the error between recorded EEO and predicted EEO for Oil Tanker B.....	102



Table 16: Modifications of the formula to calculate ship form coefficient for Container Ship A.....	109
Table 17: Ship form coefficient <i>C<sub>form</sub></i> due to ship categories and loading condition for Container Ship A.....	109
Table 18: Modifications of the formulae to calculate direction reduction coefficient .....	110
Table 19: Direction reduction coefficient <i>C<sub>β</sub></i> due to weather direction for Container Ship A .....	111
Table 20: Statistical analysis of the error between recorded FCR and predicted FCR for Container Ship A.....	115
Table 21: Increasing energy consumption rate due to fouling effect for Container Ship A and Container Ship B.....	119
Table 22: Statistical analysis of the error between recorded FCR and predicted FCR for Container Ship B.....	120
Table 23: Time-dependent corrections for Suezmax Oil Tanker A, Aframax Oil Tanker B, Post-Panamax Container Ship A, and Post-Panamax Container Ship B .....	121
Table 24: Specifications of Beaufort scale (Met Office, retrieved 2015).....	133
Table 25: Comparison of ship operational performance between the selected optimum routes and recorded route.....	144
Table 26: The range of optimum speed under specific BN for an Aframax oil tanker .....	149
Table 27: Comparison of ship operational performance with different speed sets for an Aframax oil tanker .....	150
Table 28: The range of optimum speed under specific BN for a Post-panamax Container ship .....	150
Table 29: Comparison of ship operational performance with different speed sets for a Post-panamax container ship.....	151

# Chapter 1 – INTRODUCTION

---

## 1.1 Chapter Overview

This chapter will introduce the background (§1.2) of the issues included in this thesis, define the problem studied (§1.3), followed by the aims and objectives of the work (§1.4). The innovations of this thesis will be outlined (§1.5) and its structure will be presented (§1.6).

## 1.2 Background

As quoted in the ‘Climate Change 2014: Synthesis Report’ (IPCC, 2014), the observed increase of the global temperature since the mid-20<sup>th</sup> century is very likely to be caused by the anthropogenic Global Greenhouse Gas (GHG) emissions. They grew on average 2.2% per year, from 2000 to 2010, compared to 1.3% per year, from 1970 to 2000. The total anthropogenic GHG emissions from 2000 to 2010 were the highest in human history. Carbon dioxide ( $CO_2$ ) is the most important component of GHG produced by the human activities.

The continuous growth of the world population and the increasing number of developing countries leads to increase in dependency of the world economy on international trade. Transport by shipping accounts for 90% of world trade, and it is predicted that the trade transported by ships will triple by the year 2030. (International Chamber of Shipping, 2009)

According to the International Maritime Organization (IMO) GHG Study, shipping in 2012 was estimated to have emitted 949 million tonnes of  $CO_2$ . The average shipping  $CO_2$  emissions growth by 2020 amounts to 7% of 2012 emissions. For 2030 the prediction is that

the average shipping emissions will increase by 29% and for 2050 by 95% from their 2012 levels. (Third IMO GHG Study 2014)

The focus of this thesis is to reduce the carbon emissions from shipping through fuel-efficient ship operations. More specifically, it will focus on the voyage optimization to achieve energy efficient shipping.

### **1.3 Problem Definition**

Reducing GHG emissions from shipping is a key drive for energy efficient shipping. Another primary drive towards energy efficient shipping is fierce competition in shipping. Although the large 2-stroke engine installed for merchant ship burn the cheapest 'bunker fuel', the cost of IFO 180 has risen sharply with other petroleum products, increasing from \$170/t in 2002, to \$230/t in 2005, and further to nearly \$700/t in July 2014 (Bunker Index, 2014). With such high fuel prices, the bunker costs could account for 50%-60% of a ship's total operating cost (Wang and Teo, 2013). Recently the IFO 180 dropped again to around \$200/t, but the energy efficient shipping remain a primary goal for the shipping companies in a tough market, only the most competitive ships will survive.

As the main international regulatory body for shipping, the International Maritime Organisation (IMO) has been focusing on legislating the requirements for more environmental friendly and thus achieving energy efficient shipping by controlling the marine GHG emissions. For this purpose, a number of technical and operational measures have been proposed, discussed, ratified and implemented by IMO and the Member States. These measures include:

- Energy Efficiency Design Index (EEDI);
- Energy Efficiency Operational Index (EEOI);

- Ship Energy Efficiency Management Plan (SEEMP).

The SEEMP, as part of MARPOL Annex VI, has been made mandatory since 1<sup>st</sup> January, 2013, and it is applicable to both new and existing ships of 400 tonnages and above. The SEEMP is a ‘live’ document, outlining a program that continuously improves the energy efficiency of the ships. As introduced in ‘2012 Guidelines for the Development of a Ship Energy Efficiency Management Plan (SEEMP)’ (IMO, 2012), the recommended fuel-efficient ship operations include:

- **Improved voyage planning**

‘The optimum route and improved efficiency can be achieved through the careful planning and execution of voyages’

- **Weather routing**

‘Weather routing has a high potential for energy savings on specific routes. It is commercially available for all types of ship and for many trade areas. Significant savings can be achieved, but conversely weather routing may also increase fuel consumption for a given voyage.’

- **Just in time**

‘Good early communication with the next port should be an aim in order to give maximum notice of berth availability and facilitate the use of optimum speed where port operational procedures support this approach. Port authorities should be encouraged to maximize efficiency and minimize delay.’

- **Speed optimization**

‘Speed optimization can produce significant savings. However, optimum speed means the speed at which the fuel used per tonne mile is at a minimum level for that voyage. It does not mean minimum speed; in fact, sailing at the speed lower than optimum speed will consume more fuel rather than less. Reference should be made to the engine manufacturer’s power/consumption curve and the ship’s propeller curve.’

#### **- Optimized shaft power**

‘Operation at constant shaft RPM can be more efficient than continuously adjusting speed through engine power.’

Voyage optimization is the optimization of ship operations, which include verified voyage planning, weather routing, just-in-time arrival, ballast optimization, trim optimization, and other potential optimizations. Voyage optimization can also be regarded as an optimum combination of fuel-efficient ship operations within the constraints imposed by logistics, scheduling, contractual arrangements and other constraints. Through the assessment of potential reduction of  $CO_2$  emissions from shipping, voyage optimization can achieve 1-10% saving of  $CO_2$ /tonne-mile (Second IMO GHG Study 2009, 2009). With commercial consideration, the term optimum indicates:

- a. Minimum passage time;
- b. Minimum fuel consumption within specified passage time;
- c. Minimum damage to ship and /or cargo;
- d. Maximum comfort to passengers;
- e. A desired combination of the factors above

The accuracy in determining the optimum route depends on the accuracy of ship operational performance prediction for different ship conditions and different sea states, the accuracy of weather forecast, and the optimization algorithms. Within these three factors, the accurate ship operational performance modelling is the key element for accurate voyage optimization. This is also a major research direction contained within this thesis.

For the assessment of the routing service tools, the three principles include:

- Technical status
- User acceptance
- Economic performance

The more accurate ship operational performance prediction can improve voyage optimization in technical status, and the increased user-acceptance of voyage optimization system is also critical. The following quotes are taken from IMO GHG Study (Second IMO GHG Study 2009, 2009):

*‘Several types of weather routing system, technical support systems, performance monitoring systems and other systems can be used to help achieve optimal voyage performance. These systems must be used and understood, and the skills and motivation of the crew are critical.’*

Therefore, as one important component of voyage optimization system, the ship operational performance prediction model is also expected to be easy-to-use and practical. This is also the key motivation for developing the semi-empirical ship operational performance prediction model as proposed in this study.

## 1.4 Aims and Objectives

The purpose of this PhD thesis can be summarized in the following research question:

*“Is it possible to develop an easy-to-use and practical approach to accurately model the operational performance for a specific merchant ship in different weather conditions, and based on a user friendly approach to select optimum route and optimal speed set for voyage optimization and energy efficient shipping?”*

More specifically, the main aim of this study is to develop and validate a semi-empirical ship operational performance prediction model for a specific merchant ship, and based on this model to achieve voyage optimization via weather routing and speed optimization.

In general, the optimum route is defined as the route which provides an on time arrival while using the minimum fuel consumption and avoiding safety critical conditions. In this study, the optimum routes are selected through evaluating encountered weather and sea state, passage time, and minimum fuel consumption by user’s preference. It is also important to include the fouling effect for the operational performance modelling of specific merchant ship.

The specific objectives proposed to achieve the main aim are given below:

- To develop an easy-to-use and practical model to accurately predict added resistance for specific ship type under specific speed, wave angle encountered, and sea state.
- To develop an easy-to-use and practical method to predict the specific ship operational performance under specific speed, wave angle encountered, sea state, fouling effect and engine performance degradation condition.

- To validate the accuracy of the ship operational performance prediction for specific merchant ship types using actual operational data.
- To select optimum routes for weather routing by evaluating encountered weather and sea state, passage time, and minimum fuel consumption while keeping the fixed main engine output.
- To develop an approach to select optimum speed set for speed optimization while keeping the Estimated Time of Arrival (ETA) fixed, and illustrate the effect of speed management for energy efficient shipping in actual commercial trade routes

## 1.5 Contributions to the Field of Study

The contributions of my research include:

- The development of an easy-to-use and practical semi-empirical model to predict the ship added resistance and operational performance at varying speeds and wave height and angles encountered for oil tankers and container ships.
- The integration of the fouling effect and engine performance degradation as a time-dependant correction factor in ship operational performance modelling.
- The validation of the proposed semi-empirical ship operational performance prediction model by comparing with the actual operational performance data.
- The development of a weather routing model and speed optimization model for voyage optimization based on the proposed ship operational performance prediction method, which enables the user to easily and accurately investigate the relation between fuel consumption, voyage speed, the various sea states and wave directions that the ship may encountered during her voyage.



## 1.6 Structure of thesis

The structure of thesis is summarised briefly below.

- Chapter 2 will review the literature on ship routing and scheduling, the routing service software, the algorithms applied for weather routing and speed optimization, the ship added resistance prediction methods, the ship operational performance modelling and the effects of fouling on ship operational performance
- Chapter 3 will provide an overview of the methodology for achieving voyage optimization based on the proposed semi-empirical ship operational performance prediction model. The structure of the methodology and the links between inputs, modules, and outputs of the proposed method will be introduced in the analysis diagram.
- Chapter 4 will introduce the data sets that have been adopted for the development of the semi-empirical ship operational performance prediction model for specific merchant ship. The uncertainties of the parameters in actual operational data will be clarified.
- Chapter 5 will present the development and validation of the semi-empirical ship operational performance prediction model for oil tanker and container ship.
- Chapter 6 will explain the access and utilization of weather forecast, and the development of a grid system for achieving voyage optimization. The potential routes are defined by the GRIDS system, and the sea conditions along each potential route are read from weather forecast provided by National Oceanic and Atmospheric Administration (NOAA) (NOAA, 2015). The integration of the weather forecast information and the GRIDS system for optimum route selection will be presented.

- Chapter 7 will introduce the integration of the proposed semi-empirical ship operational performance prediction model with GRIDS system. The development of weather routing and speed optimization model for achieving voyage optimization will be presented with case studies
- Chapter 8 will discuss the achievements of this study regarding the research aims and objectives. The novelties and contributions to the field within this PhD study will be highlighted.
- Chapter 9 will present the concluding remarks regarding the work performed within this thesis. The recommendations for future research will be provided

## 1.7 Chapter Summary

This chapter has provided the general background of this study and introduced the nature of the problem to be addressed in the following chapters. The purposes of the PhD thesis with specific aims and objectives have been clarified. The contributions to the field of this study have been presented. The structure of this thesis has been outlined for greater clarity.

The next chapter will review the literature on ship routing and scheduling, especially algorithm applied for weather routing and speed optimization in routing service; ship added resistance prediction; ship operational performance modelling; and the effect of fouling on ship operational performance.

# Chapter 2 – CRITICAL REVIEW

---

## 2.1 Chapter Overview

This chapter will firstly present a critical review of ship routing (§2.2), which includes algorithms applied for weather routing (§2.3), and speed optimization (§2.4). It will then review the currently available literature on ship added resistance prediction (§2.5), and ship operational performance modelling (§2.6). Then the literature of fouling effect on ship operational performance are reviewed (§2.7). The chapter will close by identifying the research gaps which currently exist (§2.8).

## 2.2 Ship Routing

Extensive surveys of research on ship routing and scheduling have been carried out almost regularly, once every 10 years (Ronen, 1982; Ronen, 2011; Christiansen et al., 2004; Christiansen et al., 2013). As concluded by Christiansen et al. (Christiansen et al., 2004; Christiansen et al., 2013), during the last decade, the research on ship routing and scheduling has blossomed, and the volume of new papers regarding ship routing and scheduling has doubled that of the former decade.

From the wider scope of fleet management, the shipping operations of shipping can be clustered into three groups (Christiansen et al., 2004):

- Liner shipping: liner vessels visit a few specific ports according to a published schedule, aiming to maximize profit.
- Industrial shipping: the cargo and ship are both owned by the industrial operator, aiming to minimize the cost of delivering the cargos.

- Tramp shipping: tramp vessels do not have fixed visiting ports or schedule, normally follow the cargoes, aiming to maximize profit.

The network design and fleet deployment of liner shipping, and the fleet size and composition, cargo routing and scheduling, maritime inventory routing and supply chains of industrial and tramp shipping have been specially addressed in recent research.

In addition, more specialized problems regarding emissions and fuel-efficient operations on ship level, such as weather routing and speed management, have attracted wider attention.

Journ e and Meijers (Journ e and Meijers, 1980) discussed the speed loss due to added resistance and the voluntary speed reduction by the ship's captain. The overall added resistance includes the following:

- Added resistance due to wind and wave
- Added resistance due to vertical ship motions
- Added resistance due to steering
- Added resistance due to fouling

By integrating the information of propeller and engine, a prediction method of speed and power of a ship in a seaway was proposed in the first section of their publication. A computer program named ROUTE was developed to calculate the ship's speed loss in a seaway. For a 200,000 tdw (tonne deadweight) tanker, the speed loss in varying voyage speed and different significant wave height in Head waves was estimated. For the other wave directions, the shapes of the energy distribution over the frequency range are assumed to be the same, which might cause significant error in added resistance prediction. In the second section of their

publication, Meijers studied the effect of routeing on the fuel cost. Four alternative routes from Port A to Port B were studied with encountered wave fields, as presented in Figure 1.

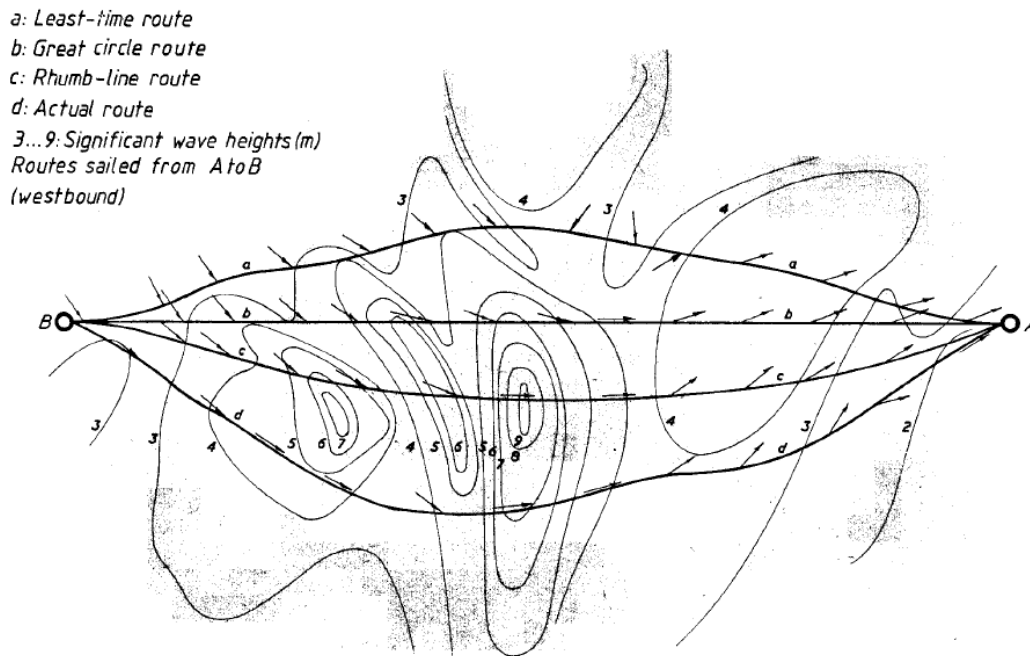


Figure 1: Four Alternative Routes between Ports A and B (Journ é and Meijers, 1980)

Journ é and Meijers (Journ é and Meijers, 1980) stated that up to 12% of fuel can be saved by utilizing the least-time route compared to the actual route while keeping the constant number of revolutions of propeller. Speed optimization was not included in their routing work. In general, it might be the first time that the relation between speed loss, voyage speed, and significant wave height has been applied to ship routing. However, as different components of added resistance were modelled separately and due to the limitations (such as the wave directions and ship motions) of their modelling methods, the prediction of added resistance (in speed loss format) seems to be complicated and not very accurate. Therefore, the accuracy of fuel consumption prediction might be affected.

Motte et al. (Motte et al., 1994a) introduced the design and operation of a computerized weather routeing system called ORION. The elements of ORION system include

environmental data, ship performance and optimal algorithm. The environmental data is sourced from the European Centre for Medium range Weather Forecasts (ECMWF), the National Meteorological Center (NMC) and the Fleet Numerical Oceanographic Center (FNOC). The optimization algorithm can be selected from dynamic programming (Calvert, 1990 and Motte et al., 1988) and the modified isochrones method (Hagiwara, 1989). However, the ship performance model is not easy-to-use as it requires the following:

- Ship body plan, or offsets at a series of specific sections along the hull. Loading scenarios for estimation of projected windage areas
- Engine and propeller data
- Ranges of operational draughts, trims, KG and GM, for example from a stability booklet
- Dry-docking data, and hull and propeller anti-fouling systems
- Seakeeping algorithms and studies, using strip theory
- Regression studies and calibration to sea-trials and log-books

Regarding the weather forecast adopted in ship routing, Chen (Chen, 1990) stated that the most practical forecast period is about 6 days by evaluating the Medium Range Forecast (MRF) model. The probability of erroneous weather forecast will obviously increase afterwards. However, Kalnay et al. (Kalnay et al., 1990) proposed the first 7-10 days is the best estimator of the 30-day mean forecast circulations. Motte et al. (Motte et al., 1994b) investigated the effect of utilizing different time range weather forecast data on weather routing (ORION). In their case study, the ship speed was assumed to be constant and the Minimum Time Route (MTR) utilizing three-day forecast, five-day forecast, ten-day forecast, and long-range extended forecast (hindcast analyses) are compared. The results indicate that

a lack of weather forecast from the 6<sup>th</sup> day has a large impact upon the route selection, and the MTR does not alter obviously by utilizing the long-range extended forecast other than the ten-day forecast. Therefore, it can be concluded that the period of weather forecast adopted for ship routing is supposed to be between 6 days and 10 days.

In recent years, the ship routing service on ship level has been well developed and can be generally categorised into an ashore based routing service, an on-board based routing service and the combination of ashore & on-board routing service.

The ashore based routing service commonly provides:

- Weather forecast, including the strength and directions of wave and wind
- Route planning, based on the advice from experienced masters and meteorologists

The on-board based routing service commonly provides:

- Weather and wave forecast, received from ashore agent or satellite
- Route planning and voyage optimization, defined routes and corresponding ship responses according to weather and wave forecast can be displayed on PC for route planning. An optimization functionality is often introduced into route planning system and automatically detect favourable routes for voyage optimization (Route optimization)

Hinnenthal (Hinnenthal, 2008) has reviewed the existing routing service or decision support systems. As presented in Table 1, sixteen routing service software have been briefly reviewed regarding their installed locations and functions.



**Table 1: Exemplary compilation of routing service or decision support systems (Hinnenthal, 2008)**

<i>Service Provider</i>	<i>Installed Location</i>	<i>Service/System</i>	<i>Weather forecast</i>	<i>Route planning</i>	<i>Route optimization</i>	<i>Ship monitoring</i>	<i>Data recording</i>
Aerospace and Marine International (USA)	ashore	Weather 3000, internet service, maps displaying fleet and weather information	X				X
Weather Routing Inc. (USA)	ashore	routing advice and Dolphin navigation program combined with a web-based interactive site	X	X			
Finish Meteorological Institute (Finland)	ashore	weather and routing advice for the Baltic sea	X	X			
Fleetweather (USA)	ashore	Meteorological consultancy	X	X			X
Networks Ltd. (UK)	ashore	meteorological consultancy	X	X			
Applied Weather Technology (USA)	on-board	BonVoyage System	X	X			
Euronav (UK)	on-board	seaPro, software or fully integrated bridge system	X	X			X
Germanischer Lloyd, Amarcon B.V. (Germany, Netherlands)	on-board	SRAS - Shipboard Routing Assistance System	X	X		X	
Transas (UK)	on-board	ship guard SSAS, software or integrated to bridge system	X	X		X	X
Norwegian met office, C-Map (Norway, Italy)	on-board	C-STAR	X	X			
US Navy (USA)	on-board	STARS	X	X	X	X	
Meteo Consult (Netherlands)	on-board	SPOS - Ship Performance Optimization System	X	X	X	X	
Oceanweather INC., Ocean Systems INC. (USA)	on-board	VOSS - Vessel Optimization and Safety System	X	X	X	X	
Weather News International, Oceanwaves (USA, Japan)	ashore & on-board	voyage planning system VPS and ORION, routing and optimization software	X	X	X		
Swedish Met and Hydrology Institute (Sweden)	ashore & on-board	Seaware Routing, Seaware Routing Plus and Seaware EnRoute Live	X	X		X	
Deutscher Wetterdienst (Germany)	ashore & on-board	MetMaster, MetFerry, routing system, advice on demand	X	X	X		

In recent years, the Ship Performance Optimization System (SPOS) and the Voyage and Vessel Optimization System (VVOS) are two most popular voyage optimization systems in commercial routing service software.

The SPOS (Spaans and Stoter, 2000) is an on-board routing system. The navigational planning is generated by a combination of the forecasted weather with the experience of the master of the ship. The ship performance characteristics are then inserted by the user. After the vessel departs from the port, the true performance data will replace the estimated ship performance data in the route management function of SPOS. Due to the feedback from users, the time of operating in bad weather can be significantly reduced with SPOS.

The advantage of using SPOS is the accurate weather forecast. The independent weather bureau Meteo Consult provides a global marine weather forecast up to five days in advance for five different Ocean areas daily. Nautical MeteoBase (NMB) has been developed by MeteoGroup in 2005. It is used to integrate the sources of marine weather forecast, which include:

- ECMWF (European Centre for Medium Range Weather Forecasting), a model from the joint European weather services
- UK Meteorological Office
- NCEP of the American National Weather Service, part of NOAA

The weather information can be graphically displayed on screen with the ocean chart as a background, as presented in Figure 2.

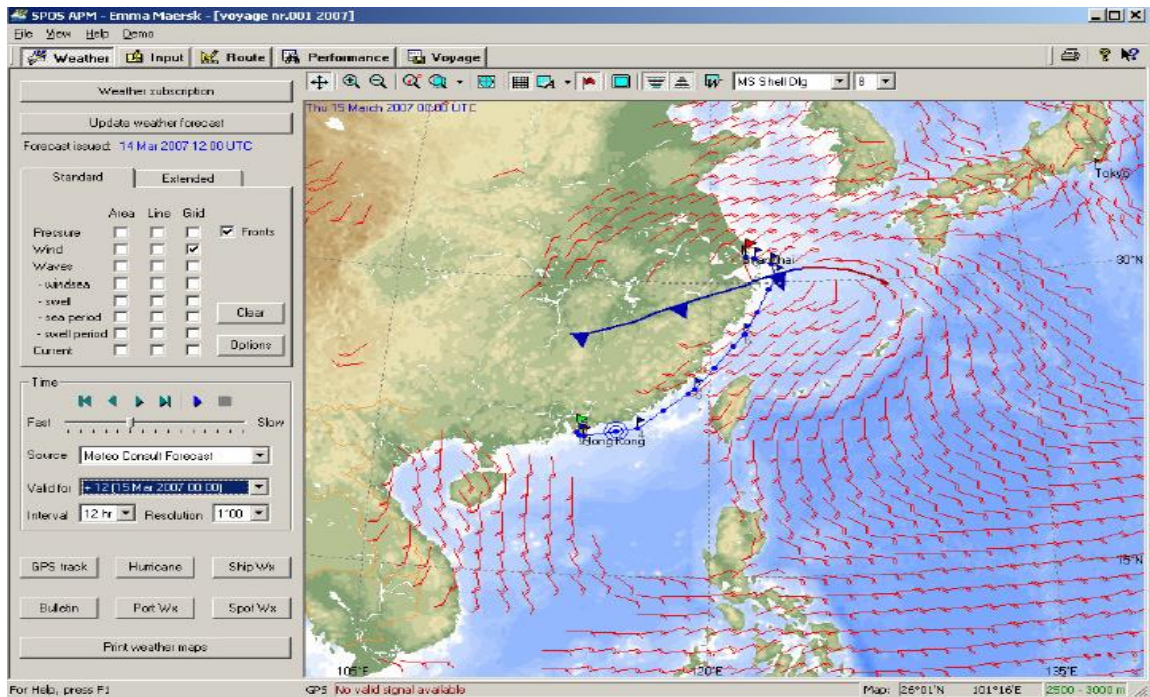


Figure 2: Marine Weather Forecast displayed by SPOS (Spaans and Stoter, 2000)

In SPOS, the ship performance characteristics for voyage optimization are read from the recorded ship performance database. As the database is highly dependent on the manual input, the accuracy of ship performance is determined by the quality of manual input, which is a disadvantage in using SPOS. Furthermore, the optimum route provided by SPOS is the minimum time route while assuming the engine power is fixed. The function of speed optimization is not included.

The VVOS (Jeppesen, accessed 2014) is an on-board tool for voyage optimization. The optimum routes are selected by considering sophisticated hydrodynamic modelling, computations and ocean forecasts. Firstly, the ship's body plan, bilge keels and other appendages are digitized, its loading conditions are modelled with fore and aft drafts and GM. Then added mass and damping coefficients are computed with a sophisticated hydrodynamic program to solve the equation for motion. Engine and propeller characteristics are also involved in VVOS. Next, based on this model, the ship speed is estimated under the forecasted wind, wave and current for a given engine power and propeller RPM.

The sources of input include the Ocean area forecasts downloaded via satellite communication, and the VVOS motion sensor; which is used to monitor excessive motions and accelerations. In the output module, the VVOS recommends speed and heading changes to reduce ship motions and minimize heavy weather damage with respect to a fixed estimated time of arrival (ETA).

The Jeppesen Commercial Marine Operations (Ballou, Chen, and Horner, 2008) has been using the grids, as presented in Figure 3, to illustrate all the possible routes between Seattle, Washington to Nojima, Saki, Japan. The red column chart in Figure 3 lists the estimated time of arrival with corresponding fuel consumption, and the blue column meets the required ETA.

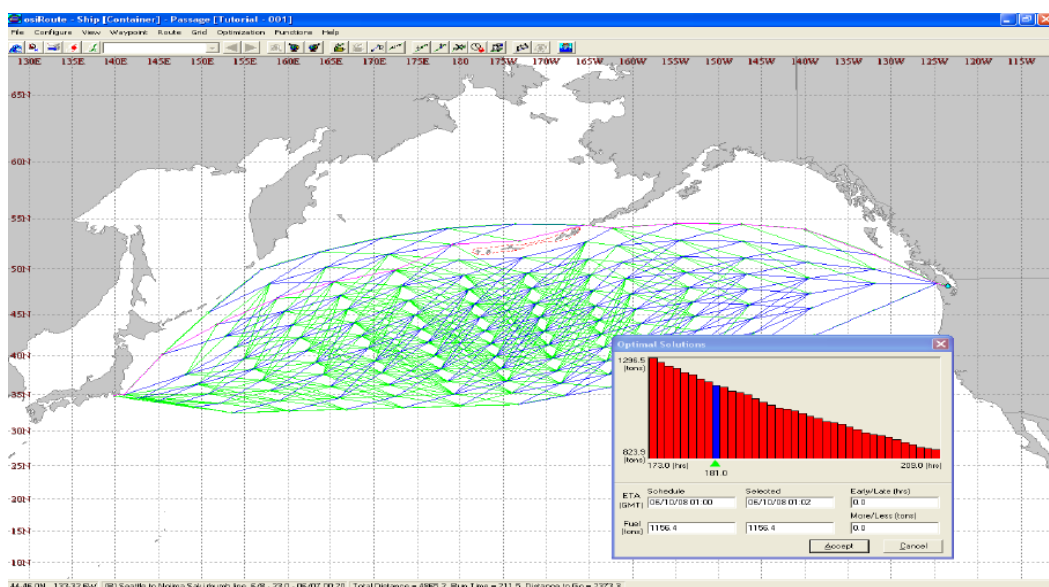


Figure 3: VVOS screen showing route optimization for trans-Pacific passage (Jeppesen, accessed 2014)

The VVOS is able to provide the minimum fuel speed plan for required arrival time and optimal speed management compared to constant speed, which is theoretically more advanced than SPOS. As the ship's body plan, bilge keels and other appendages are essentially required and requested to be digitized by using the motion sensor system installed on-board, and then the added mass and damping coefficients are computed with sophisticated

seakeeping software, the complicated system and high expense of using VVOS become the disadvantages.

## 2.3 Algorithm Applied for Weather Routing

When summarizing the literature of ship routing and scheduling, optimization algorithm has been identified to be widely used for weather routing. In this section, the Calculus of Variations, Isochrone Method, Dynamic Programming, Isopone Method, Evolutionary Method and Dijkstra's Method applied for weather routing will be reviewed.

### 2.3.1 *Calculus of Variations*

The calculus of variations is an analytical method that views ship routing as a continuous optimization problem. The real optimal route is selected by refining the gradients of the objective function while the course, ship position, and time are assumed to be deterministic. Bijlsma (Bijlsma, 1975) develops an incremental plotter using 6 days' recorded wave information, fictitious ship's data, and a 12 hour time step. The least time track is estimated, as presented in Figure 4. Based on the calculus of variations, optimal control theory, and the previous research of minimization of transit time, a study of minimum fuel routing is carried out in 2001 (Bijlsma, 2001). The same author in a later publication (Bijlsma, 2002) combines optimal control and dynamic programming for weather routing. Without the restricted grid in discrete dynamic programming method, the sailing paths can vary in the navigation area as a continuous process. Two years later, a computational method for the solutions of minimum time/fuel routing with limited manoeuvrability is proposed. This method is equivalent to the application of Pontryagin's maximum principle (Pontryagin, 1962), and provides a more realistic approach for weather routing by considering the manoeuvrability (Bijlsma, 2004). As the air pollution caused by the use of heavy fuel oil in shipping is drawing more attention, an approach to compute a Minimum Time Route (MTR) between specific ports and given

amount of fuel is proposed. Within this approach, the MTR with fixed fuel consumption is derived from the corresponding results generating from the calculus of variations (Bijlsma, 2008).

The advantage of using calculus of variations is its generality principle. As a mathematically elegant method, the calculus of variations can provide the optimal solution for each specific objective. The disadvantages include the fact that it assumes many variables to be deterministic, which make it not easy-to-use; and the sailing speed is always assumed to be a constant value, which is not able to achieve speed optimization.



Figure 4: Least time track (dashed line) (Bijlsma, 1975)

### 2.3.2 *Isochrone Method*

The isochrone method was firstly applied for weather routing by James (James, 1957). From start point, after each certain time unit, the boundaries of attainable regions are generated by computing isochrones continuously. However, the ship speed could be very different due the varying sea conditions in different attainable locations, after a certain time, the shape of the

isochrones which is normally irregular, will cause ‘isochrone loops’ problem for the computer program.

Hagiwara (Hagiwara, 1989) develops the modified isochrone method to overcome the ‘isochrone loops’ problem. Regarding the generation of new isochrone in the sub-areas, the point having maximum distance from each particular starting point (located on previous isochrone) is selected as the point within the new isochrone. Based on the modified isochrone method and forecasted wind/wave, the ship’s speed, drift angle, rudder angle, heel angle and engine power are predicted with equilibrium equations for the forces and moments acting on the ship. In the simulations of minimum time/fuel routing, the number of propeller revolutions is assumed to be constant, a set of routes with corresponding standard deviations of passage time and fuel consumption are calculated. According to the results, the optimum route is decided from a stochastic point of view. From Tokyo to San-Francisco, all minimum time routes generated by the modified isochrone method are shown in Figure 5. The minimum fuel consumption is calculated by varying propeller revolutions along the minimum time route.

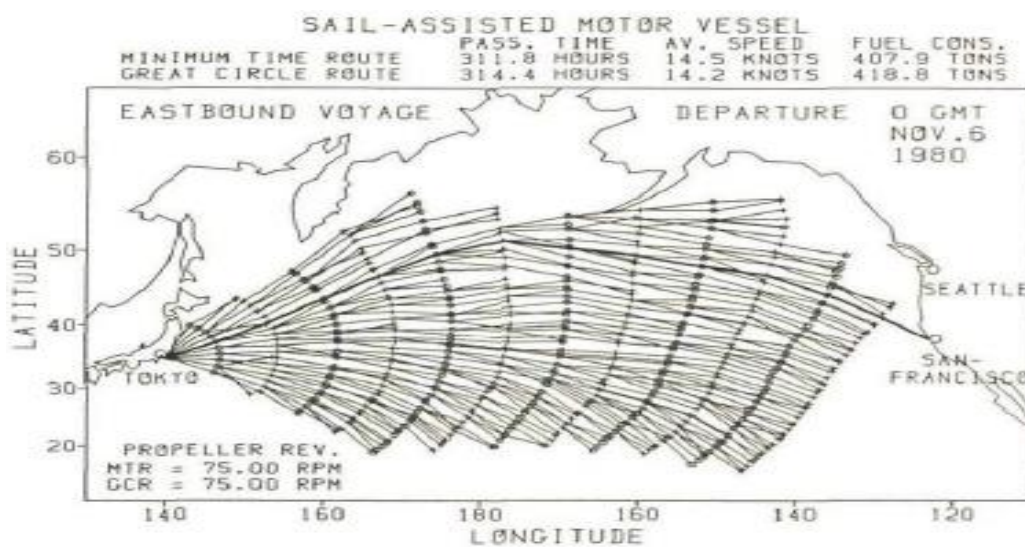


Figure 5: All minimum time routes of the sail-assisted motor vessel reaching each isochrone (eastbound voyage)

(Hagiwara, 1989)

The advantage of using the isochrone method is that it is straightforward, easy to understand, and can be used manually, which is helpful to increase user-acceptance. The other advantage is its flexibility. The isochrone method can be relative easily implemented in a modified way. The disadvantage is the fact that the propeller rotation speed of the vessel is assumed to be constant, and the minimum fuel route is the selected along with the minimum time passage, these assumptions may lead to the lack of speed optimization for optimal fuel consumption.

### 2.3.3 *Isopone Method*

Isopone method is an extension of the modified isochrone method. Klompstra et al. (Klompstra et al., 1992) propose the three dimensional isopone method by adding a time axis to the position (longitude and latitude). The minimum fuel consumption is obtained by computing energy fronts instead of computing time fronts in modified isochrone method as Hagiwara proposed (Hagiwara, 1989). With given weather conditions, the isopones in a three dimensional space, as presented in Figure 6, are derived from the speed-fuel relation. The isopones are defined as the outer boundary of the attainable region from the initial state  $(x_{10}, x_{20}, t_0)$  after consuming fixed amount of fuel  $(\Delta F)$  with varying time  $t$ . Since the first isopone has been generated, all the points on it are assumed to be the initial points for the determination of the next isopone. By repeating this procedure, a set of isopones are developed until the last isopone is tangent to the line  $l_f$  indicating the destination, as presented in Figure 7. Therefore, the minimum fuel consumption route is figured out by tracing backwards to the departure point  $\bar{x}_0$ , and the corresponding optimum course and speed are obtained.



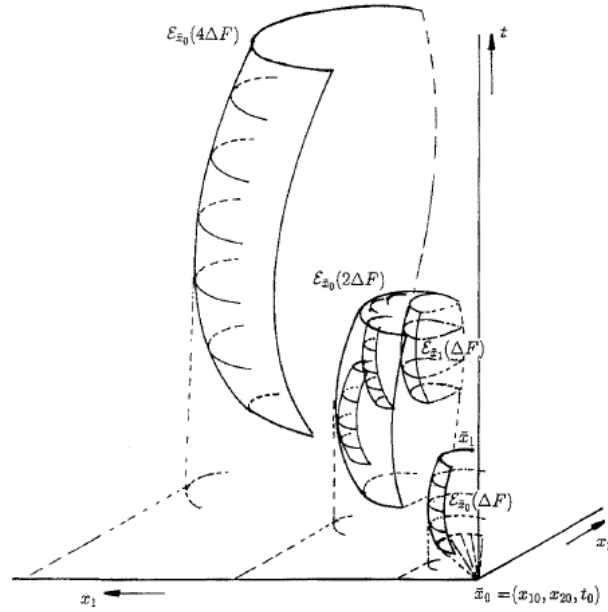


Figure 6: Isozones in three-dimensional state space (Klompstra et al., 1992)

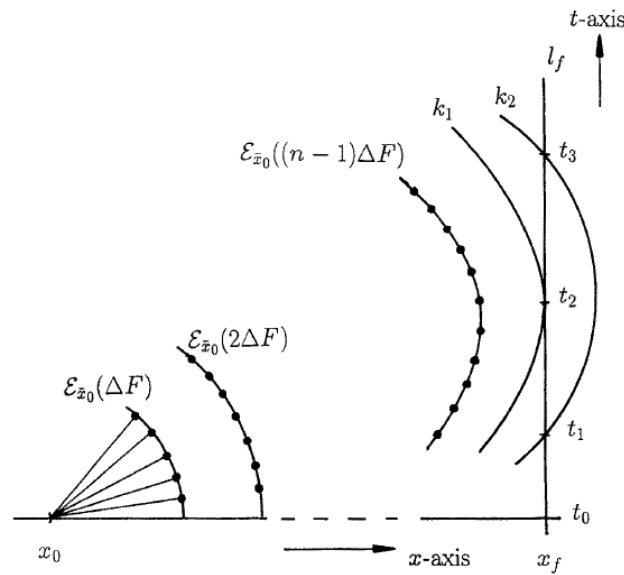


Figure 7: The last few isozones in a two-dimensional state space (Klompstra et al., 1992)

The advantage of isopone method is that it includes the ship engine power as a variable for weather routing. As the isopone method is mathematically more elegant and supposed to provide more accurate results compared to the modified isochrone method, the isopone method is adopted at the beginning development of the SPOS (Spaans and Stoter, 2000), which is commercial weather routing software. The disadvantage of isopone method is the

fact that the isopone method is difficult to be understood by ship operator, which is also the main reason that the isopone method has been replaced by the modified isochrone method in the development of SPOS (Spaans and Stoter, 2000).

#### *2.3.4 Dynamic Programming*

Dynamic programming is originally developed based on Bellman's principle of optimality (Bellman, 1957). The principles of dynamic programming indicate to divide a complex problem into relative simple sub problems; the sub problems are iteratively solved; and then the sub solutions are combined to conclude an overall solution. For weather routing, a grid system containing stages and points is widely adopted. The decision of selection control variables between two adjacent stages is assumed to be sub problems of weather routing. The points within the grid represent the geographical position and the corresponding weather conditions in specific time. The prediction of ship response to the sea conditions under each point is assumed to be the sub problems of routing between the corresponding stages. A prefixed grid of points for selecting a fixed time ocean route is proposed by De Wit (De Wit, 1990), as presented in Figure 8. In this research, the ship is assumed to sail with a fixed pitch propeller at a constant rotating rate; the objective is to obtain a route with minimum rotating rate for weather routing. By utilizing dynamic programming techniques, Calvert et al. (Calvert et al., 1991) proposed one minimum time optimization model and one minimum fuel optimization model for routing study. For the minimum time optimization model, the engine power, engine revolutions and departure time are fixed; the control variable is only the ship heading direction. For the minimum fuel optimization model, the engine power, RPM and the departure time are fixed; the arrival time is given as a boundary conditions; a minimum fuel consumption route is deduced by selecting the minimum time route within the boundary conditions. As the traditional dynamic programming methods take ship's heading (2 Dimensions: longitude and latitude) as variables for weather routing, while the engine power

and engine revolutions are assumed to be fixed during the voyage, Shao and Zhou (Shao and Zhou, 2012) proposed a three dimensional dynamic programming (3DDP) method to select minimum fuel consumption route. Both ship power setting (speed) and ship's heading (longitude and latitude) are assumed to be variables. The analysis diagram of using 3DDP for the fuel consumption between two stages is presented in Figure 9. Another three-dimensional (3D) dynamic programming announced by Chen (Chen, 2013) has been adopted by VVOS, which provides commercial weather routing service.

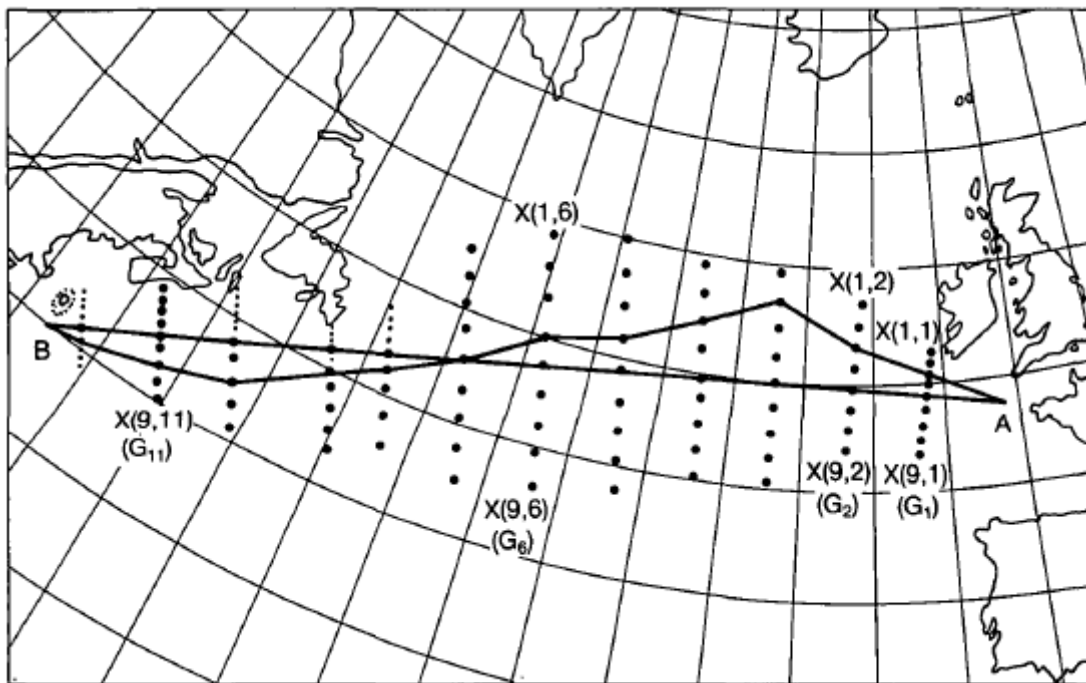


Figure 8: Example of a grid track from A (Quessant) to B (Nantucket L. V.) (De Wit, 1990)

The advantage of using dynamic programming for weather routing is that it simplifies route design by the development of a grid system. The weather conditions within the grid boundary can be easily captured. Compared to the analytical method of calculus of variations, the logical process is easier to be understood. The computation of the ship operational performance along a voyage course is also faster as the ship's heading directions is pre-defined by the grid points. The disadvantage of this method is the great demand of

computational power and time due to complicated loop in logic programming. As the accuracy of the optimum route selection is based on the density of the grid, the demand of computation increases sharply with finer grid.

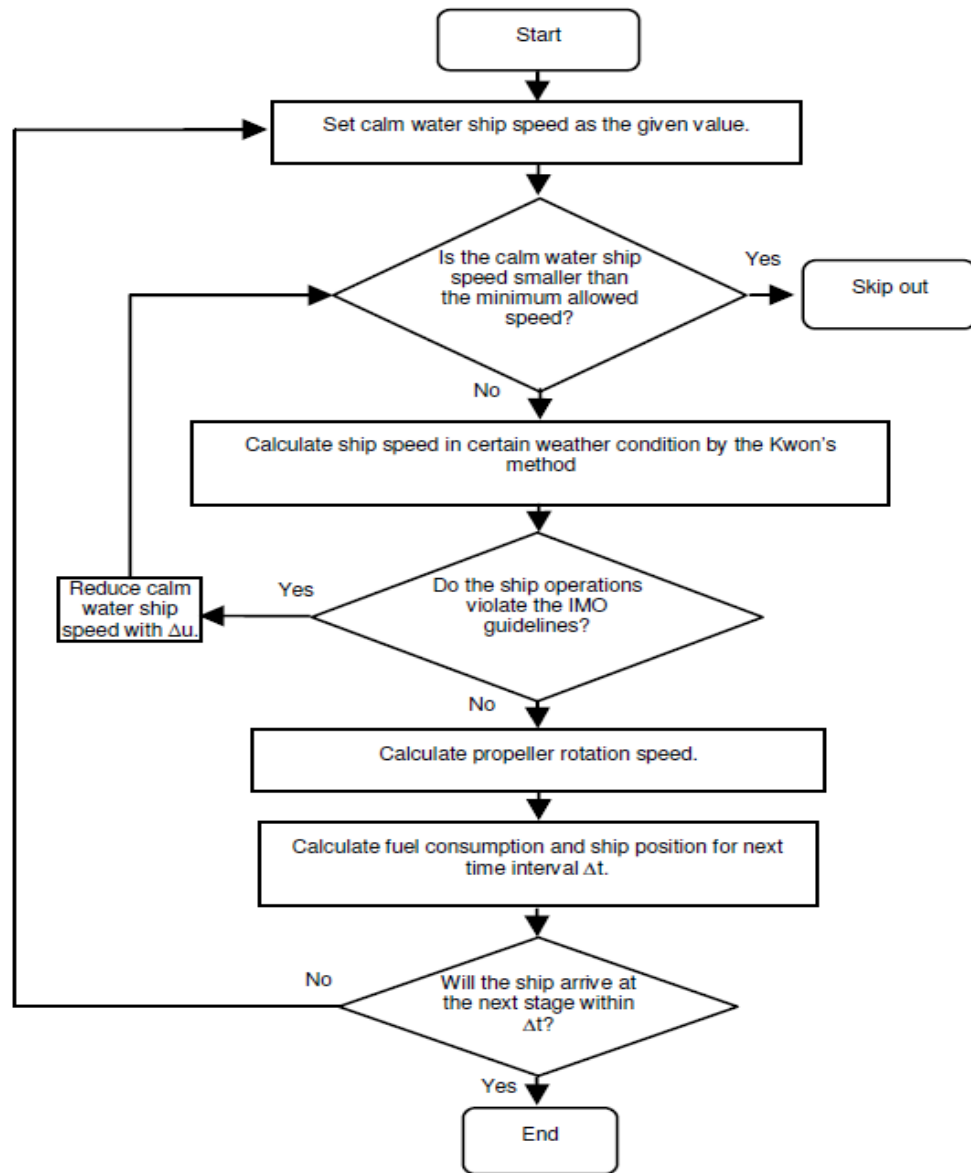


Figure 9: Estimate of fuel consumption between two stages (Shao and Zhou, 2012)

### 2.3.5 Evolutionary Method

Evolutionary algorithms include genetic algorithms. As a computational model simulating the biological evolution process of the genetic selection theory of Darwin, evolutionary methods have become popular in the last two decades and widely applied to multi-objective

optimization in weather routing. Pareto-optimal set is developed by a purely mathematical approach to optimization with multiple goal functions. Szlapczynska (Szlapczynska, 2007), Hinnenthal (Hinnenthal, 2008), and Marie and Courteille (Marie and Courteille, 2009) have proposed the multi-objective Pareto-based approach towards weather routing. Szlapczynska and Smierzchalski (Szlapczynska and Smierzchalski, 2009) describe the Multicriteria Evolutionary Weather Routing Algorithm (MEWRA) in detail and present the simulation results for the hybrid ship passing North Atlantic routes. A new engine-based MEWRA has been presented by Szlapczynska (Szlapczynska, 2013) and adopted as a plugin for NaviWeather software.

The advantages of Evolutionary algorithms include their remarkable characteristics of stability, especially its practicability in solving a multi-objective optimization problem. However, the Evolutionary approach is an elegant mathematical method requires many parameters during the optimization process, and ship operators need to know the value settings during the optimization process.

### **2.3.6**      *Dijkstra's Method*

An algorithm for finding the shortest paths between nodes within a network was proposed by Dijkstra (Dijkstra, 1959). The geographical space is discretized into a grid with rectangle shape, and the ship can sail to the centre points of the eight different neighbouring rectangles, as presented in Figure 10. The power of the engine, engine fuel consumption per unit of time, the ship speed and weather conditions between two centre points are assumed to be constant. Based on the Dijkstra's algorithm, Padhy (Padhy, 2008), Panigrahi (Panigrahi, 2008) and Sen (Sen, 2010) investigated the minimum time routing over the Indian Ocean under WAM (Third Generation Wave Model) forecasts. Mannarini et al. (Mannarini et al., 2013) developed an operational ship routing decision support system using time-dependent meteo-

oceanographic fields. The shortest path is recovered by utilizing a modified Dijkstra's algorithm.

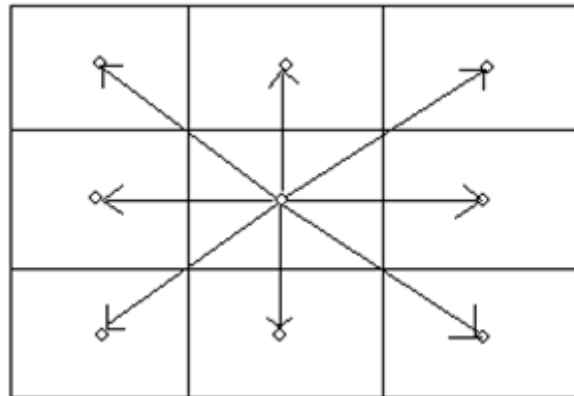


Figure 10: Different possible directions (Korving, 2011)

The advantage of Dijkstra's algorithm is its simplicity in providing solution to weather routing as it can be easily implemented with ship response in waves and added resistance. The disadvantage of this method is that it requires high density grid generation, better approximations can be provided with finer grid, but this also requires more calculation power.

## 2.4 Speed Optimization

Many studies on the optimization of shipping operations have assumed that the ship's speed is fixed during the voyage (Christiansen et al., 2004; Shintani et al., 2007; Gelareh et al., 2010; Wang and Meng, 2011, 2012). However, compared to the given speed, optimal speed for the voyage is very likely to contribute to energy efficient shipping. Some researchers (Corbett et al., 2010; Meng and Wang 2011; Ronen, 2011) have investigated the optimal speed issue for container ships based on the third power relationship between speed and approximately proportional bunker consumption (Ronen, 1982). Besides the investigation of speed optimization for container ship, Norstad et al. (Norstad et al., 2011) also looked into the bulk carrier. By utilizing the nine cases (as presented in Table 2) from bulk shipping

companies, the effect of speed optimization using the multi-start local search heuristic was evaluated with five approaches, which include:

- (1) The speed of each case was fixed with service speed of 17 knots. This approach was taken as baseline solution.
- (2) Based on the baseline solution, the speed was optimized for each route separately, as proposed by Fagerholt et al. (2010).
- (3) The speed of each was fixed with maximum speed of 20 knots. Fuel consumption increases but additional spot cargoes may be carried for higher profits.
- (4) The maximum speed with speed optimization for each route, as proposed by Fagerholt et al. (2010).
- (5) Variable speed (in the range of 14-20 knots) for each case, where the speed on each route leg was optimized with fleet schedule.

**Table 2:** Characteristics of test cases for speed optimization (Norstad et al., 2011)

Case No.	1	2	3	4	5	6	7	8	9
No. of contracted cargoes	18	8	17	12	15	41	28	12	16
No. of spot cargoes	0	1	0	2	2	9	2	3	2
No. of vessels	6	3	6	7	13	13	13	4	6
Planning horizon (days)	23	75	75	40	35	150	20	35	90

**Table 3:** Speed optimization – profit and fuel cost differences (in percent) from fixed service speed (Norstad et al., 2011)

Approach	Case No.	1	2	3	4	5	6	7	8	9	Average
Service speed + speed opt (2)	Profit	0.4	0.5	2.0	4.0	1.7	6.8	0.8	0.4	8.7	2.7
	Fuel	-2.4	-3.1	-14.0	-24.6	-9.7	-43.9	-10.4	-7.9	-11.1	-14.1
Max speed (3)	Profit	-1.6	1.9	-7.0	-7.9	-6.1	-6.3	-1.9	-1.7	-25.6	-6.2
	Fuel	31.7	53.7	45.6	46.2	35.4	40.1	24.9	31.8	74.7	42.7
Max speed + speed opt (4)	Profit	1.8	6.4	2.0	4.0	2.0	7.2	1.1	0.4	26.3	5.7
	Fuel	-15.3	27.6	-14.0	-24.4	-11.5	-45.2	-14.2	-7.9	8.5	-10.7
Variable speed (5)	Profit	2.2	7.7	2.0	6.6	2.1	10.9	1.3	0.5	30.0	7.0
	Fuel	-21.3	20.1	-14.0	-38.3	-12.4	-70.0	-18.0	-8.8	3.9	-17.6

Corresponding results of the last four approaches were compared with the baseline provided in approach 1, as presented in Table 3. Compared to the results generated with approach 1 and 3, speed optimization (approach 2, 4) contributes to profit increasing and fuel savings. It can be concluded that the speed optimization with variable speed range achieves best profit and fuel savings.

Lang and Veenstra (2010) have optimized sailing speed by assuming that fuel consumption varies linearly with the sailing speed to avoid nonlinearity, but the potential speed range must be very narrow. Golias et al. (2010) and Norstad et al. (2011) have taken a heuristic method to achieve speed optimization while the optimality cannot be guaranteed. Gelareh and Meng (2010) and Alvarez et al. (2010) have been discretizing the sailing speed range to address the nonlinearity. The benefits of this approach include:

- Widely applicable to continuous nonlinear functions
- Easily control approximation error by the number of discretization intervals

However, according to Fagerholt and Ronen (2013), the non-linearity of the bulk fleet scheduling problem with speed optimization is not able to find optimal solutions within any reasonable time frame for realistic size problems.

## **2.5 Ship Added Resistance Prediction**

Based on the experience of similar ships sailing on the same route, ship owners and designer stated that there is a 15-30% power increase in open water sailing than at the design stage (Péres Arribas, 2006). The 15-30% power increase is believed to be mainly caused by added resistance.



### **2.5.1 Causes of Added Resistance**

Added resistance is generally caused by the unsteady wave-making phenomenon, and the causes can be specified as follows (Wind n, 2011):

- Reflection of incident waves at the bow
- Heaving and pitching due to unfavourable shifts in buoyancy forces
- Boundary layer distortion due to flow disturbances around the hull
- Poor power plant performance and propeller performance in unsteady running conditions
- Strong head winds

### **2.5.2 Approach to Determine Added Resistance**

The methodologies for estimating added resistance can be generally categorized into empirical and semi-empirical, potential theory, Computational Fluid Dynamics (CFD) and experimental methods. The potential theory methods are subdivided into 2D or strip theory method and 3D panel methods. The details of these methods will be addressed below for greater clarity.

#### **2.5.2.1 The strip theory method and radiated energy method**

The strip method and radiated energy method are combined in the same section as these two methods are widely applied together for added resistance prediction.

The far-field method based on the principle of momentum and energy conservation was first proposed by Maruo (Maruo, 1960). The strip theory is able to predict the added resistance when the effect of radiation wave is dominant, but the added resistance caused by scattering wave near the ship bow cannot be predicted through strip theory (Kashiwagi et al., 2010).

According to this short-coming, a few practical approaches have been proposed to predict the added resistance due to scattering wave near the ship bow. The approaches include:

- Fujii & Takahashi (1975)
- Faltinsen et al. (1980)

Gerritsma and Beukelman's method (1972) adopts a radiated energy method to calculate added resistance. Although Gerritsma and Beukelman's method (1972) is widely used because of its equally accurate added resistance prediction for most ship forms, there are still several limitations of utilising this method:

- Only valid for head waves:

Gerritsma and Beukelman's method (1972) provides questionable results in following waves as it is only sensitive to low encountered frequencies. The accuracy of added resistance prediction may drop for high frequency waves.

- Only valid for radiation waves:

As Gerritsma and Beukelman's method (1972) is closely related to strip theory, it contains the common drawback of added resistance prediction using strip theory: only valid to predict the added resistance when the effect of radiation wave is dominant.

Another far-field method based on radiated energy method was proposed by Salvesen (1978). Salvesen's method (1978) is able to provide accurate added resistance prediction in the longer waves region ( $L/\lambda < 1.5$ ). On the other hand, the shortcoming of Salvesen's method (1978) is that it is not fit for shorter waves region ( $L/\lambda \geq 1.5$ ).

### ***2.5.2.2 The Rankine panel method***

The Rankine panel method is also known as pressure integration method. Boese (1970) proposed to integrate pressure directly on the wetted hull surface, and the force caused by the pressure can be divided into horizontal force and vertical force.

The comparison of S-175 containership added resistance prediction between Boese's method and experimental data has been carried out by Journ e (2001). The results indicated that the Boese's method is able to accurately predict ship added resistance in the longer waves region ( $L/\lambda < 1.2$ ) for S-175 containership in the preliminary design stage and not work well in shorter waves region ( $L/\lambda \geq 1.2$ ) in reverse.

### ***2.5.2.3 The Cartesian grid method and CFD method***

The Cartesian grid method and CFD method are reviewed in the same section as these two methods are widely applied together for added resistance prediction recently.

Seo et al. (Seo et al., 2013) has computed the added resistance and motions using a non-viscous Cartesian grid method through CFD programme. Case studies have been conducted for Wigley hulls, Series 60 hulls ( $C_B = 0.7, 0.8$ ) and the S175 containership. The predicted added resistance was compared to that of using strip theory and Rankine panel method, as well as experimental data. In an overview, there was a fairly good agreement for all methods (ITTC, 2014). The representation of ship solid body shape is significantly affected by the grid system (such as grid spacing) in the Cartesian grid method. However, the grid system has its limitations including aspect ratio and computational resource, which means that it is hard to use more grid in CFD method.

#### ***2.5.2.4 The semi-empirical method***

As the added resistance in short waves is not accurately predicted by using the numerical methods referred above, some researches have been carried out to fill this gap. Generally, an empirical or experimental correction is added to the existing added resistance prediction models/formulae to increase the compatibility and accuracy in added resistance prediction. These methods are so called semi-empirical methods.

As Salvesen's method (1978) is only able to provide accurate results for the longer waves region ( $L/\lambda < 1.5$ ), Faltinsen et al. (1980) has added a correction via approximated formula for different short wave lengths region. Overall the approximated formulae proposed by Faltinsen et al. (1980) was used to evaluate wave reflection added resistance and then the Salvesen's results were combined with the wave reflection added resistance in a semi-empirical way.

However, the selection of encountered angle (approximate 90 degree and 180 degree) is limited due to trigonometric function included in the correction formula. Furthermore, the term of 'short waves region' is not well defined as it depends on the ship length, which is another uncertainty in added resistance prediction.

As the calculated results of added resistance in short waves commonly give poor agreement with the experimental data, Fujii-Takahashi (1975) considered the reason for the discrepancy as added resistance due to wave reflection. They proposed a semi-empirical method considering the drift force acting on an upright barrel and correction coefficient for ship shape and speed. Although it has been widely used to predict ship added resistance, but the added resistance due to reflected waves acting on the bulbous-bow is not included. The bow flare above the water surface and the presence of a bulbous bow below the waterline water

may change the reflected waves, which may lead to significant error in the prediction of the added resistance.

According to the expressions of added resistance due to wave reflection proposed by Fujii-Takahashi (1975), Kuroda et al. (2008) modified the terms of added resistance due to wave reflection based on a tank test in a semi-empirical way, the effect of hull form above the water line was also included in the added resistance calculation. However, the added resistance due to reflected waves acting on bulbous-bow is still not taken into account.

Kashiwagi (1995) developed the Enhanced Unified Theory (EUT), which adopted the wave reflection at the bow through the body boundary condition. However, the EUT proposed in 1995 was not able to predict added resistance in short waves as the wave diffraction near the ship bow was not involved. Therefore, Kashiwagi et al. (2010) proposed an empirical correction factor (including Froude number and the ratio of wavelength to ship length) into the EUT. Compared to the measured added resistance in tank test, the semi-empirical EUT is able to obtain reasonable added resistance prediction. However, the correction factor can be applied only to the component due to diffraction of an incident wave.

Liu and Papanikolaou (2013) proposed a semi-empirical formula to predict the added resistance of ships in short oblique seas based on some easy-to-calculate ship data. Due to the complexity of the physical problem and the viscous effect, the experimental data are required to fine-tune relevant semi-empirical coefficients. As the adopted experimental data was pretty out-of-date, Liu, Papanikolaou and Zaraphonitis (2015) then modified the previous proposed formula by reconsideration of the effect of local and global ship's hull form, of bow flare and local draft and of newly available experimental data for different types of hull forms (Takahashi, 1988; Guo and Steen, 2011; SHOPERA, 2013). The updated formula is validated by applications to a tanker, a bulk carrier, a Series 60 ship and two containers, and the

prediction of ship added resistance in head seas, beam seas and quartering seas is reasonable. However, this added resistance prediction approach only works in short waves.

#### ***2.5.2.5 The experimental method***

There are two methods of towing that could be applied to predict added resistance (ITTC, 2011a):

- Constant thrust (model free to surge)

Constant thrust is believed to allow more freedom to model motions and less oscillations of instantaneous resistance force about its average. However, complicated towing apparatus construction is required by utilizing this method.

- Constant speed (surge restricted)

Compared to constant thrust method, constant speed method is much easier for realization, as the sub-carriage can be firmly attached to the main carriage. However, utilizing constant speed method may result in large oscillations of resistance force and the accuracy at instant overshooting of force gauge limits could be quite low, especially in high waves.

#### ***2.5.2.6 The empirical method***

Townsin and Kwon (1983) proposed the approximate formulae to estimate the added resistance due to weather effect. The added resistance was represented by the speed loss from the service speed under constant thrust. The wave added resistance was assumed to increase as the second power of the wave height based on Maruo's method (1957a, 1957b, 1957c, and 1957d) and the added resistance due to reflection in regular waves based on Kwon's method (1982). Based on large amount of wave and wind data recorded on board, wind and wave are predominantly in proportional relationship and come from the same direction. A particular

family of wind and wave spectra were identified in terms of Beaufort Number (BN). Therefore, the Response Amplitude Operator (RAO) for added resistance was linked to Beaufort Number (BN) via ITTC spectrum. Finally, the head weather formulae are derived from calculations for container ships in their normal service condition and tankers both laden and in ballast. Based on the head weather formulae, the weather direction reduction factors were introduced as a correction factor, and then the added resistance under bow, beam and following weather can also be estimated. The percentage speed loss is given by

$$\mu \frac{\Delta V}{V} 100\% \quad (1)$$

where,

$\Delta V$  : Speed loss due to head weather

$V$  : Design service speed

$\mu$  : The weather direction reduction factor

The Townsin and Kwon's method (1983) was assumed to be one of the first empirical added resistance prediction methods that were simple enough to be incorporated into more involved voyage management procedures. However, there are limitations to utilize the Townsin and Kwon's method (1983):

- Few ship details are included as prediction inputs and therefore the prediction accuracy might be unsatisfactory for specific ship
- The accuracy of the prediction may become unreliable for BN above 6
- As only the head weather direction correction is derived from full scale data, the other weather direction corrections are not as accurate as head weather direction correction

In order to solve the first limitation of the Townsin and Kwon's method (1983), as outlined above, Kwon (2008) proposed the correction factors with block coefficient ( $C_B$ ) and Froude number ( $F_n$ ) to involve more detailed characteristics of the ship. The Kwon's method extends Townsin-Kwon's approximate formulae to include block coefficients ( $C_B$ ) from 0.55 to 0.85 and include Froude number ( $F_n$ ) from 0.05 to 0.30. The percentage speed loss is given by

$$\alpha\mu\frac{\Delta V}{V}100\% \quad (2)$$

where,

$\Delta V$ : Speed loss due to head weather

$V$ : Design service speed

$\alpha$ : The correction factor for block coefficient ( $C_B$ ) and Froude number ( $F_n$ )

$\mu$ : The weather direction reduction factor

The results of the above formula were compared with some published model test data (Takahashi et al., 1977) and full scale data (Aertssen & van Sluys, 1972). The comparison results indicate that the Kwon's method (2008) provides a good approximation for practical purposes, which is an advantage of using Kwon's method (2008). Another advantage is this method provides a simpler and easier way to estimate the effect of wind and waves over a wider range of parameters compared to Townsin-Kwon's approximate formulae (Townsin & Kwon, 1983). As the Kwon's method (2008) was developed and validated with series 60 hullform, which might be the weakness of applying the empirical formulae on the modern hullforms.



## 2.6 Ship Operational Performance Modelling

The fundamentals of voyage optimization include ship operational performance modelling for different ship conditions and different sea states, weather forecast and optimization algorithms. As the accurate ship operational performance modelling is the key element of voyage optimization and major research direction in this study, this section will focus on the review of ship operational performance modelling.

Currently, there are two sources of ship operational performance modelling for voyage optimization. The first option is the ship operational performance database, which records the historical ship operational performance under different ship conditions and different sea states. In the route evaluation process, with given sea states, vessel speed, draft, and other ship conditions, the corresponding ship operational performance will be extracted from the database. The large amount of ship operational performance records is one of the preconditions of using this option, and mostly the performance records need to be inputted manually. The second option is the ship operational performance prediction model, which predicts the ship operational performance with given ship characteristics and sea conditions.

Generally, the prediction of ship total resistance in waves ( $R_T$ ) can be performed in two steps (ITTC, 2011):

- a) Prediction of calm water resistance,  $R_{CW}$ , at speeds of interest
- b) Prediction of added resistance in waves,  $R_{AW}$ , at the same speeds

Then, the prediction of ship total resistance in waves is obtained as a combination of the above two predicted values:

$$\mathbf{R}_T = \mathbf{R}_{CW} + \mathbf{R}_{AW} \quad (3)$$

There are several methods to determine the calm water resistance of ships; in this thesis the Holtrop and Mennen method (1982) has been adopted to calculate the calm water resistance. Compared to the well-developed prediction of ship resistance in calm water, there is still an enhancement potential in added resistance prediction. The review of added resistance prediction has been carried out in Section 2.5, and this section will review the methods of ship performance modelling.

### 2.6.1 Overview of Ship Performance Monitoring and Analysis Systems on the Market

In recent years, many ship performance monitoring and analysis systems have been developed. Regarding the data collection for the performance evaluation systems, some systems have utilized automatic data acquisition systems, but most of them still adopt manual data collection. Since the details of ship operational performance modelling in the merchant ship performance monitoring and analysis systems are confidential, it is difficult to review or comment on their performance modelling methods, input parameters and the accuracy of output. Therefore, most shipping companies prefer to utilize their own methods for monitoring and analysing ship performance. Table 4 provides a general overview of available ship performance monitoring and analysis systems:

**Table 4: Exemplary compilation of ship performance monitoring and analysis systems (Hasselaar, 2010)**

<b>System Provider</b>	<b>System</b>	<b>General Introduction</b>
Mitsui OSK lines (MOL 2003)	TOMAS	Onshore analysis of daily abstract logbooks via regression analysis
BMT Seatech Ltd (BMT-SeaTech 2004)	SMART <sup>POWER</sup>	On-board real-time data collection, analysis and performance analysis. Both instantaneous and long-term performance feedback is given
MARINTEK	SOPRANweb <sup>TM</sup>	Onshore analysis of daily abstract logbooks for

		both operational feedback as well as long-term condition monitoring
Kyma AS (KYMA 2006)	Kyma Ship Performance	On-board real-time data collection and analysis
Propulsion Dynamics Inc. (Munk 2006)	CASPER	Onshore analysis of daily ship logbooks. Periodical performance reports are sent to the customer. Correction of wind, waves and displacement variations.
Force Technology (Force-Technology 2008)	Seatrend	On-board manual data collection, analysis onshore with corrections for wind, wave and displacement variations.
Ocean Systems Inc. (OSI 2010)	Performance Monitoring	On-board manual data collection, analysis onshore with corrections for wind, wave and displacement variations.

Based on the general review of the available ship performance monitoring and analysis systems, it can be concluded that the ship operational performance data is still often collected and entered manually once a day. Even if the on-board computer has been used for data recording, the uncertainties (such as mistype and misread) of the manually collected data are not ignorable.

### **2.6.2**      *Methods of Ship Performance Modelling*

In this section, the ship performance modelling methods have been generally categorized into trend assembles and regression method; deterministic performance analysis method; system identification method; and bond graph method. The input requirement, general ship performance modelling procedures of these four methods will be introduced and a brief comment for each method will be included.

### **2.6.2.1 *Trend Assembles and Regression Method***

For ship operational performance modelling, the trend assembles and regression method can be generally grouped into two levels, one basic level and one premier level:

The basic level of trend assembles and regression method is utilizing the derivation of the relationship between some basic ship performance parameters, such as main engine fuel consumption, speed, Admiralty coefficient, and RPM. Large amount of data related to ship's performance are used as input. The required data should be collected in relatively calm water under similar speeds. As the added resistance caused by wave and wind is ignored in the ship performance modelling, the basic trend assembles and regression method is very easy to use and thus widely adopted by some shipping companies. However, this method requires huge amount of consistently collected ship performance data, and deviations in the trend regression are rather large without necessary performance corrections (such as draft, weather and sea conditions). Molland et al. (Molland et al., 2011) have introduced the basic level trend assembles and regression method for resistance data analysis and power data analysis.

The premier level of trend assembles and regression method is utilizing statistical analysis and multiple regression analysis techniques to include more ship performance related parameters, such as wave and wind, ship draft, sea directions, and ship speed. The corrections for ship operational data are also introduced into ship performance modelling. Thus the ship performance trend can be generated with higher accuracy. Even though the premier trend assembles and regression method is not difficult to understand and increase the ship performance modelling accuracy, this method still requires a huge amount of voyage performance data. The accuracy of ship performance modelling is quite dependent on the accuracy of actual ship performance data. Pedersen and Larsen (Pedersen and Larsen, 2009) have tested different regression method on full-scale propulsion power prediction, and concluded that the Artificial Neural Network (ANN) was the best solution. Aas-Hansen (Aas-

Hansen, 2010) introduced the linear regression on the corrected power for specific ship. Pedersen and Larsen (Pedersen and Larsen, 2013) stated that the Gaussian Process Regression (GPR), which is a non-parametric model that provides a flexible framework for regression, can provide a better prediction on energy consumption than ANN.

### **2.6.2.2 *Hydrodynamic Analysis Method***

A vast number of ship performance modelling approaches utilizing hydrodynamic analysis methods have been developed since the last century. Based on the ship performance prediction procedure presented by ITTC (ITTC, 1999) for full scale ships, the ship performance prediction is supposed to start with the ship's total resistance prediction, then modelling the full scale wake and operating condition of propeller, which is in general separately studied as wake fraction  $w$ , and thrust deduction coefficient  $t$ .

The ship's total resistance in waves consist of calm water resistance and added resistance (ITTC, 2011a). Holtrop and Mennen method (1982) and Holtrop method (1984) were developed through a regression analysis of experiments and full-scale data. Their methods are widely used to predict calm water resistance. The literature of added resistance prediction methods have been reviewed in Chapter 2.5. Regarding the prediction of required power in open sea, the propulsive efficiency has been studied. Hasselaar (Hasselaar, 2010) has reviewed the methods to predict corrected power by deducing added resistance, and categorized these methods into three groups:

- *Utilizing constant propulsive efficiency and constant speed*

Andersen et al. (Andersen et al., 2005) established a simple method to evaluate the service performance of ships. The daily operational performance data of two sister ships, one has a conventional propeller, the other one is fitted with a high-efficiency propeller were collected. During a period of two years steaming for both vessels, the propulsive efficiencies (under

constant speed) of these two ships are assumed to be constant and compared. The comparison results indicate 4% improvement of propulsion efficiency by utilizing the high-efficiency propeller.

- *Utilizing calculated propulsive efficiency and constant revolutions*

Schoenherr (Schoenherr, 1931) stated that a propeller delivers a definite amount of thrust and absorbs a definite amount of power at given shaft speed. Nowadays, Schoenherr's statement has been extended and accurately quantified. By using the propeller open-water diagram, the propeller efficiency under different delivered power, engine RPM, and ship speed can be identified and involved correctly. When the propeller revolutions and wake fraction are assumed to be constant, and the open-water diagram is available, this method is able to predict the corrected power and speed in calm water, and it can include the effect from weather and loading conditions through the given added resistance. This method has been widely used for speed trial analysis, which has been adopted by (Townsin and Svensen, 1980; and Toki, 2005).

- *Utilizing calculated propulsive efficiency and constant ship speed*

The two approaches above both assumed that the difference in torque between the performance in actual service sea conditions and the performance in calm water is only caused by added resistance. However, the change of hull resistance due to ship speed variation is often ignored. Thus, Taniguchi and Tamura (Taniguchi and Tamura, 1966) proposed a load coefficient (determined by the correction of wind and wave resistance component from the total resistance of the hull) to avoid the changes in hull resistance from speed reduction as the effect of sea conditions. This method is valid when the wake fraction for actual sea conditions and calm water are assumed to be equal. Similar methods can be found in (Kim et al., 2001; and ISO15016 2002).

All of these three types of ship hydrodynamics methods referred to above can provide reasonable ship performance predictions. The propeller open-water diagram, wake fraction, wind resistance coefficients, wave response resistance coefficients and thrust deduction factor are the parameters partially or all requested for greater prediction accuracy. These parameters are normally accessible during ship design stage, however, not always available for the ship owner or ship charterer to access them. Thus the prediction of ship performance using the referred hydrodynamics analysis methods may be unavailable or not accurate enough due to the absence of the proper values for these parameters.

### **2.6.2.3 System Identification Method**

System identification method is aiming to evaluate the capabilities of the vessel by conducting acceleration-deceleration manoeuvres trials. Based on the first principles of physics, the calm water resistance of a ship can be obtained without the need for any predefined propulsive characteristics, thus the model test is not essential and the uncertainties from scaling effect can be avoided. Abkowitz (1989) proposed to describe the hydrodynamic force using multiple polynomial equations, which contain the variables related to manoeuvring motion, propeller RPM, and rudder angle. The acceleration-deceleration trials are carried out during a regularly scheduled voyage.

The system identification method seems to be able to provide reasonable ship performance (including manoeuvring) prediction for long-term ship performance analysis. However, as described by Schmiechen and Abkowitz, the short-term predicted resistance using the system identification techniques (Abkowitz 1980; Abkowitz 1988; Abkowitz 1989; Schmiechen 1991; Schmiechen 1998) is commonly lower than the traditional techniques, which is not satisfying the shipping companies.

#### 2.6.2.4 Bond Graph Method

The Bond Graph Method was developed in 1960 by H. Paynter, MIT, and has been utilized to describe dynamic systems (Broenink, 2000). For ship performance modelling, the Bond Graph Method bonds the energetic states of two interacting systems, and illustrates the exchange of power between the two systems or subsystems at both ends of the bond. Hansen (Hansen, 2011) proposed a ship performance monitoring system modelled in General Energy System (GES) by utilizing the Bond Graph Method. The general analysis diagram of his modelling is expressed in Figure 11.

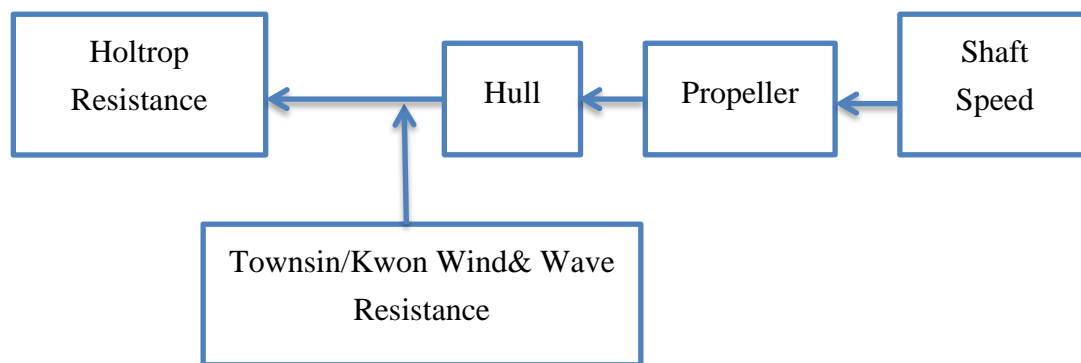


Figure 11: The ship performance modelling diagram (Hansen, 2011)

The analysis steps can be briefly described as following:

- The shaft speed is measured from the diesel engine to the propeller; the propeller torque is measured on the shaft, and then the torque coefficient can be found.
- The corresponding thrust coefficient and advanced coefficient can be figured out based on the given torque coefficient and propeller open-water diagram; then the propeller thrust and the speed of advance can be found; together with wake fraction and propeller slip, the ship speed is found.
- The hull and appendages (rudder and stabilisers) resistance can be found based on the thrust deduction coefficient and propeller thrust.



- The added resistance due to weather effect can be modelled by using Townsin/Kwon's method (Townsin, 1993; Kwon, 2008).
- The total resistance can be calculated by using the Holtrop model (Holtrop/Mennen, 1982; Holtrop, 1984).

In general, the Hansen's model (Hansen, 2011) is an easy-to-use method to predict the ship operational performance, especially by integrating the empirical Townsin/Kwon's method (Townsin, 1993; Kwon, 2008). However, as illustrated in Chapter 2.5.2.6, the Townsin/Kwon's method are developed and validated based on out-of-date hullform. This weakness is supposed to be overcome by modifying their formulae based on the latest actual operating data. This is also the major objective of this PhD thesis.

## 2.7 Effect of Fouling on Ship Operational Performance

The added resistance caused by the fouling effect is considerable for ship operational performance prediction. As fouling is a biological progress and the extent of fouling depends on the paint type, temperature, the sailing routes and area, it is not easy to provide an accurate prediction of fouling effect on ship operational performance. However, based on the docking period and the time since the last docking of the specific ship, it is still possible to predict the general trend of fouling effect.

Aertssen (Aertssen, 1969) investigates the fouling effect by utilizing full-scale experiments. The results indicate that, for a ship sailing on the Atlantic route, the added friction resistance ( $\Delta R_F$ ) caused by fouling effect is expressed in the order of:

$$\frac{\Delta R_F}{R_F} * 100\% = 3.6 * y_a + \frac{40 * y_d}{1 + 2 * 2 y_d} \quad (4)$$

in which:

$y_a$  age of the ship in years

$y_b$  years since the last docking

Journ e and Meijers (Journ e and Meijers, 1980) investigate the fouling effect by utilizing a log data of a 200,000 TDW tanker. The results indicate the calm water resistance increases by 26%- 29% one year after the last docking, and increases by 47%- 52% two years after last docking. To maintain the speed of 13 knots, the main engine load is required to increase from 50% to 80%, as presented in Figure 12.

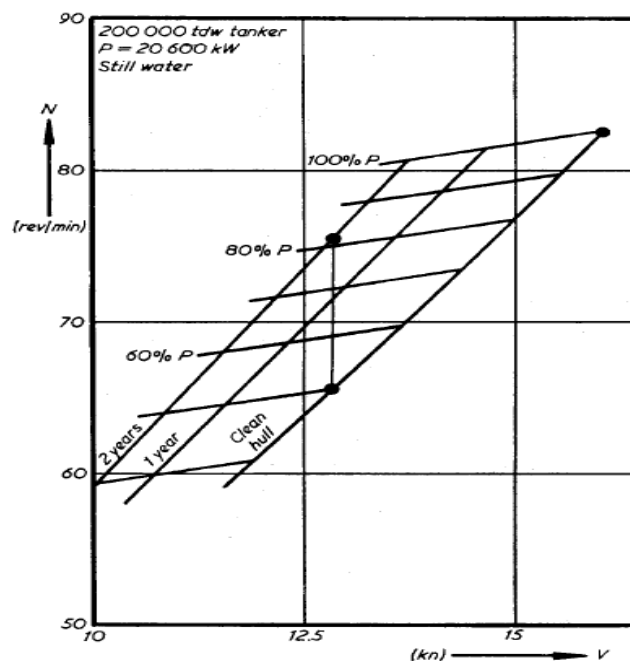


Figure 12 Power Increase due to Fouling (Journ e and Meijers, 1980)

Recently, Yokoi (Yokoi, 2004) looked into the changes in speed, shaft power and fuel consumption of a training ship over 8 years. Based on the recorded ship operational performance, there is a 10% - 20% increase in the shaft power per year due to fouling (ITTC, 2011). Munk (Munk, 2006) studied the resistance change before and after dry-docking for the ship in service, which has highlighted the importance of hull and propeller cleaning. Corbett et al. (Corbett et al., 2011) compared the fuel consumption of a bulk carrier and a tanker

before and after utilizing a foul release coating. Compared to the utilization of traditional tributyltin-free (TBT-free) Self-Polishing Copolymers (SPC) coating, the fuel savings can achieve 10% and 22% for the bulk carrier and tanker respectively.

## 2.8 Research Gaps

This chapter will clarify the research gaps in added resistance prediction, ship operational performance prediction and voyage optimization, especially look into the motivations for developing an easy-to-use and practical ship added resistance and operational performance prediction model.

Based on the critical review of ship added resistance prediction, it can be concluded that the prediction accuracy of using strip method; radiated energy method or Rankine panel method is commonly limited for some wave directions and in the shorter wave region; The Cartesian grid method and CFD method are widely applied together to provide fairly good added resistance prediction, but will take long time in calculation and may be limited with aspect ratio and computational resource; The reviewed semi-empirical methods partially make up the drawbacks of some existing added resistance prediction methods, and provide very reasonable added resistance prediction, but their modelling procedures are still complicated and not easy-to-use; The experimental methods have been verified to provide compatible results for added resistance and not influencing motion measurements. However, the experimental methods are not simple enough to be quickly incorporated into ship operational performance prediction and voyage management procedures. The empirical Townsin and Kwon's method (1983) is assumed to be the first added resistance prediction method that is simple enough to be involved into voyage management procedure. Kwon (2008) further improved the Townsin and Kwon's method (1983) by involving a correction factor, which is related to block coefficient ( $C_B$ ) and Froude number ( $F_n$ ) to involve more detailed aspects of

ship for more practical ship added resistance prediction. However, as the Kwon's method (2008) was developed to predict the added resistance for a very general ship type and the results of the approximate formulae are validated with out-of-date hullform, the prediction accuracy might be unsatisfactory for specific commercial ship with latest hullform. Therefore, the first research gap has been identified and the motivation is to develop an easy-to-use ship added resistance prediction model for specific commercial ship.

Based on the critical review of ship operational performance modelling, the trend assembles and regression method are simple enough to be involved into voyage management procedures, but these methods require huge amounts of ship performance data, and the accuracy of ship performance modelling is quite dependent on the accuracy of ship voyage records, which might be not good enough to quantify the effect of fouling on ship operational performance; The hydrodynamic method, system identification method, and bond graph method can provide very reasonable ship performance prediction, However, the propeller open-water diagram, wake fraction, wind resistance coefficients, wave response resistance coefficients and thrust deduction fraction are the parameters partially or fully requested for utilizing these three methods. These parameters are normally accessible during ship design stage, but in actual industry field, it is often unable for ship owner or ship charter to access the values of those parameters. On the other hand, the fouling conditions and other time-dependent factors are also not commonly included. The actual ship conditions may affect the ship operational performance significantly. Thus the prediction of ship performance using the referred hydrodynamics analysis method, system identification method, and bond graph method may be unavailable or not accurate enough due to the lacking of necessary values for the parameters. Therefore, the second research gap has been identified and the motivation is to develop a practical ship operational performance prediction model including the time-

dependant correction factor of fouling effect and engine performance degradation for specific commercial ship.

Based on the critical review of algorithm applied for weather routing, the basic principles, advantages and disadvantages of each algorithm have been clarified. Considering the effectiveness of voyage optimization for energy efficient shipping, the accurate ship operational performance modelling is prerequisite. By reviewing the existing commercial routing service software, it can be concluded that voyage optimization has been commonly involved in routing service. The ship performance characteristics for voyage optimization are commonly read from the recorded ship performance database, which is highly dependent on the quality of manual input, such as SPOS. Some advanced routing software, such as VVOS, have been using motion sensor system installed on-board. The ship's body plan, bilge keels and other appendages are all requested to be digitized. Then the added mass and damping coefficients are computed with sophisticated seakeeping software. The ship performance prediction in VVOS seems to be complicated and expensive as it requires the installation of sensor system. Therefore, the practical ship operational performance prediction model for specific commercial ship needs to be easy-to-use and provide good results with absence of hull form or other sensitive parameters, which sometimes cannot be accessed by ship owners.

Based on the critical review of speed optimization, most studies are still using the third power relationship to roughly estimate the proportional fuel consumption, which is not able to provide accurate ship operational performance prediction with varying sea conditions. Some studies have been using the historical operating data for regression. It has been concluded that speed optimization is an effective ship operation for voyage optimization. By studying the effect of fouling on ship operational performance, it has been concluded that the involvement of fouling effect for specific commercial ship is essential for accurate ship operational performance modelling. Therefore, the effect of fouling is supposed to be involved in the

easy-to-use and practical ship operational performance prediction model for specific commercial ship.

Within this thesis, a semi-empirical added resistance prediction approach will be developed for specific commercial ship based on existing empirical added resistance prediction method. The corresponding semi-empirical ship operational performance prediction approach will be developed based on the bond graph method. The effect of fouling on ship operational performance will be included as a time dependent correction in the proposed performance prediction approach.

## 2.9 Chapter Summary

In this chapter, the literature currently available on ship added resistance prediction, ship operational performance prediction, effect of fouling on ship operational performance, algorithm applied for weather routing, and speed optimization were reviewed, while the important research gaps were identified and highlighted towards the motivation of this PhD thesis.

The next chapter will clarify the proposed methodology for achieving voyage optimization.

# Chapter 3 – METHODOLOGY FOR VOYAGE OPTIMIZATION

---

## 3.1 Chapter Overview

This chapter will start with a few practical questions regarding voyage optimization (§4.2), and then present a flowchart of the method followed by a brief description of each module to clarify how to address these practical questions (§4.3).

## 3.2 Practical Questions Regarding Voyage Optimization

When a merchant ship is expected to have a long-distance voyage, with specified departure, destination and average voyage speed (decided by the given ETA and distance to go), a few practical questions regarding voyage optimization might be proposed by the ship owner and charterer to the captain.

- *‘With fixed ETA, what is the specific voyage plan (route selection and speed management), why not go with other potential routes?’*
- *‘What are the expected fuel consumption and sea conditions that the ship will encounter during her voyage?’*

In general, the captains are required to report to ship owners or charterers in daily basis. As the practical questions above are commonly answered based on the experience of the captains or rough estimation, there are many uncertainties included in their answers.



### 3.3 Overview of the Methodology for Voyage Optimization

In order to accurately answer the questions raised by ship owner and charterer, an easy-to-use and practical method to achieve voyage optimization will be introduced in this section. The flowchart of this methodology is presented in Figure 13.

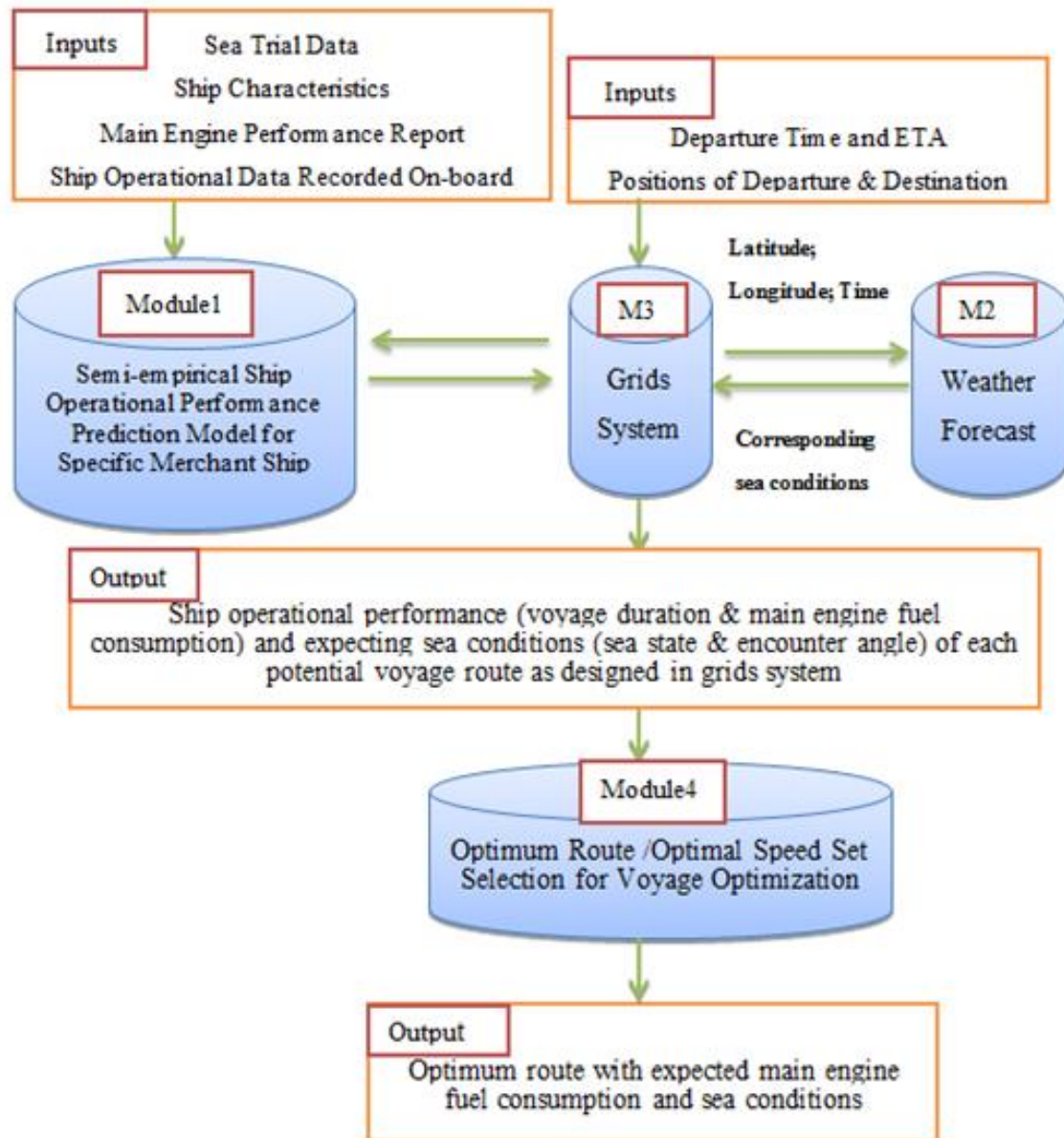


Figure 13: Flowchart of the Proposed Method for Voyage Optimization

From Figure 13, it has been observed that there are four modules included in the methodology for voyage optimization. These four modules will be briefly introduced as following:

### **Module 1 Semi-empirical ship operational performance prediction model for specific merchant ship**

The ship operational performance prediction for specific merchant ship starts from the prediction of calm water resistance with the input of ship characteristics. Then the added resistance caused by wave and wind is predicted based on a set of semi-empirical formulae which have been developed based on the actual operational data and empirical added resistance formulae. Next the relation between total resistance and speed under varying sea states and sea directions is converted into the relation between required effective power and speed under varying sea states and sea directions. By utilizing the Speed-Power Curve in sea trial document, the propulsion efficiency for the specific ship is then determined. Thus the relation between required effective power and speed under varying sea states and sea directions is converted into the relation between required engine power and speed under varying sea states and sea directions, as presented in Figure 14. By utilizing the Specific Fuel Oil Consumption (SFOC) diagram in the main engine performance report, the relation between Fuel Consumption Rate (FCR) and engine load (percentage of MCR) is determined for specific main engine. Therefore the relation between required engine power and speed is converted into the relation between FCR and speed under varying sea states and sea directions. Finally, the specific merchant ship's operational performance at varying speeds, in different sea states and sea directions can be accurately predicted. The details of Module 1 will be further clarified in Chapter 5.

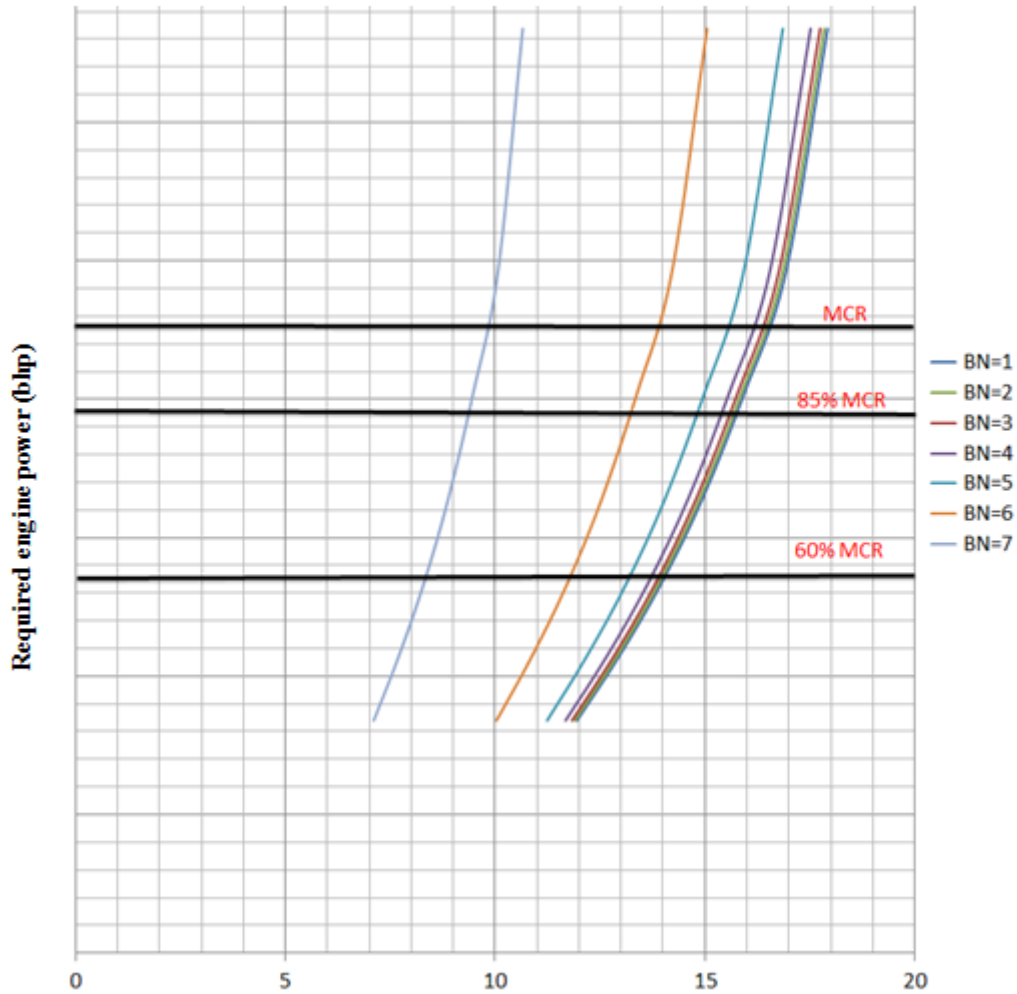


Figure 14: Relation between required main engine power and ship speed under varying sea state

## Module 2 Weather forecast

In this thesis, the weather forecast come from the National Oceanic and Atmospheric Administration (NOAA), and the historical weather and sea conditions records come from European Centre for Medium-Range Weather Forecasts (ECMWF). The decoding program has been written to get access to the ‘GRIB’ files from NOAA and ECMWF. With a given position (latitude and longitude) and time, the decoding program can provide the corresponding wind speed/direction, significant wave height, and wave direction/period. The details of Module 2 will be further clarified in Chapter 6.2.

### **Module 3 GRIDS system**

With the given positions of departure and destination, the GRIDS system is aiming to create all potential routes. The nodes in the GRIDS system contain the information of latitude, longitude and time, which will be used to read the corresponding sea conditions from Module 2. As each potential route has been divided into route legs by the nodes, and the weather condition during each route leg has been identified, Module 1 will predict the ship operational performance during each potential route and provide the feedback to the GRIDS system. The details of Module 3 will be further clarified in Chapter 6.3.

### **Module 4 Optimum route / optimal speed set selection for voyage optimization**

By integrating the GRIDS system with the semi-empirical ship operational performance prediction model, the relation between the FCR of main engine and ship speed under varying sea states is determined.

For weather routing, the voyage duration, the main engine fuel consumption, the expected sea state and encountered angle for each potential voyage route are taken as objective parameters and recorded into a database. Within this database, the optimum route is selected by sorting the value of single objective or multi-objective optimization. The details of optimum route selection regarding weather routing will be further clarified in Chapter 7.3.

For speed optimization, the optimum speed range of each route leg is firstly determined based on the optimum power output range of main engine (defined by the user). Then a speed optimization programme has been written to evaluate the fuel consumption with all possible speed combinations along the given route. By taking the fixed ETA as constraint, the optimum speed set for minimum fuel consumption is developed. Therefore, the ship masters are able to manage the optimum speed within specific ETA.

By evaluating the ship performance with varying speed sets and ETA, the ship masters are also able to trade-off the weight between fuel consumption and voyage time. If the extra voyage time is available, the corresponding amount of fuel savings can be easily presented to ship masters. The details of optimal speed set selection regarding speed optimization will be further clarified in Chapter 7.4.

### 3.4 Chapter Summary

This chapter referred a few practical questions raised by ship owner and charterer regarding voyage optimization, then presented the flowchart of the methodology and followed by a brief description of each module to answer these questions.

The next chapter will introduce the data sets adopted for the development of the semi-empirical ship operational performance prediction model.

# Chapter 4 – DATA DESCRIPTION

---

## 4.1 Chapter Overview

This chapter will introduce the data sets that have been adopted for the development of the semi-empirical ship operational performance prediction model for specific merchant ship. The data sets include actual operational data (§4.2), sea trial data (§4.3), and the main engine performance report (§4.4). The uncertainties of these three data sets will also be discussed.

## 4.2 Actual Operational Data

Sailing ships have to collect operational data on a daily basis and these are known as ship logs and ship reports (often referred to as noon reports as they are typically recorded every 24 hours at noon). The type of data fields that are included in the ship reports cover: date/time of the report, ship position, and estimated time of arrival, arrival/departure port, observed distance, achieved speed, mean draft, Beaufort Number, wind directions, and total main engine fuel consumption per day. There is no standard for the recording of operational parameters within the ship reports and therefore the content tends to differ between companies, which make it difficult to analyse the operational datasets from different sources. Besides the varying recording format, it has also been observed that often the mean draft is not recorded or additional parameters such as rpm, power (if a torque meter is installed), propeller slip, speed through water, and fore and aft drafts (providing trim information) are given.

However, there are some common parameters available to study the ship operational performance. These parameters contain a vast amount of uncertainty in their accuracy. This uncertainty originates from the methods used to obtain data, the type of measurement, and the

assumptions made during the analysis. Some of the uncertainties related to the parameters of interest that are discussed here:

- Ship date/time: this parameter is generally accurate although care should be taken to adjust for changes in time zone that the ship passes through. Uncertainty also occurs with human input error. The recorded date and time can be used to calculate the duration of the ship reports in hours, which is typically 24 hours.
- Ship position: this is recorded by GPS and is considered sufficiently accurate. Uncertainty occurs through human input error.
- Observed distance: this is calculated using GPS.
- Achieved speed: the achieved speed is calculated by dividing the observed distance by the report duration. The speed is therefore given as an average value for the whole report duration. It does not take into account the speed profile over the report duration which, due to the approximately cubic relationship between ship speed and power for the low and medium Froude number ships, could have a significant influence over the fuel consumed during the reporting period. The achieved speed is also the speed over ground and therefore, the effects of currents and tides are not taken into account. To improve the accuracy of performance prediction, the speed through water should be obtained.
- Mean draft: The mean draft is the draft amidships (average of the fore and aft draft) and is typically recorded using draft marks before departure. The recorded draft in the ship reports does not change over the course of the voyage although in reality it changes with the consumption of fuel, although only by a very small amount. Furthermore, without the fore and aft drafts it is not possible to determine the trim of the vessel (if it is not recorded separately) despite the fact that it is known that it influences the fuel consumption. A small



amount of the ship reports for the tankers used in this thesis have the fore and aft trim recorded. By analysis of these few reports it appears that the tankers operate at even keel trim during loaded voyages and with predominantly the same aft trim in ballast which prohibits the emergence of the propeller.

- Beaufort Number (BN): The Beaufort measurement itself contains uncertainty as one number is used to represent a range of wind speeds and depending on the sea area it corresponds to different combinations of wave heights and periods. More accurate added resistance performance prediction methods depend on the wave height as an input along with the type of sea spectrum (including surface waves and developed seas). Additional uncertainty is created with the measurement of Beaufort Number typically being made via judgement of the sea conditions out of the window on the bridge by the officer on watch. Not only is this measurement subjective as it is a judgement, it is also made from some distance away from the sea surface. There is also ambiguity as to whether the Beaufort Number recorded is representative of the conditions at the observation point, or an average of the conditions observed over the report duration. In general, the strongest BN ( $BN_{Strongest}$ ) and the average BN ( $BN_{Average}$ ) are both recorded in noon reports.

- Wind direction: recording of the wind directions is typically aided by the use of an anemometer. Obstructing super structure in different wind directions is known to produce inaccuracies in the measurement, along with variations in wind strength at different heights. Uncertainty due to averaged measurements also applies in the same way as for Beaufort Number. Furthermore, the wind direction is assumed to be the same as the wave direction, which may be true in most instances of surface waves, but it could also be very different for swell direction. To improve sea and wind condition measurements, the wave, swell and wind direction and strength or height, should be recorded.

- Ship heading direction: The angle between the direction of ship bow and the North Pole. The angle is measured clockwise from north, in degrees from 0 to 359, which can be read from GPS.
- Encountered angle: Derived from wind direction, which is relative to the ship. It is also known as the heading angle relative to the waves. The encountered angle is generally categorised into four groups: Head Sea, Bow Sea, Beam Sea and Following Sea, as presented in Figure 15.

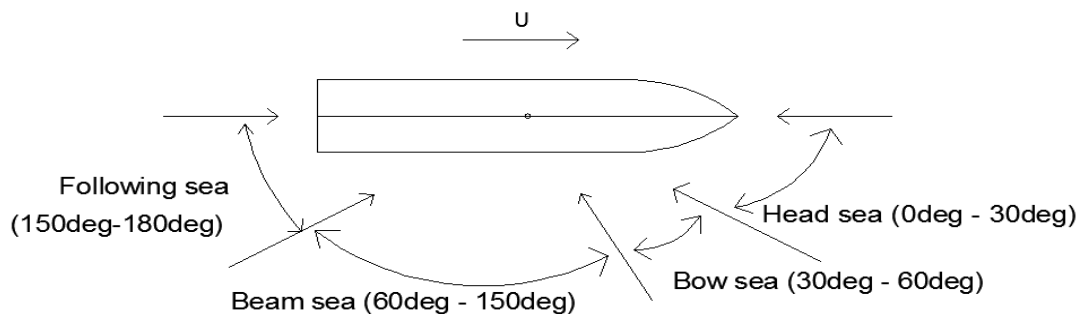


**Figure 15: Encountered angle**

- Main engine fuel consumption: Fuel flow meters improve the accuracy of fuel consumption measurements if they are calibrated and working correctly. However, in most cases the main engine fuel oil consumption is recorded by tank sounding. Not only could the measurements contain a vast amount of inaccuracy, but there is room for error in the tank sounding calculations and the recorded value is susceptible to transcription error and intentional falsification for various reasons.

Despite all of the uncertainties described, the parameters in the ship reports provide an insight into the operating conditions of the ship in sailing and thus provide a value to performance prediction modelling.

## 4.3 Sea Trial Data

Sea trial data is providing the actual operation performance test results of a new launched ship. The following contents of a sea trial document will be utilized in the development of the semi-empirical ship operational performance prediction model for specific merchant ship

- I. Principal particulars
- II. General condition of sea trial
- III. Test results
  1. Speed trial result
    - 1) Result of speed test (scantling & ballast draft)
    - 2) Speed – power – RPM curve
    - 3) Speed trial analysis (scantling & ballast draft)

For the ship operational performance study in this research, the principal particulars, general condition of sea trial and speed trial results are taken as a reference for specific ship type. The principal particulars and general condition of sea trial can provide the ship dimensions, displacement with corresponding scantling & ballast draft, trim, wetted surface area (W.S.A), departure time and the main engine type & output. Theoretically, there is no uncertainty in these two sections of sea trial data.

The results of speed indicate the engine brake horse power (B.H.P) and Revolutions per minute (R.P.M) under specific draft, ship speed, encountered angle, wind speed & direction, wave height & direction. Based on the results of speed, the speed – power – RPM curve can be generated. In speed trial analysis, more details (ship waterline length, displacement, block

coefficient, wetted surface area, propulsion coefficient, ship speed, engine BHP and RPM, resistance correction and draft) of the sea trial are illustrated. These details are very helpful for calm water resistance modelling and the development of the semi-empirical ship added resistance prediction model for specific merchant ship. As the sources of sea trial data include the model test results, the analysed results and the actual measured results, the uncertainties of model test results and analysed results may lead to reasonable error in the speed – power – RPM curve and sea trial analysis.

In general, the error caused by the uncertainties of sea trial data is quite limited. The principal particulars, general condition of sea trial and speed trial results are very supportive for the specific ship total resistance prediction with respect to draft, ship speed, and encountered angle. Based on the instructions of propulsion coefficient from sea trial analysis, the required engine power is generated with corresponding ship total resistance.

In this thesis, two oil tankers and two container ships have been used to develop the semi-empirical ship operational performance prediction model. The basic particulars of these ships are recorded in their Sea Trial documents as shown below.

	<i>Suezmax Oil Tanker A</i>	<i>Aframax Oil Tanker B</i>
<b><i>Loa(m)/Beam(m)/Draft(m)</i></b>	<b><i>258/45.7/16.2</i></b>	<b><i>239/43.8/15</i></b>
<b><i>DWT(t)</i></b>	<b><i>142K</i></b>	<b><i>117K</i></b>
	<b><i>Post-Panamax Container Ship A</i></b>	<b><i>Post-Panamax Container Ship B</i></b>
<b><i>Loa(m)/Beam(m)/Draft(m)</i></b>	<b><i>299.9/40/14</i></b>	<b><i>304/40/14</i></b>
<b><i>TEU</i></b>	<b><i>6200</i></b>	<b><i>6800</i></b>

Based on the ship daily reports during the past few years, the operational zones for Oil Tanker A and Oil Tanker B are majorly located within Pacific Ocean (between Japan and Los

Angeles) and Gulf of Mexico; the operational zones for Container Ship A and Container Ship B are majorly located within North Atlantic Ocean (between West Africa and Europe).

## 4.4 Main Engine Performance Report

As presented in Table 5, main engine performance report provides the expected fuel consumption under different engine shaft power and engine speed with given fuel type at ISO reference conditions:

- Ambient air pressure            1,000 mbar
- Ambient air temperature        25 degree
- Cooling water temperature    25 degree

The relation between specific fuel oil consumption (SFOC), engine shaft power and engine speed (Figure 16) is able to converting the required engine power referred in Section 2.2 into main engine fuel consumption rate for specific ship. Obviously, the quality of the fuel and the actual ambient conditions will affect the SFOC of the engine (MAN Diesel & Turbo, 2013)

**Table 5:** Sample Expected Fuel Consumption at ISO Reference Conditions (MAN Diesel & Turbo, accessed 2014)

Engine shaft power % Specified engine MCR (SMCR)	Engine shaft power BHP	Engine speed r/min	Specific fuel oil consumption g/BHP	Fuel consumption per day t/24h
100	72000	94	125.2	216.27
95	68400	92.4	124.3	204.09
90	64800	90.8	123.7	192.34
85	61200	89	123.2	180.98
80	57600	87.3	123	170.06
75	54000	85.4	123.1	159.51
70	50400	83.5	123.3	149.10
65	46800	81.4	123.6	138.82
60	43200	79.3	124.1	128.63
55	39600	77	124.7	118.49
50	36000	74.6	125.4	108.38

45	32400	72	126.4	98.25
40	28800	69.3	127.4	88.07
35	25200	66.2	128.6	77.80
30	21600	62.9	130	67.40
25	18000	59.2	131.5	56.83

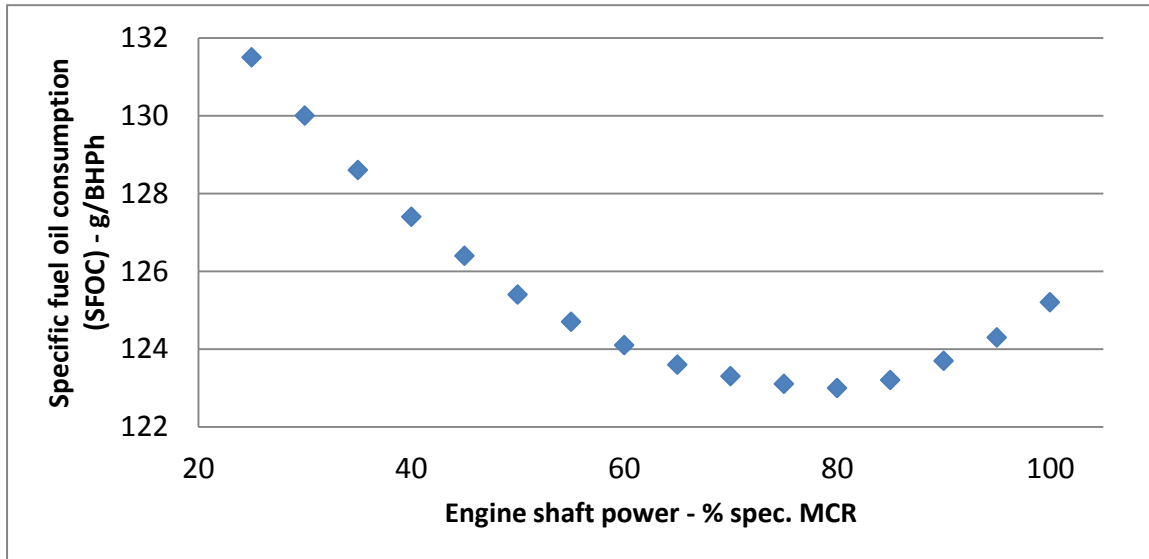


Figure 16: Sample Expected Specific Fuel Oil Consumption Rate at ISO Reference Conditions (MAN Diesel & Turbo, accessed 2014)

In main engine performance report, as stated by the main engine manufacturer, the margin for SFOC is +/- 5%, which is one uncertainty factor for ship operational performance prediction. Another uncertainty from main engine part is the specific engine tuning, which can lead to different Maximum Continuous Rating (MCR) for the same engine.

## 4.5 Chapter Summary

This chapter has introduced the data sets adopted for the development of semi-empirical ship operational performance prediction model for specific merchant ship. The uncertainties of the specific parameters in typical operational data, potential error sources in sea trial data and main engine performance report have been analysed.

The next chapter will present the development and validation of the semi-empirical ship operational performance prediction model for oil tankers and container ships.

# Chapter 5 – SEMI-EMPIRICAL SHIP OPERATIONAL PERFORMANCE PREDICTION MODEL

---

## 5.1 Chapter Overview

This chapter will first provide an overview of the proposed semi-empirical ship operational performance prediction model with flowchart (§5.2), and then specify the calm water resistance prediction (§5.3), added resistance prediction (§5.4), and ship operational performance prediction (§5.5). The development and validation of semi-empirical ship operational performance models for oil tankers (§5.6, §5.7) and container ships (§5.8, §5.9) are carried out, the discussion on time-dependent correction for oil tanker and container ship (§5.10) is presented at the end of this chapter.

## 5.2 Overview of the Semi-empirical Ship Operational Performance Prediction Model

The semi-empirical ship operational performance prediction model aims to predict the main engine FCR of a particular merchant ship under varying speeds, sea states and wave angle encountered (between sea directions and ship headings). The fouling effect on fuel consumption is included as a correction coefficient. The innovations and contributions of the proposed semi-empirical ship operational performance prediction model include:

- The development of the semi-empirical wave added resistance prediction formulae adapted for specific ship type by utilizing the actual ship operation data.



- The integration of the fouling effect and engine performance degradation as a time-dependant correction factor in ship operational performance modelling.
- The validation of the proposed semi-empirical ship operational performance prediction model by utilizing the recorded ship performance in actual shipping activities.

The approach adopted to develop this model is briefly explained below.

Initially, the calm water resistance is predicted by using Holtrop and Mennen's Method (Holtrop and Mennen, 1982), and thus the relation between the required effective power in calm water and the ship's speed is determined.

Then, the added resistance caused by the wave, wind, sea directions and other sea conditions is modelled by the semi-empirical ship operational performance model, which has been developed for oil tankers and container ships and will be presented in Section 5.6 and 5.8. As a result, the speed loss due to added resistance under varying speeds, sea states and wave encountered directions is determined. Based on the relation between required effective power and ship speed in calm water, the relation between required effective power and actual ship speed (by deducting the speed loss from the speed in calm water) is determined.

Next, the required effective power from the second step is converted into required main engine power by using the propulsive efficiency, which comes from the sea trial documents.

Based on the main engine Specific Fuel Oil Consumption (SFOC) diagram and the time-dependent fouling correction, the required main engine power from previous step is converted into main engine fuel consumption rate.

Finally, the main engine fuel consumption rate of the particular merchant ship under varying speeds, sea states and wave angle encountered can be estimated. By comparing the predicted

operational performance with the recorded one (during the period that fouling effect on fuel consumption is not significant, such as the first 5 months since launching, a decision will be made. The flowchart of the development of semi-empirical added resistance model is presented in Figure 17 for greater clarity.

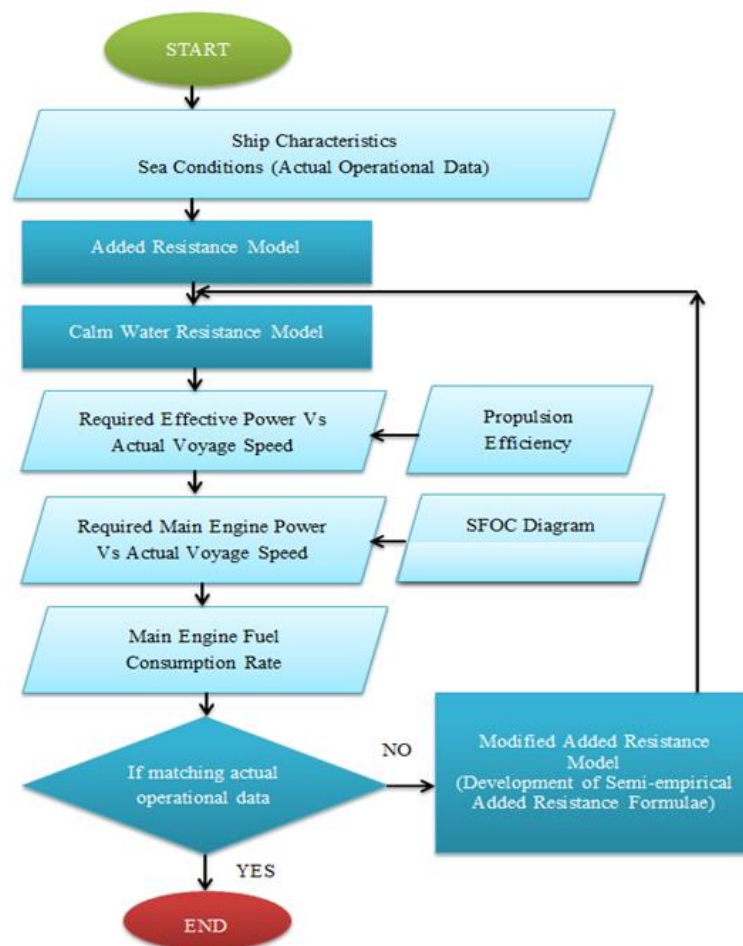


**Figure 17:** Flowchart of the Development of Semi-empirical Ship Operational Performance Prediction Model

If there is a good match in the comparison results, the flowchart will end, which indicates that an accurate semi-empirical added resistance model has been developed. If not, a new set of semi-empirical added resistance formulae will be developed, and replace the original empirical added resistance formulae.

Based on the proposed semi-empirical added resistance model, the predicted ship operational performance is compared with all available actual ship performance in time-dependant manner. A trend line is derived from the error between the predicted and recorded ship performance. It indicates the increasing fuel consumption rate caused by the time-dependent factors. By integrating the time-dependent correction, the semi-empirical ship operational performance prediction model is able to further improve the prediction accuracy.

### 5.3 Calm water Resistance Prediction

The well-known Holtrop and Mennen's Method (Holtrop and Mennen, 1982) is used to estimate the calm water resistance of the ship. This method is widely used to calculate the total calm water resistance of a ship with a good accuracy for a wide range of ship types, sizes, hull forms and for a range of Froude numbers. The equation for total ship resistance in calm water is given as follows:

$$R_{total} = R_F(1 + k_1) + R_{APP} + R_w + R_B + R_{TR} + R_A \quad (5)$$

where,

- $R_{total}$  Ship total resistance in calm water
- $R_F$  Frictional resistance according to the ITTC-1957 friction formula
- $1 + k_1$  Form factor describing the viscous resistance of the hull form in relation to  $R_F$
- $R_{APP}$  Resistance of appendages
- $R_w$  Wave-making and wave-breaking resistance
- $R_B$  Additional pressure resistance of bulbous bow near the water surface
- $R_{TR}$  Additional pressure resistance of immersed transom stern
- $R_A$  Model-ship correlation resistance

Based on Holtrop and Mennen's Method (Holtrop and Mennen, 1982), a calm water resistance prediction model has been developed in this study. In order to validate the prediction accuracy of this model, a case study for a post-panamax container ship has been carried out, as presented in Figure.18.

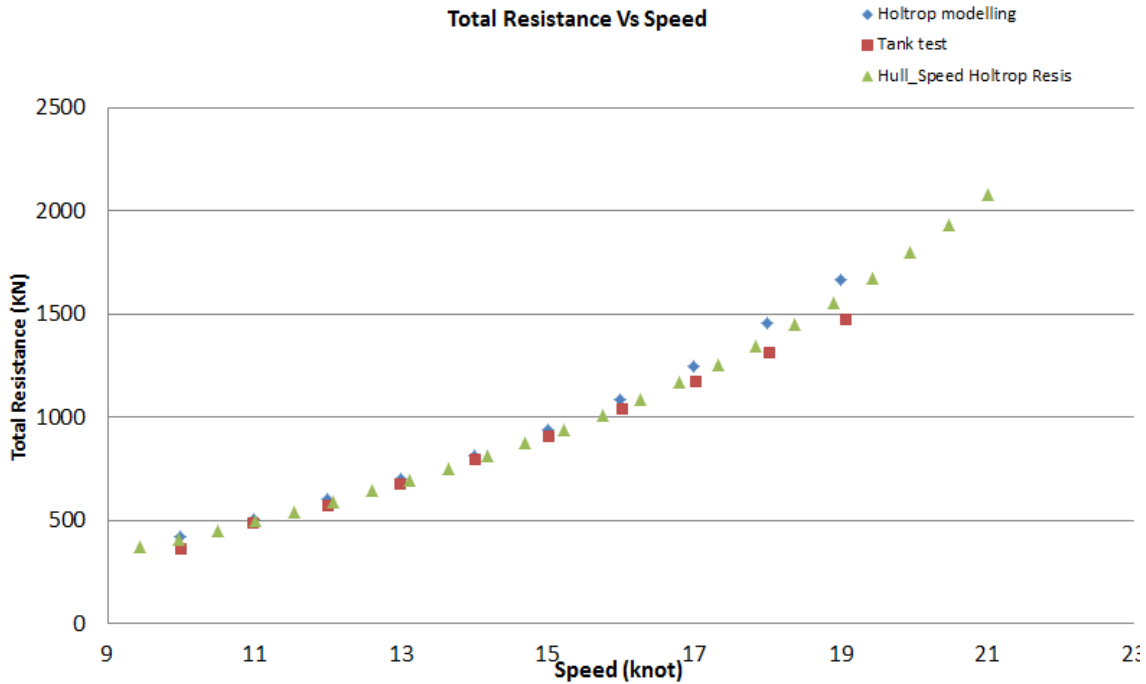


Figure 18: Validation Case Study for the H&B Resistance Prediction Model

As presented in Figure 18, the predicted resistance using the H&B resistance prediction model has been compared with the measured resistance in tank test and the predicted resistance using H&B method from commercial software – Hullspeed (MAXSURF, Accessed in 2014). The results indicate that the developed calm water resistance prediction model based on H&B method provide accurate resistance prediction.

## 5.4 Speed Loss Prediction

Based on the critical review of the existing added resistance prediction methods, as presented in Chapter 2.5, it has been concluded that the Kwon’s added resistance prediction method (Kwon, 2008) is one of the best empirical added resistance prediction methods. As an approximate method for the prediction of speed loss due to added resistance in weather condition (irregular waves and wind), its prediction accuracy is not limited with short wave length. Another advantage of using this method is that it is simple enough to be incorporated

into voyage management procedures and does not require hullform information or other documents that are not easily accessible by ship owners.

Compared to ship speed in calm water conditions, the added resistance caused by weather effect is presented in the form of speed loss ( $\Delta V$ ). This percentage of speed loss is expressed in the following way using Kwon's method for modelling added resistance (Kwon, 2008):

$$\frac{\Delta V}{V_1} 100\% = C_B C_U C_{Form} \quad (6)$$

$$V_2 = V_1 - \left( \frac{\Delta V}{V_1} 100\% \right) \frac{1}{100\%} V_1 = V_1 - (C_B C_U C_{Form}) \frac{1}{100\%} V_1 \quad (7)$$

where,

$V_1$  Design (nominal) operating ship speed in calm water conditions (no wind, no waves), given in m/s.

$V_2$  Ship speed in the selected weather (wind and irregular waves) conditions, given in m/s.

Note:  $V_2 < V_1$ .

$$\Delta V = V_1 - V_2 \quad (8)$$

Speed difference, given in m/s.

$C_B$  Direction reduction coefficient, dependent on the weather direction angle (with respect to the ship's bow) and the Beaufort Number (BN), as shown in Table 6.

$C_U$  Speed reduction coefficient, dependent on the ship's block coefficient  $C_B$ . The loading condition and the Froude Number ( $F_n$ ), as shown in Table 7.

$C_{form}$  Ship form coefficient ( $C_{form}$ ), as shown in Table 8.

**Table 6:** Direction reduction coefficient  $C_R$  due to weather direction (Kwon, 2008)

Weather direction	Direction angle (with respect to the ship's bow) (deg)	Direction reduction coefficient $C_R$
Head sea (irregular waves) and wind	0	$2C_R=2$
Bow sea (irregular waves) and wind	30-60	$2C_R=1.7-0.03*((BN-4)^2)$
Beam sea (irregular waves) and wind	60-150	$2C_R=0.9-0.06*((BN-6)^2)$
Following sea (irregular waves) and wind	150-180	$2C_R=0.4-0.03*((BN-8)^2)$

**Table 7:** Speed reduction coefficient  $C_U$  due to Block coefficient  $C_b$  (Kwon, 2008)

Block coefficient $C_b$	Ship loading conditions	Speed reduction coefficient $C_U$
0.55	normal	$1.7-1.4*Fn-7.4*(Fn^2)$
0.6	normal	$2.2-2.5*Fn-9.7*(Fn^2)$
0.65	normal	$2.6-3.7*Fn-11.6*(Fn^2)$
0.7	normal	$3.1-5.3*Fn-12.4*(Fn^2)$
0.75	loaded or normal	$2.4-10.6*Fn-9.5*(Fn^2)$
0.8	loaded or normal	$2.6-13.1*Fn-15.1*(Fn^2)$
0.85	loaded or normal	$3.1-18.7*Fn+28.0*(Fn^2)$
0.75	ballast	$2.6-12.5*Fn-13.5*(Fn^2)$
0.8	ballast	$3.0-16.3*Fn-21.6*(Fn^2)$
0.85	ballast	$3.4-20.9*Fn+31.8*(Fn^2)$

**Table 8:** Ship form coefficient  $C_{form}$  due to ship categories and loading condition (Kwon, 2008)

Type of (displacement) ship	Ship form coefficient $C_{form}$
All ships(except container ships) in loaded loading condition	$0.5BN+(BN^6.5)/(2.7*(\Delta^{2/3}))$
All ships(except container ships) in ballast loading condition	$0.7BN+(BN^6.5)/(2.7*(\Delta^{2/3}))$
Container ships in normal loading conditions	$0.7BN+(BN^6.5)/(2.2*(\Delta^{2/3}))$

As presented in Table 6, 7 and 8, the prediction of speed loss is determined by direction reduction coefficient, speed reduction coefficient and ship form coefficient.

For direction reduction coefficient, it has been observed that there are four weather directions (depends on encountered angle between sea direction and ship's heading direction) and four corresponding formulae, which are only related to the parameter of BN. In this thesis, there is non-filtered nature of the performance data for the co-directional wind and wave. The wave directions are assumed to be the weather directions.

For speed reduction coefficient, it has been observed that under loaded and normal loading condition, there are 7 block coefficient (0.55 – 0.85) and 7 corresponding formulae; under ballast loading condition, there are 3 block coefficient (0.75 – 0.85) and 3 corresponding formulae. In an overview, these 10 formulae are only related to Froude number.

$$F_n = \frac{V}{\sqrt{gL}} \quad (9)$$

Where

$V$  is ship speed

$L$  is ship length

$g$  is acceleration of gravity

As presented in the Formula above, the Froude number is only related to ship speed while the ship length is fixed for specific ship. Therefore, it can be also assumed that the formulae to calculate speed reduction coefficient is only related to the parameter of speed.

For ship form coefficient, it has been observed that the ship type has been generally grouped into container ships and all ships except container ship. The loading conditions of container ships are always assumed to be in loaded, and there is one corresponding formula, which is related to BN and displacement. For all ships except container ships, there are two loading

conditions and corresponding ship form coefficients, which are related to the parameters of BN and displacement.

As the Kwon's added resistance prediction method (Kwon, 2008) was originally developed based on series 60 hullform, there is a great potential that the existing formulae will not provide very accurate added resistance prediction for modern ship hullform. Besides the hullform issue, the Kwon's added resistance formulae are also developed for a general type of merchant ship, which is not able to provide very accurate prediction for a specific ship. For improving the added resistance prediction accuracy, a semi-empirical added resistance method has been developed, tailor-made for oil tankers and container ships, as presented in Chapter 5.6.1 and 5.8.1

The approach to develop the semi-empirical added resistance prediction method for specific merchant ship includes 3 steps as given below:

- Firstly, the predicted ship operational performance using Kwon's method (Kwon, 2008) is compared with the actual operational data recorded on-board (as referred in Chapter 4.2). During the comparison process, it should be noted that there are two sources may cause the error between the predicted performance and recorded performance:
  - The shortcomings of existing Kwon's added resistance prediction formulae, which is not able to accurately predict the added resistance caused by wave for specific commercial ship.
  - The fouling effect on fuel consumption, which is included in the actual operational data, but not include in the Kwon's added resistance prediction method.

In order to minimize the error caused by fouling effect, the comparison has been carried out during the first 5 months since launching date and the first 5 months after dry-



docking (The fouling effect on fuel consumption during these specific periods are assumed to be ignorable). The statistical analysis of the error between predicted and recorded ship operational performance under different speed, BN and sea direction are carried out.

- Secondly, the formulae to predict direction reduction coefficient, speed reduction coefficient, and ship form coefficient are modified based on the comparison results derived in the first step.

Based on the predicted added resistance using the modified formulae, the corresponding ship operational performance is predicted and compared with the recorded ship operational performance from noon reports. By comparing the error between predicted ship operational performance (using different modified added resistance prediction formulae) and actual recorded field data, the modified empirical added resistance prediction formulae providing minimum error for specific ship type are proposed. In general, the selection process as described above determines which formula needs to be adjusted.

- Thirdly, the semi-empirical added resistance prediction method as referred in step 2 is applied to another ship (the same ship type) to verify its compatibility and improvement in prediction accuracy. The statistical analysis of the error between the corresponding predicted and recorded ship operational performance are carried out.

In summary, the Kwon's method (Kwon, 2008) predicts the involuntary drop in speed due to the effect of weather loading on a displacement type of ship in an empirical way. The modifications of the formulae in original Kwon's method are determined based on the analysis of the actual ship operational performance data. Thus the empirical added resistance prediction method is turned out to be a semi-empirical added resistance prediction method.

Based on the proposed added resistance prediction method, the development and validation of the semi-empirical ship operational performance model for oil tankers and container ships are carried out. The procedures will be illustrated in Section 5.6 – 5.9.

## 5.5 Ship Operational Performance Prediction

Since the ship calm water resistance has been predicted by utilizing Holtrop and Mennen's Method (Holtrop and Mennen, 1982), the relation between calm water speed and total calm water resistance has been extracted, as presented in Figure 19. Under varying calm water speed ( $V_1$ ), the required effective power ( $P_E$ ) to overcome resistance is determined as:

$$P_E = R_{total} * V_1 \quad (10)$$

As the added resistance has been modelled by utilizing Kwon's method (Kwon, 2008), the speed loss under varying Beaufort Number (BN) and encountered angle has been modelled for specific merchant ship. The corresponding original calm water speed ( $V_1$ ) is calculated by summing the actual vessel speed ( $V_2$ ) in a seaway and speed loss ( $\Delta V$ ) due to added resistance.

$$V_1 = V_2 + \Delta V \quad (11)$$

Thus, under specific BN and encountered angle, there is a corresponding original calm water speed ( $V_1$ ) for each actual ship speed ( $V_2$ ). By taking the calm water speed ( $V_1$ ) as the interface parameter between actual ship speed ( $V_2$ ) and required effective power ( $P_E$ ), the relationship between actual ship speed ( $V_2$ ) and required effective power ( $P_E$ ) under each specific BN and encountered angle is determined.

From effective power the required brake power ( $P_B$ ) of main engine is determined as:

$$P_B = P_E / \eta_T \quad (12)$$

Where

$\eta_T$  is the total propulsive efficiency

Based on the Principles of Naval Architecture (SNAME, 1988) the total propulsive efficiency  $\eta_T$  is defined as:

$$\eta_T = \eta_H * \eta_O * \eta_R * \eta_S \quad (13)$$

where,

$\eta_H$  is the hull efficiency

$\eta_O$  is the open water efficiency

$\eta_R$  is the relative rotative efficiency

$\eta_S$  is the shaft efficiency

With the availability of the Speed-Power Curve from the sea trial report, the propulsive efficiency for specific merchant ship can be determined directly and more accurately by dividing engine brake power ( $P_B$ ) from the effective power ( $P_E$ ):

$$\eta_T = P_E / P_B \quad (14)$$

It needs to be noted that the propulsive efficiency also depends on the loading conditions and propellers (Fixed Pitch Propeller/ Controllable Pitch Propeller). In this thesis, the performance data under laden conditions and Fixed Pitch Propeller (FPP) are used. Since the total power transmission efficiency from effective power to brake power has been determined, the relationship between actual ship speed ( $V_2$ ) and required engine brake power ( $P_B$ ) under varying sea states is generated. For each specific ship, the corresponding main engine performance documents contain the expected fuel consumption based on ISO reference conditions, which illustrate the Specific Fuel Oil Consumption (SFOC) with corresponding engine load, engine power and engine speed. The ship main engine Fuel Consumption Rate (FCR) can be determined as:

$$FCR = P_B * SFOC \quad (15)$$

Finally, the ship main engine fuel consumption rate under varying speeds, sea states and wave angle encountered is predicted.

## 5.6 Development of Semi-empirical Ship Operational Performance Model for Oil Tanker

In this section, the development of semi-empirical ship operational performance model for oil tanker is explained. ‘Energy Efficiency of Operation’ (EEO) is defined as the indicator used to illustrate the main engine fuel consumption efficiency and the ship’s operational performance.

$$EEO = \frac{FC}{m_{cargo} \times Distance} \quad (16)$$

where,

$FC$  is the main engine fuel consumption (tonnes), which is generally in 24 hours basis.  $m_{cargo}$  is the mass of cargo carried on-board (tonnes), and  $Distance$  is the distance in nautical miles corresponding to the cargo carried or work done.

An advantage of using the EEO as an indicator is that it contains many of the same elements and could be easily converted to the Energy Efficiency Operational Index (EEOI), which is recommended within the Ship Energy Efficiency Management Plan (SEEMP) (IMO, 2012).

The basic expression for EEOI for a voyage is defined as:

$$EEOI = \frac{\sum_j FC_j \times C_{F_j}}{m_{cargo} \times Distance} \quad (17)$$

where,  $j$  is the fuel type,  $FC_j$  is the mass of consumed fuel  $j$  at one voyage, and  $C_{F_j}$  is the fuel mass to CO<sub>2</sub> mass conversion factor for fuel  $j$ .

For ballast voyage, the cargo onboard is assumed to be zero, which is not able to illustrate the ship operational performance for voyage optimization. In order to use EEO as the energy efficiency indicator, this thesis will focus on the loading condition of laden. The development

procedures of the semi-empirical ship operational performance model for oil tanker will be clarified in the following sections.

### 5.6.1 Development of semi-empirical added resistance prediction method for oil tanker

Based on the approach to develop the semi-empirical added resistance method as described in Chapter 5.4, the development of semi-empirical added resistance method for oil tanker includes the following steps:

Firstly, based on the recorded ship voyage conditions and sea states in ship daily reports of Suezmax Oil Tanker A, the predicted EEO using the empirical added resistance prediction formulae from the Kwon’s method (Kwon, 2008) was compared to the corresponding recorded EEO, as presented in Figure 19.

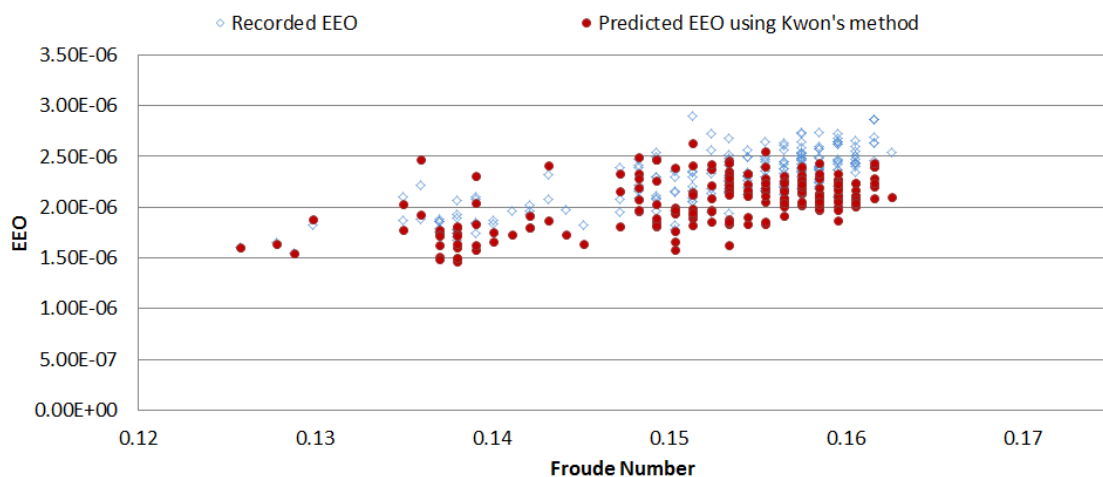


Figure 19: Overview of the comparison between the predicted EEO using original Kwon’s method and recorded EEO

From Figure 19, it has been observed that there is a big difference between the recorded EEO and predicted EEO using Kwon’s method. The statistical analysis of the error between the predicted EEO and recorded EEO has been carried out. The results (Table 13) indicate that average absolute error is 11.08%. The coefficient of determination ( $R^2$ ), which is a statistical

measure to indicate how close the predicted ship operational performance fit the recorded ship operational performance, is 82.3%.

As referred in Chapter 5.4, the shortcoming of Kwon’s empirical added resistance prediction formulae and the effect of fouling are the two major sources of the error. In order to focus on the improvement of the added resistance prediction formulae for specific ship, the error caused by the effect of fouling needs to be excluded from the total error. During the first 5 months since launching, the effect of fouling is assumed to be minimum and ignorable. In order to verify this assumption, the error between recorded EEO and predicted EEO using sea trial has been studied in time manner, as presented in Figure 20. This comparison was carried out under low BN and similar speed to exclude the error caused by weather and speed.

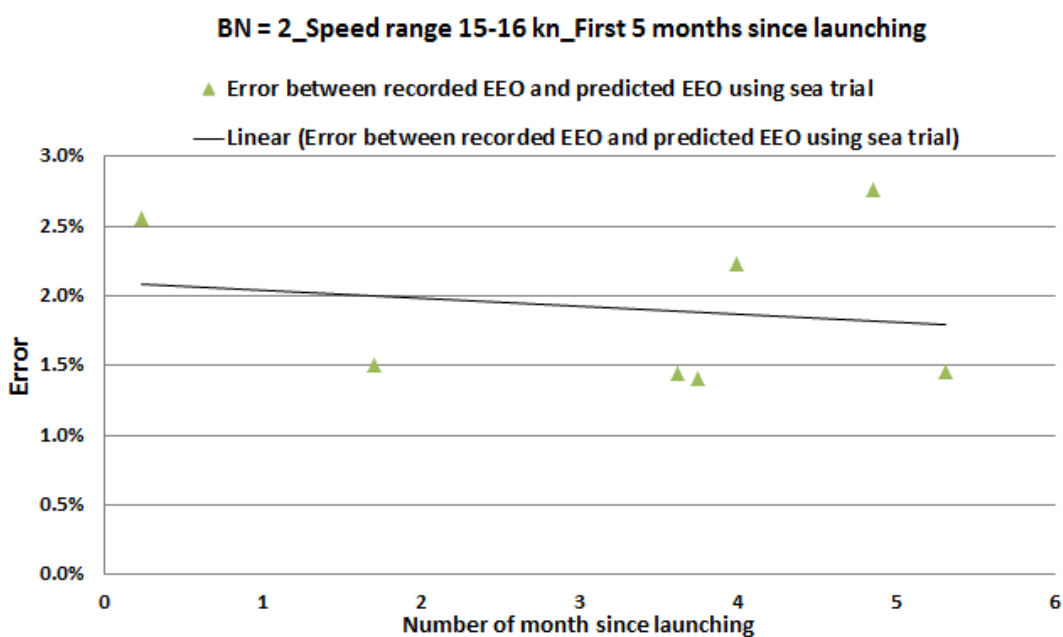


Figure 20: Time-dependent error between recorded EEO and predicted EEO using sea trial

In Figure 20, the error indicates the fouling effect on fuel consumption efficiency. It has been observed that the trend of this error is not obviously increasing, which verified the assumption above: ‘During the first 5 months since launching, there is no time-dependent added resistance increase due to fouling, the effect of fouling is ignorable’.

Therefore, the predicted EEO using the empirical added resistance prediction formulae from the Kwon's method (Kwon, 2008) was compared to the corresponding recorded EEO during the first 5 months since launching, as presented in Figure 21.

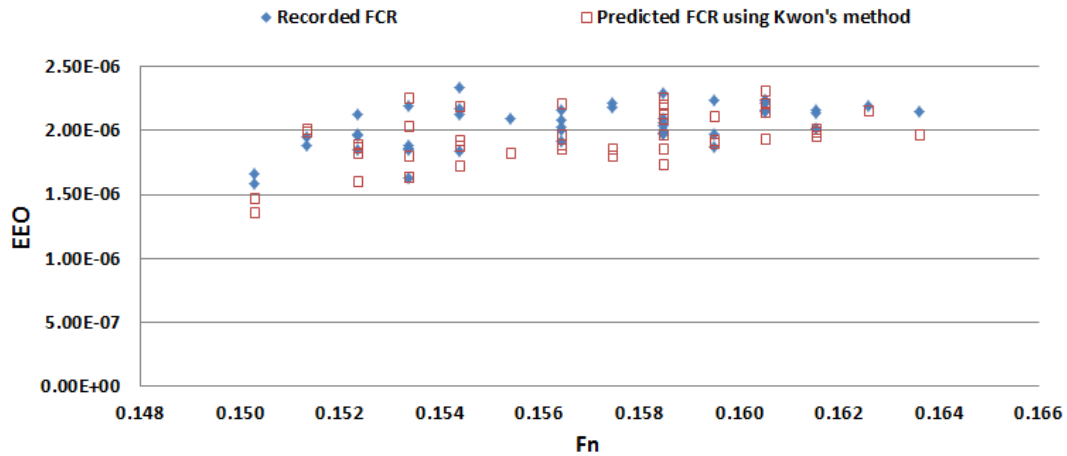


Figure 21: Comparison between the predicted EEO using original Kwon's method and recorded EEO during the first 5 months since launching

From Figure 21, it has been observed that the predicted EEO using Kwon's added resistance prediction method is commonly smaller than the recorded EEO (actual ship operational performance). The average absolute error between the predicted EEO and recorded EEO is 7.41%. It has been also noted that the error between them is not directly related to Froude number. Thus the formula to calculate speed reduction coefficient  $C_U$  (as the speed reduction coefficient is only related to the parameter of Froude number) should not be modified. The formulae to predict direction reduction coefficient and ship form coefficient may either or both need to be modified.

Secondly, in order to determine which empirical formula (determining direction reduction coefficient and ship form coefficient in Kwon's method) needs to be adjusted for Suezmax Oil Tanker A, the predicted EEO using Original Kwon's method (Kwon, 2008) under each BN and each wave angle encountered has been compared to the corresponding recorded EEO. The comparison results under BN = 2, BN = 3, and BN = 4 are presented in Figure 22, Figure

23, and Figure 24 respectively. The comparison results under Head Sea, Bow Sea, Beam Sea and Following Sea are presented in Figure 25, Figure 26, Figure 27, and Figure 28 respectively.

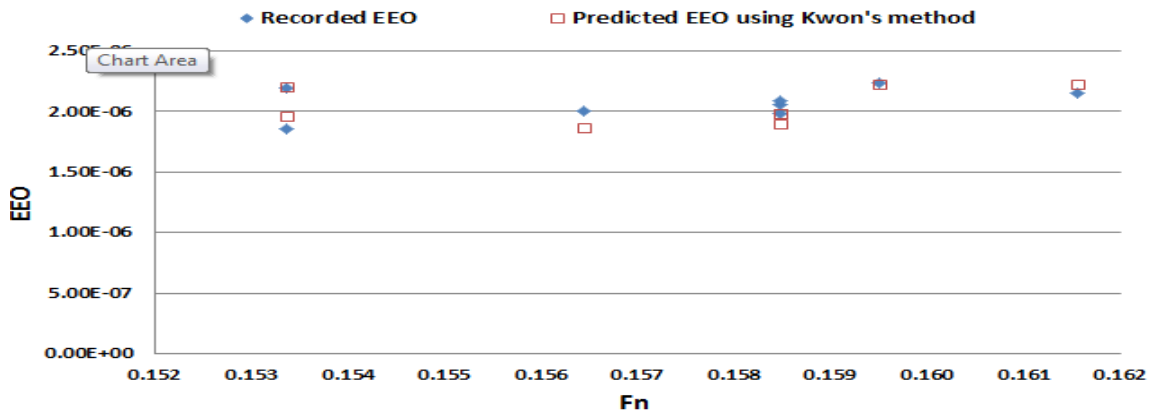


Figure 22: Comparison between the predicted EEO using original Kwon's method and recorded EEO during the first 5 months since launching under BN = 2

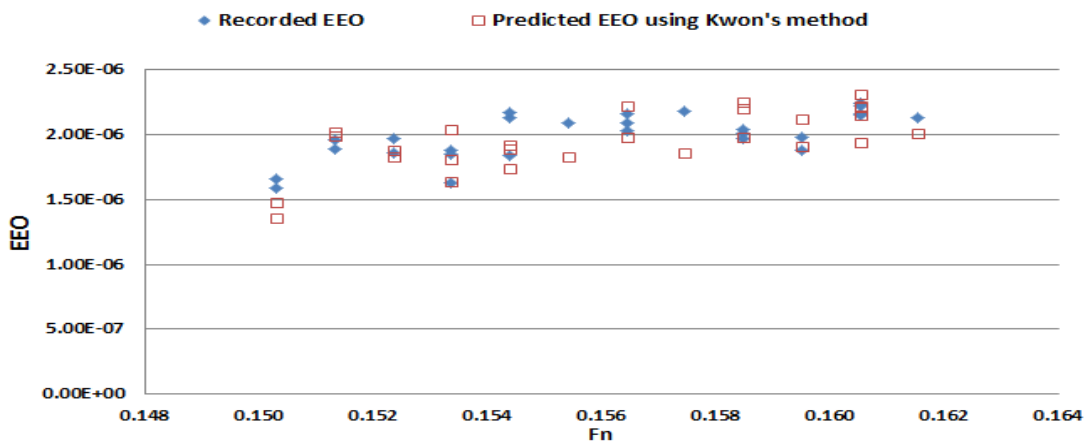


Figure 23: Comparison between the predicted EEO using original Kwon's method and recorded EEO during the first 5 months since launching under BN = 3



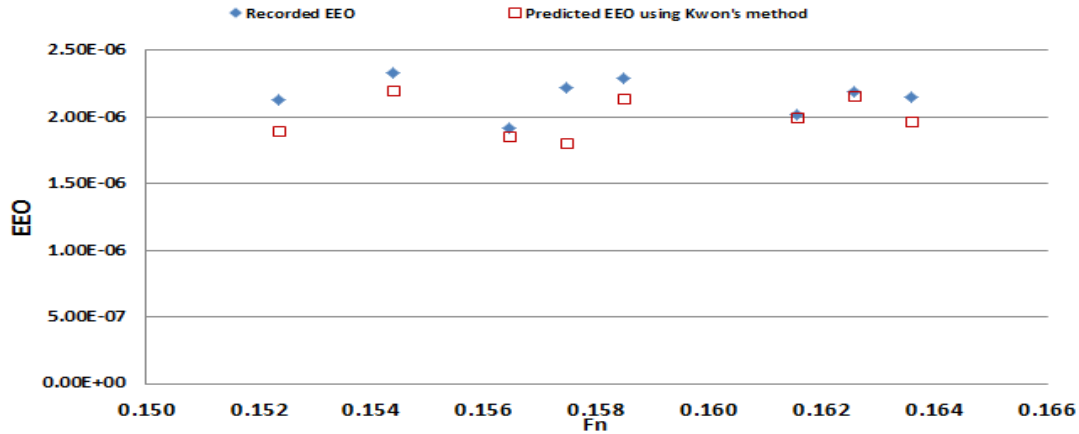


Figure 24: Comparison between the predicted EEO using original Kwon's method and recorded EEO during the first 5 months since launching under BN = 4

As presented in Figure 22, Figure 23, and Figure 24, the average absolute error under BN= 2, BN=3, BN=4 are 1.92%, 6.82%, 7.14%. The results indicate that the average error increase with BN. Under each BN, there are some points indicating that the predicted EEO is much lower than the recorded EEO (such as  $F_n = 0.1565$  in Figure 22,  $F_n = 0.150, 0.155$  and  $0.157$  in Figure 23,  $F_n = 0.152$  and  $0.157$  in Figure 24). By studying the corresponding noon reports of these points, it has been noted that their strongest BN ( $BN_{strongest}$ ) is bigger than their average BN ( $BN_{Average}$ ), while the Kwon's added resistance prediction formulae only include the average BN. Therefore, it can be concluded that both strongest BN and average BN should be included in the empirical added resistance prediction formulae, the BN related formulae to calculate direction reduction coefficient and ship form coefficient both need to be improved.

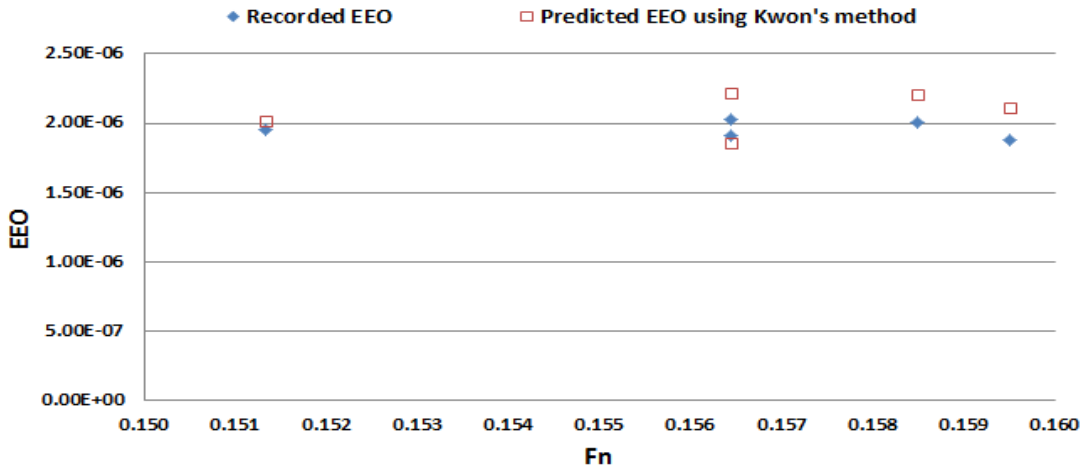


Figure 25: Comparison between the predicted EEO using original Kwon's method and recorded EEO during the first 5 months since launching in Head Sea

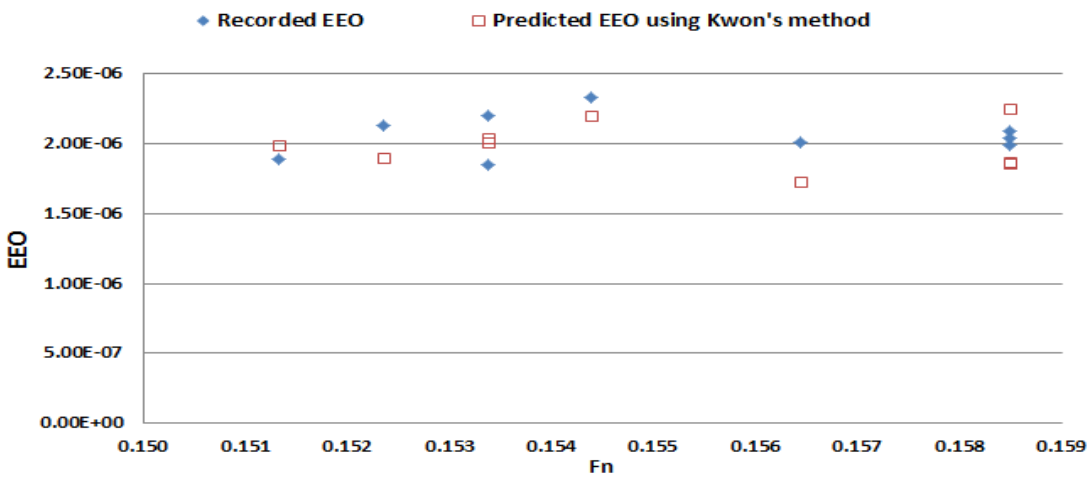


Figure 26: Comparison between the predicted EEO using original Kwon's method and recorded EEO during the first 5 months since launching in Bow Sea

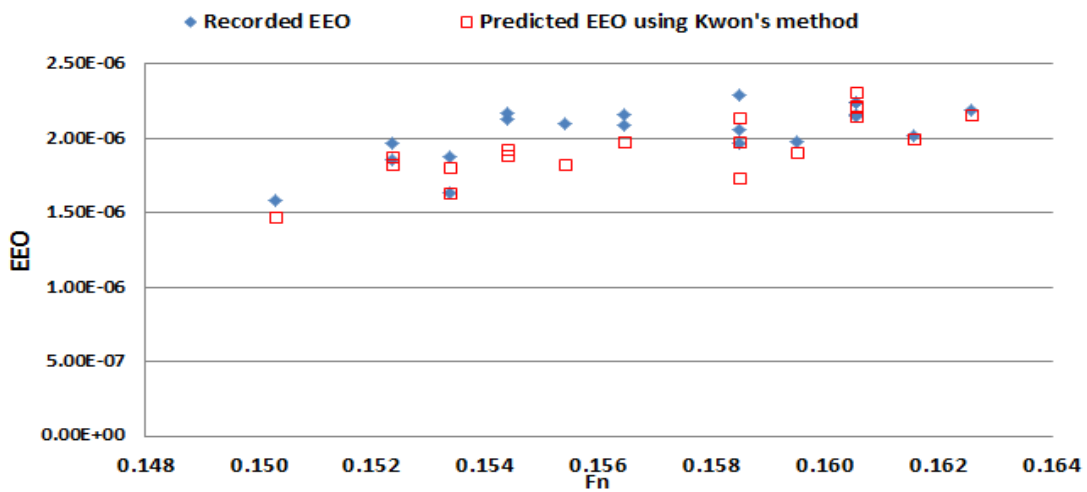


Figure 27: Comparison between the predicted EEO using original Kwon's method and recorded EEO during the first 5 months since launching in Beam Sea

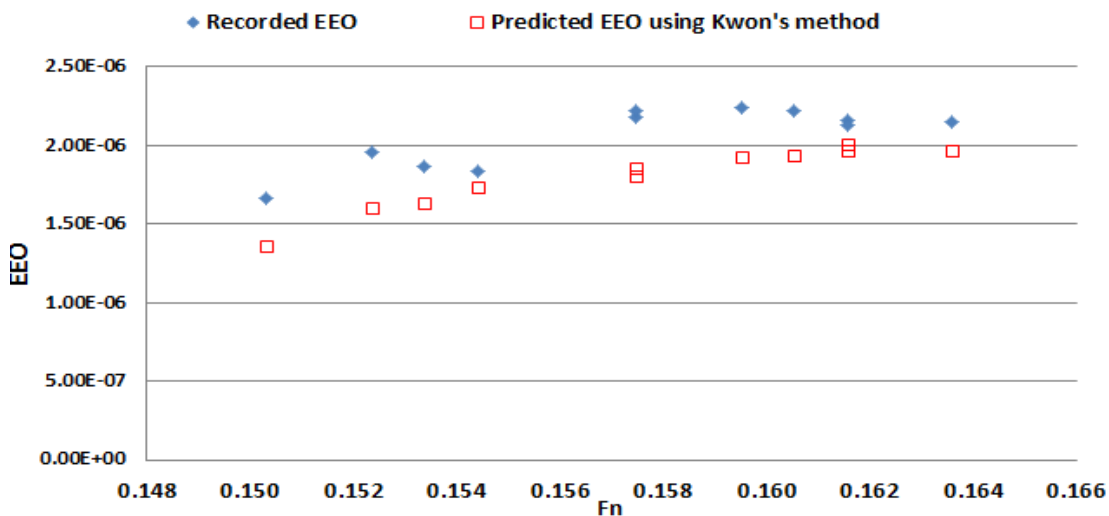


Figure 28: Comparison between the predicted EEO using original Kwon's method and recorded EEO during the first 5 months since launching in Following Sea

As presented in Figure 25, Figure 26, Figure 27, and Figure 28, the average absolute error under Head Sea, Bow Sea, Beam Sea and Following Sea are 6.54%, 8.05%, 5.26%, and 12.16%. The results indicate that the error between the recorded EEO and predicted EEO using Kwon's added resistance prediction formulae is rather different in different wave angle encountered, especially in following sea. Besides the error caused by the exclusion of strongest BN, it has been identified that error also comes from the formulae to calculate direction reduction coefficient.

Based on the observations and conclusions drawn in the second step, the modifications of the formulae to calculate ship form coefficient are presented in Table 9. The variation of each coefficient is used to test the sensitivity of the coefficients. The average absolute error between the predicted EEO and the recorded EEO during the first 5 months since launching are compared as following.

**Table 9: Modifications of the formula to calculate ship form coefficient**

Loading condition	Name	Ship form coefficient	Average absolute error
Laden	Original	$0.5BN + BN^{6.5} / (2.7 * (\Delta^{2/3}))$	7.41%
	Modification1	$0.5 * \frac{BN_{Strongest} + BN_{Average}}{2} + (\frac{BN_{Strongest} + BN_{Average}}{2})^{6.5} / (2.7 * (\Delta^{2/3}))$	6.63%
	Modification2	$0.45 * \frac{BN_{Strongest} + BN_{Average}}{2} + (\frac{BN_{Strongest} + BN_{Average}}{2})^{6.5} / (2.7 * (\Delta^{2/3}))$	6.87%
	<b>Modification3</b>	$0.55 * \frac{BN_{Strongest} + BN_{Average}}{2} + (\frac{BN_{Strongest} + BN_{Average}}{2})^{6.5} / (2.7 * (\Delta^{2/3}))$	6.37%
	Modification4	$0.6 * \frac{BN_{Strongest} + BN_{Average}}{2} + (\frac{BN_{Strongest} + BN_{Average}}{2})^{6.5} / (2.7 * (\Delta^{2/3}))$	6.58%
	Modification5	$0.5 * \frac{BN_{Strongest} + BN_{Average}}{2} + (\frac{BN_{Strongest} + BN_{Average}}{2})^7 / (2.7 * (\Delta^{2/3}))$	6.76%
	Modification6	$0.5 * \frac{BN_{Strongest} + BN_{Average}}{2} + (\frac{BN_{Strongest} + BN_{Average}}{2})^6 / (2.7 * (\Delta^{2/3}))$	6.81%
	Modification7	$0.5 * \frac{BN_{Strongest} + BN_{Average}}{2} + (\frac{BN_{Strongest} + BN_{Average}}{2})^{6.5} / (2.2 * (\Delta^{2/3}))$	6.64%
	Modification8	$0.5 * \frac{BN_{Strongest} + BN_{Average}}{2} + (\frac{BN_{Strongest} + BN_{Average}}{2})^{6.5} / (3.2 * (\Delta^{2/3}))$	6.74%

From Table 9, it has been observed that the first coefficient in the ship form coefficient formula has the strongest sensitivity in determining the average absolute error. The Modification 3 is providing the minimum average absolute error 6.37%. Compared to Modification1, the modifications of other coefficients (Modification 5-8) are not able to reduce the average absolute error. Therefore, the semi-empirical formulae to calculate ship form coefficient for oil tanker is determined, as presented in Table 10.

**Table 10: Ship form coefficient  $C_{form}$  due to ship categories and loading condition for Suezmax oil tanker**

Type of ship	Ship form coefficient $C_{form}$	
	modified	original
Suez-Max oil tanker in laden condition	$0.55 * \frac{BN_{Strongest} + BN_{Average}}{2} + (\frac{BN_{Strongest} + BN_{Average}}{2})^{6.5} / (2.7 * (\Delta^{2/3}))$	$0.5BN + BN^{6.5} / (2.7 * (\Delta^{2/3}))$

According to the proposed formulae to calculate ship form coefficient as described above, the modifications of the formulae to calculate direction reduction coefficient are then carried out,

the corresponding average absolute error of each combination of modifications during the first 5 months since launching is compared, as presented in Table 11. The modified formulae providing minimum average absolute error are selected as the proposed semi-empirical formulae to calculate direction reduction coefficient for Suezmax Oil Tanker A.

**Table 11: Modifications of the formulae to calculate direction reduction coefficient**

Weather direction	Name	Direction reduction coefficient	Average absolute error
Head Sea	Original	$2C_{\beta} = 2.0$	6.37%
	Modification 9	$2C_{\beta} = 1.9$	6.64%
	<b>Modification 10</b>	$2C_{\beta} = 1.8$	6.13%
	Modification 11	$2C_{\beta} = 1.7$	6.45%
Bow Sea	Original	$2C_{\beta} = 1.7 - 0.03 * (BN - 4)^2$	6.37%
	Modification 12	$2C_{\beta} = 1.7 - 0.03 * (\frac{BN_{Strongest} + BN_{Average}}{2} - 4)^2$	6.21%
	<b>Modification 13</b>	$2C_{\beta} = 1.6 - 0.03 * (\frac{BN_{Strongest} + BN_{Average}}{2} - 4)^2$	6.15%
	Modification 14	$2C_{\beta} = 1.5 - 0.03 * (\frac{BN_{Strongest} + BN_{Average}}{2} - 4)^2$	6.32%
	Modification 15	$2C_{\beta} = 1.7 - 0.02 * (\frac{BN_{Strongest} + BN_{Average}}{2} - 4)^2$	6.43%
	Modification 16	$2C_{\beta} = 1.7 - 0.04 * (\frac{BN_{Strongest} + BN_{Average}}{2} - 4)^2$	6.37%
	Modification 17	$2C_{\beta} = 1.7 - 0.03 * (\frac{BN_{Strongest} + BN_{Average}}{2} - 3.5)^2$	6.27%
	Modification 18	$2C_{\beta} = 1.7 - 0.03 * (\frac{BN_{Strongest} + BN_{Average}}{2} - 4.5)^2$	6.29%
Beam Sea	Original	$2C_{\beta} = 0.9 - 0.06 * (BN - 6)^2$	6.37%
	Modification 19	$2C_{\beta} = 0.9 - 0.06 * (\frac{BN_{Strongest} + BN_{Average}}{2} - 6)^2$	6.24%
	Modification 20	$2C_{\beta} = 1.0 - 0.06 * (\frac{BN_{Strongest} + BN_{Average}}{2} - 6)^2$	6.17%
	<b>Modification 21</b>	$2C_{\beta} = 1.1 - 0.06 * (\frac{BN_{Strongest} + BN_{Average}}{2} - 6)^2$	6.06%
	Modification 22	$2C_{\beta} = 1.2 - 0.06 * (\frac{BN_{Strongest} + BN_{Average}}{2} - 6)^2$	6.09%
	Modification 23	$2C_{\beta} = 0.9 - 0.05 * (\frac{BN_{Strongest} + BN_{Average}}{2} - 6)^2$	6.43%
	Modification 24	$2C_{\beta} = 0.9 - 0.07 * (\frac{BN_{Strongest} + BN_{Average}}{2} - 6)^2$	6.34%
	Modification 25	$2C_{\beta} = 0.9 - 0.06 * (\frac{BN_{Strongest} + BN_{Average}}{2} - 5.5)^2$	6.29%
	Modification 26	$2C_{\beta} = 0.9 - 0.06 * (\frac{BN_{Strongest} + BN_{Average}}{2} - 6.5)^2$	6.32%
Following Sea	Original	$2C_{\beta} = 0.4 - 0.03 * (BN - 8)^2$	6.37%
	Modification 27	$2C_{\beta} = 0.4 - 0.03 * (\frac{BN_{Strongest} + BN_{Average}}{2} - 8)^2$	5.92%
	Modification 28	$2C_{\beta} = 0.5 - 0.03 * (\frac{BN_{Strongest} + BN_{Average}}{2} - 8)^2$	5.87%
	<b>Modification 29</b>	$2C_{\beta} = 0.6 - 0.03 * (\frac{BN_{Strongest} + BN_{Average}}{2} - 8)^2$	5.51%
	Modification 30	$2C_{\beta} = 0.7 - 0.03 * (\frac{BN_{Strongest} + BN_{Average}}{2} - 8)^2$	5.88%
	Modification 31	$2C_{\beta} = 0.4 - 0.02 * (\frac{BN_{Strongest} + BN_{Average}}{2} - 8)^2$	6.07%
	Modification 32	$2C_{\beta} = 0.4 - 0.04 * (\frac{BN_{Strongest} + BN_{Average}}{2} - 8)^2$	6.18%
	Modification 33	$2C_{\beta} = 0.4 - 0.03 * (\frac{BN_{Strongest} + BN_{Average}}{2} - 7.5)^2$	6.03%
	Modification 34	$2C_{\beta} = 0.4 - 0.03 * (\frac{BN_{Strongest} + BN_{Average}}{2} - 8.5)^2$	6.05%

Based on the comparison results presented in Table 11, it has been observed that the Modification 10 in Head Sea, Modification 13 in Bow Sea, Modification 21 in Beam Sea, and Modification 29 in Following Sea are providing the minimum average absolute error in each weather direction. Therefore, the semi-empirical formulae to calculate direction reduction coefficient for oil tanker have been determined, as presented in Table 12.

**Table 12:** Direction reduction coefficient  $C_{\beta}$  due to weather direction for Suezmax oil tanker

Weather direction	Encounter angle (with respect to the ship's bow) (deg)	Direction reduction coefficient	
		Proposed semi-empirical formula	Original Kwon's formula
Head Sea	0-30	$2C_{\beta} = 1.8$	$2C_{\beta} = 2.0$
Bow Sea	30-60	$2C_{\beta} = 1.6 - 0.03 * \left( \frac{BN_{Strongest} + BN_{Average}}{2} - 4 \right)^2$	$2C_{\beta} = 1.7 - 0.03 * (BN - 4)^2$
Beam Sea	60-150	$2C_{\beta} = 1.1 - 0.06 * \left( \frac{BN_{Strongest} + BN_{Average}}{2} - 6 \right)^2$	$2C_{\beta} = 0.9 - 0.06 * (BN - 6)^2$
Following Sea	150-180	$2C_{\beta} = 0.6 - 0.03 * \left( \frac{BN_{Strongest} + BN_{Average}}{2} - 8 \right)^2$	$2C_{\beta} = 0.4 - 0.03 * (BN - 8)^2$

In the second step, based on the study of error between predicted EEO using empirical Kwon's added resistance prediction method and recorded EEO from field data under each specific BN and weather direction, a semi-empirical added resistance prediction method for Suezmax oil tanker, as presented in Table 10 and Table 12, has been proposed by adjusting the direction reduction coefficient  $C_{\beta}$  and ship form coefficient  $C_{form}$ .

By utilizing the proposed semi-empirical formulae, the predicted EEO has been compared to the recorded EEO during the first 5 months since launching, as presented in Figure 29.

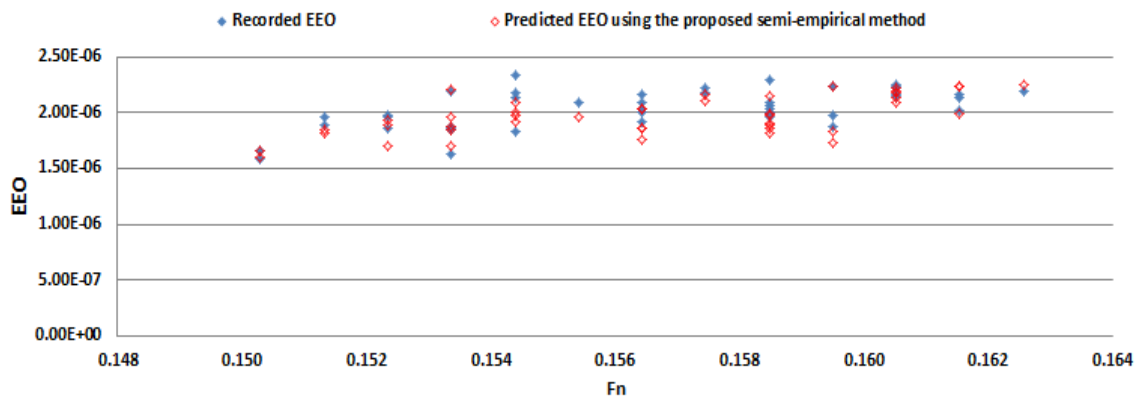


**Figure 29:** Comparison between the predicted EEO using the proposed semi-empirical method and recorded EEO

During the first 5 months since launching, the statistical analysis of the error (between the predicted EEO and recorded EEO) has been carried out. Compared to the Kwon's added resistance prediction method, the average absolute error reduces from 7.41% to 3.93% by utilizing the proposed semi-empirical added resistance prediction method. Considering the uncertainty of actual operational data (referred in Chapter 4.2), the error of 3.93% indicates that the proposed semi-empirical added resistance prediction formulae provides a good prediction of the added resistance caused by wave for Suezmax oil tanker.

Thirdly, the proposed semi-empirical added resistance prediction method is applied along all available daily ship performance reports, as presented in Figure 30.

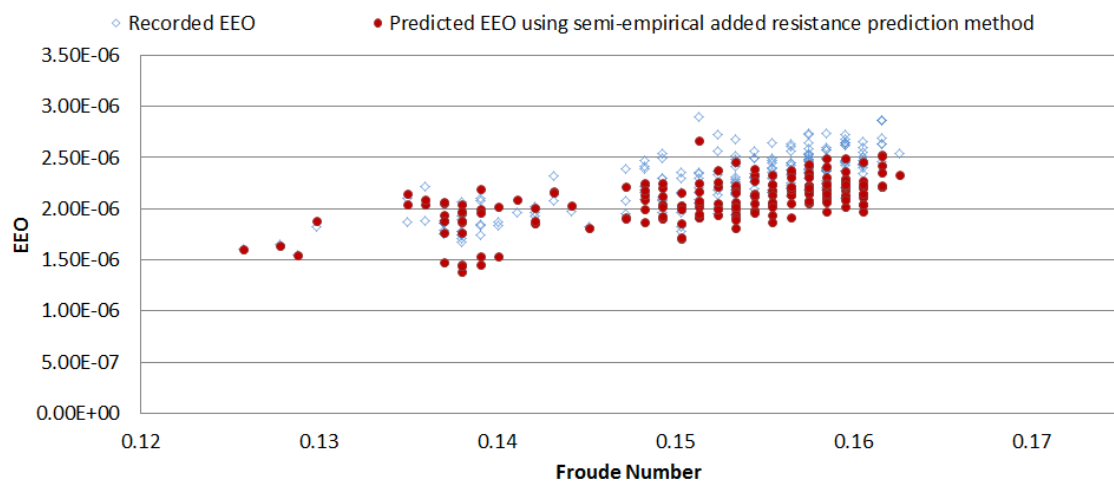


**Figure 30:** Overview of the comparison between the predicted EEO using the semi-empirical added resistance prediction method and recorded EEO

By comparing Figure 21 and Figure 30, it has also been observed that the predicted EEO using the proposed semi-empirical added resistance prediction method is better matching the corresponding recorded EEO. In order to include the fouling effect, the error between the predicted EEO using the semi-empirical method and recorded EEO is then investigated in time-dependent manner, as illustrated in the following section.

### 5.6.2 Integrating the time-dependent correction for oil tanker

Since the ship hull and propeller fouling, main engine performance degradation, and hull surface/propeller damage are not taken into account within the semi-empirical added resistance prediction model, these factors, especially the fouling effect are likely to be the source of error causing the predicted EEO to be lower compared to the corresponding recorded EEO. This error in prediction can be taken as the increase in fuel consumption in percentage, which is known to increase over time since ship launch date and dry-docking. Therefore, the error between recorded EEO and predicted EEO using the semi-empirical added resistance prediction method for Suezmax oil tanker has been investigated in time-dependant manner, as presented in Figure 31. The correction factors are derived from the trend lines.

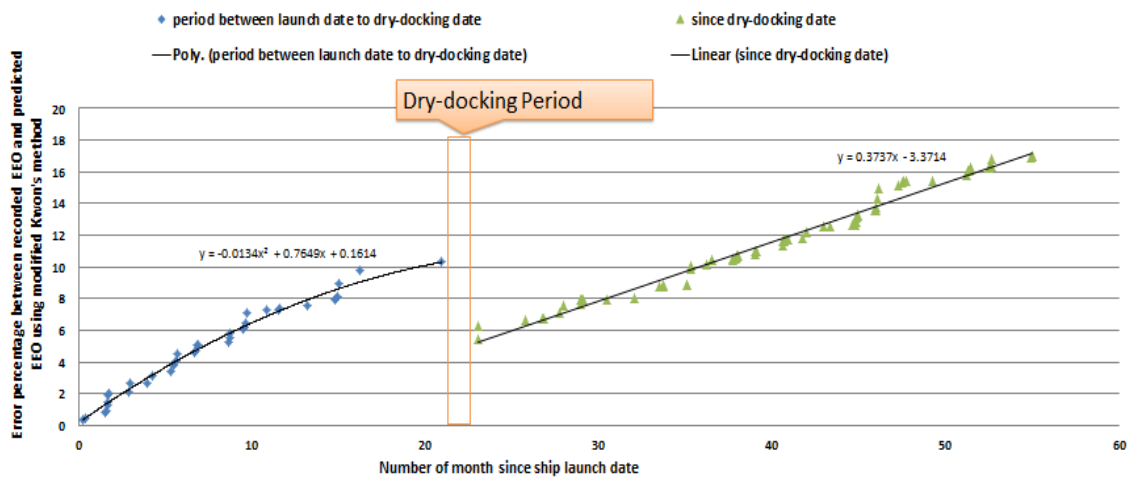


Figure 31: Error between predicted EEO and recorded one since ship launch date for Suezmax Oil Tanker A

As presented in Figure 31, from the launch date to the 21<sup>st</sup> service month of Suezmax oil tanker A, the fuel consumption due to fouling effect is increased with 0.53% per month. After dry-docking, the error caused by fouling increases with 0.44% per month.

By integrating the correction factor withdrawn from Figure 31, the updated predicted EEO using the semi-empirical added resistance prediction method for Suezmax oil tanker was



compared to the corresponding recorded EEO again. The overview of the comparison is presented in Figure 32.

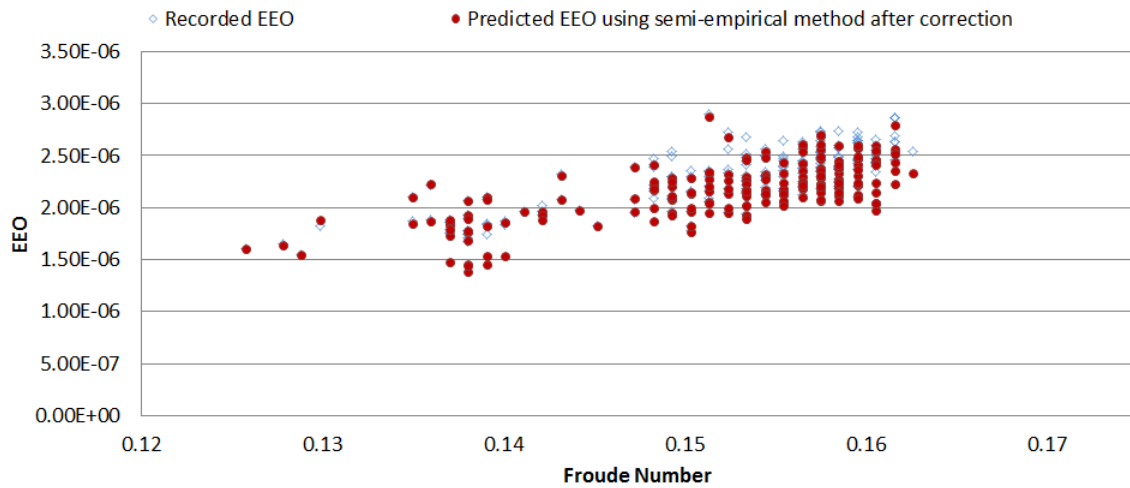


**Figure 32:** Overview of the comparison between the predicted EEO using the semi-empirical added resistance prediction method after time-dependent correction and recorded EEO

The statistical analysis of the error between the recorded EEO and predicted EEO using the semi-empirical added resistance prediction method after the correction has been carried out, as presented in Table 13.

**Table 13:** Statistical analysis of the error between recorded EEO and predicted EEO for Oil Tanker A

Statistical analysis of the error between recorded EEO and predicted EEO for Oil Tanker A			
Modelling method for predicted EEO	Empirical method	Semi-empirical method	Semi-empirical method with correction
Sample time duration (No. of months)	55	55	55
Sample size (No. of daily reports)	243	243	243
Average absolute Error	11.08%	9.00%	4.60%
Coefficient of determination ( $R^2$ )	82.3%	84.7%	91.3%

The same sample of operational data for Oil Tanker A has been used to compare each of the method so that a direct comparison of prediction accuracy can be included. The average absolute error is used to illustrate the prediction accuracy; the coefficient of determination ( $R^2$ ) is a statistical measure to indicate how close the predicted ship operational performance fit the recorded one, the higher  $R^2$  represents the better model matches the recorded ship

operational performance data. From Table 13 it can be observed that the semi-empirical added resistance prediction method improves the prediction accuracy compared to the empirical Kwon's added resistance prediction method, the average absolute error decreased from 11.08% to 9.00%, and the coefficient of determination ( $R^2$ ) increased from 82.3% to 84.7%. Especially after the time-dependant correction, the average absolute error further drops to 4.60% and the  $R^2$  value reaches to 91.3%.

In summary, within the development of semi-empirical ship operational performance model for oil tanker, the semi-empirical added resistance prediction method for oil tanker has been proposed. The comparison between recorded EEO and predicted EEO using Kwon's method, the semi-empirical added resistance prediction method and the semi-empirical added resistance prediction method with time-dependent correction have been carried out. Based on the statistical analysis, it has been observed that the semi-empirical added resistance prediction method for Suezmax oil tanker can provide more accurate ship operational performance prediction compared to original empirical method, and the integration of the time-dependent correction can further improve the prediction accuracy.

As the semi-empirical ship operational performance model for oil tanker was developed based on Suezmax Oil Tanker A, then a question comes out:

*'Whether the proposed semi-empirical model for Suezmax oil tanker is also compatible to other oil tanker size classification?'*

Therefore, a validation study by applying the proposed semi-empirical model on Aframax Oil Tanker B has been carried out to answer this question in the following section.

## 5.7 Validation of Semi-empirical Ship Operational Performance Model for Oil Tanker

As described in Chapter 5.6, the semi-empirical ship operational performance prediction model for oil tanker has been developed. In this section, the proposed method will be applied on another oil tanker – Aframax Oil Tanker B. The improvement of the performance prediction accuracy will be assessed to validate the suitability of the proposed semi-empirical method for oil tanker.

Firstly, before applying the proposed semi-empirical model on Aframax Oil Tanker B, the predicted EEO using the empirical Kwon’s added resistance prediction method (Kwon, 2008) was compared to the corresponding recorded EEO. The overview of the comparison is listed in Figure 33. The statistical analysis of the error between the predicted EEO and recorded EEO has been carried out. The results (Table 15) indicate that average absolute error is 12.56%. The coefficient of determination ( $R^2$ ) is 83.9%.

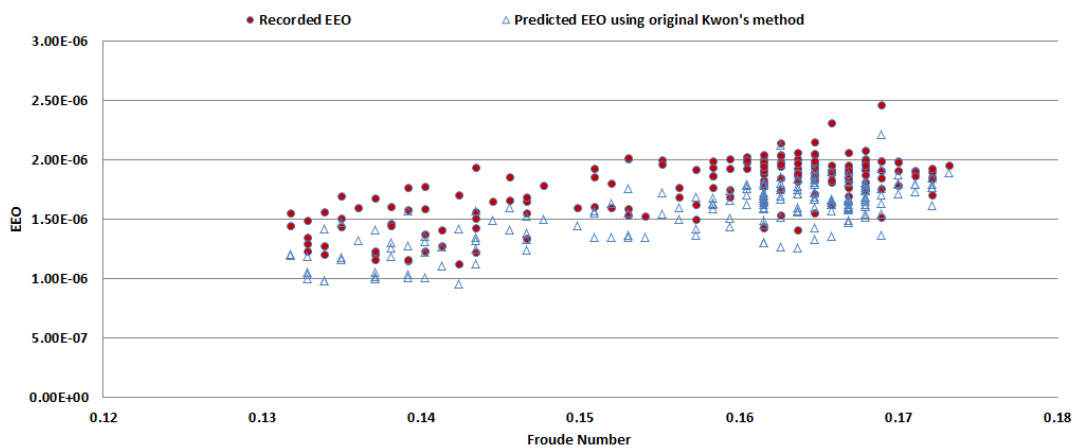
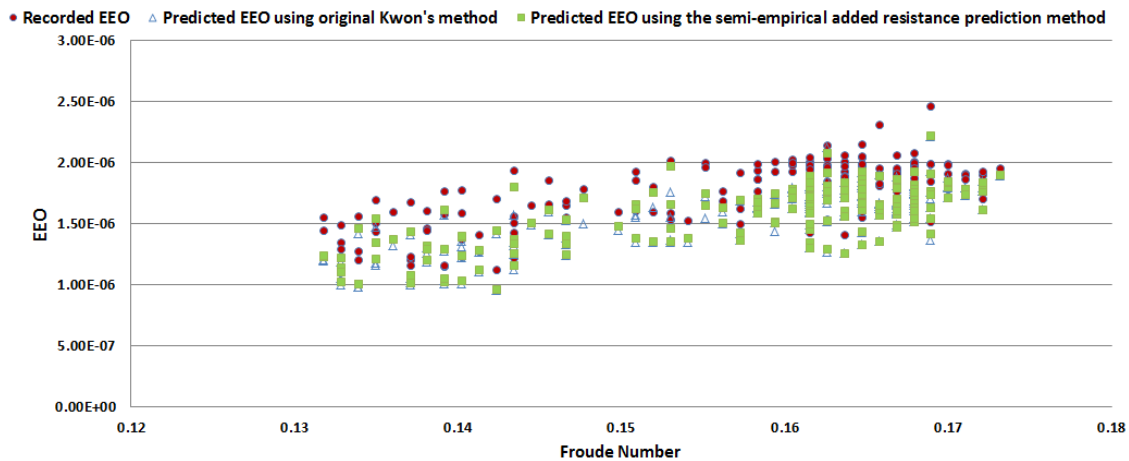


Figure 33: Overview of the comparison between the predicted EEO using original Kwon’s method and recorded EEO

Secondly, the predicted EEO using the proposed semi-empirical added resistance prediction method was compared to the corresponding recorded EEO. Together with the predicted EEO using original Kwon's method, the overview of the comparison is presented in Figure 34.



**Figure 34:** Overview of the comparison between the predicted EEO using the semi-empirical added resistance prediction method, the predicted EEO using original Kwon's method and recorded EEO

As presented in Figure 34, it has been observed that the predicted EEO by utilizing the proposed semi-empirical method for oil tanker has a better matching the corresponding recorded EEO. Based on the statistical analysis results (Table 15), compared to original empirical method, the average absolute error between the predicted EEO and recorded EEO is reduced from 12.56% to 10.83%, which indicates the increased ship operational performance prediction accuracy by utilizing the proposed semi-empirical added resistance prediction method for oil tanker; The coefficient of determination ( $R^2$ ) is increased from 83.9% to 84.6%, which indicates a better match between predicted EEO and recorded EEO by utilizing the semi-empirical added resistance prediction method. Therefore, it can be concluded that the semi-empirical added resistance prediction method developed based on Suezmax Oil Tanker A is also compatible to Aframax Oil Tanker B.

Thirdly, the error percentage between recorded EEO and predicted EEO using the semi-empirical added resistance method was studied in time-dependent manner. The time-dependant correction is derived and presented in Figure 35.

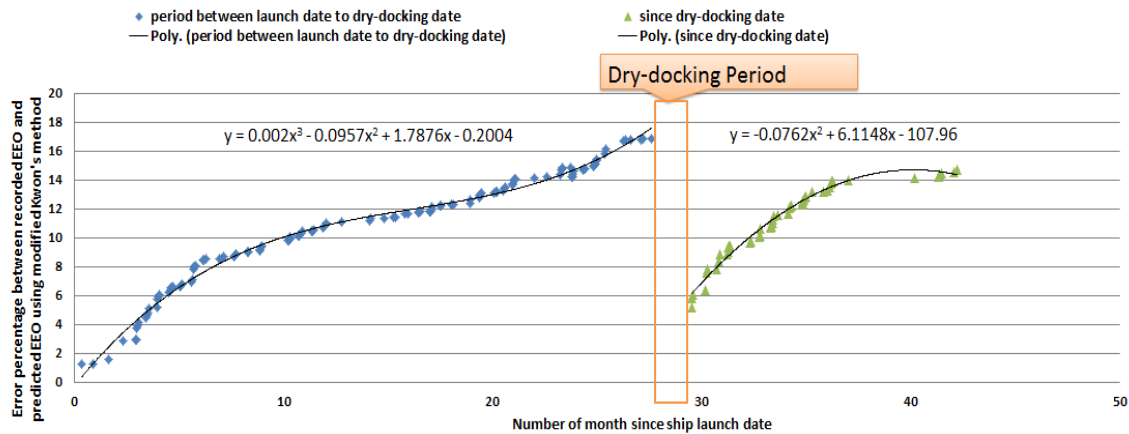


Figure 35: Error between predicted EEO and recorded one since ship launch date for Aframax Oil Tanker B

As presented in Figure 35, the fuel consumption due to fouling effect stays relatively low from the ship launch date to the fourth months, and increases sharply with 0.7% per month until the 12<sup>th</sup> month, then increases slowly with 0.5% per month between the 13<sup>th</sup> month and 27<sup>th</sup> month. On average, from the ship launch date to the 27<sup>th</sup> month, the fuel consumption due to fouling effect is increased with 0.63% per month. After the dry-docking, the fuel consumption due to fouling effect increases with 0.75% per month on average.

For Suezmax Oil Tanker A and Aframax Oil Tanker B, the average increasing energy consumption rates due to fouling effect are compared in Table 14.

Table 14: Increasing energy consumption rate for Oil Tanker A and Oil Tanker B

	Before dry-docking	After dry-docking
Suezmax Oil Tanker A	0.53% per month	0.44% per month
Aframax Oil Tanker B	0.63% per month	0.75% per month

From Table 14, it has been observed that the increasing rates from launch date to the first dry-docking for Suezmax Oil Tanker A and Aframax Oil Tanker B are relatively similar. After the dry-docking, the increasing energy consumption rate for Suezmax Oil Tanker A is 0.44%

per month, which indicates a better performed anti-fouling painting has been applied to Oil Tanker A during dry-docking; the increasing energy consumption rate for Aframax Oil Tanker B is 0.75% per month (higher than 0.63% per month before dry-docking), which might be caused by the hull surface damage or the less effective anti-fouling painting has been applied to Oil Tanker B during dry-docking. The sources of the variation (before and after dry-docking) will be further clarified in Chapter 5.10.

Fourthly, after the time-dependent correction, the updated predicted EEO was compared to the corresponding recorded EEO. The overview of the comparison is listed in Figure 36.

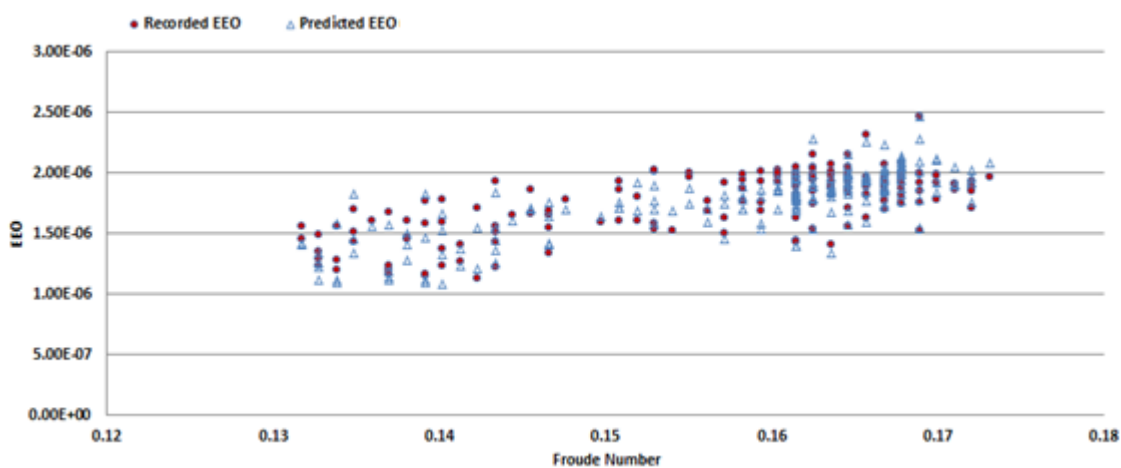


Figure 36: Overview of the comparison between the predicted EEO using the semi-empirical added resistance prediction method after time-dependent correction and recorded EEO

By comparing Figure 34 and Figure 36, it has been observed that there is an obvious improvement of prediction accuracy by including the time-dependent correction. The statistical analysis of the average absolute error between the predicted EEO using the semi-empirical method with correction and recorded EEO has been carried out and presented in Table 15.

**Table 15:** Statistical analysis of the error between recorded EEO and predicted EEO for Oil Tanker B

Statistical analysis of the error between recorded EEO and predicted EEO for Oil Tanker B			
Modelling method for predicted EEO	Empirical method	Semi-empirical method	Semi-empirical method with correction
Sample time duration (No. of months)	42	42	42
Sample size (No. of daily reports)	189	189	189
Average absolute Error	12.56%	10.83%	4.3%
R <sup>2</sup>	83.9%	84.6%	88.7%

As presented in Table 15, after the time-dependant correction, the average absolute error between the predicted EEO and recorded EEO is further reduced from 10.83% to 4.3%. The coefficient of determination ( $R^2$ ) is further increased from 84.6% to 88.7%, which indicates a better matching between predicted EEO and recorded EEO.

In summary, based on the comparison results and the statistical analysis of the error between recorded EEO and predicted EEO for Aframax Oil Tanker B, it has been verified that the proposed the semi-empirical added resistance prediction method developed based on Suezmax Oil Tanker A is also suitable to Aframax Oil Tanker B. By integrating the time-dependent correction, the proposed semi-empirical ship operational performance prediction model for oil tanker can provide accurate ship operational performance prediction for specific oil tanker under varying speeds, sea states and wave angle encountered.

## **5.8 Development of Semi-empirical Ship Operational Performance Model for Container Ship**

In this section, the development of semi-empirical ship operational performance model for container ship has been clarified. Fuel Consumption Rate (FCR) has been taken as the parameter to indicate the ship operational performance. The development steps of semi-empirical ship operational performance model for container ship are identical with that of oil tanker (referred in Chapter 5.6).

### 5.8.1 Development of semi-empirical ship operational performance model for container ship

Firstly, for Container Ship A, the predicted Fuel Consumption Rate (FCR) using the original Kwon's added resistance prediction method (Kwon, 2008) was compared to the corresponding recorded FCR, which is collected from ship daily reports. The comparison results are presented in Figure 37. Based on the statistical analysis of the error between the recorded FCR and predicted FCR using original Kwon's method (Table 20), the average absolute error is 11.85%, and the coefficient of determination is 88.0%.

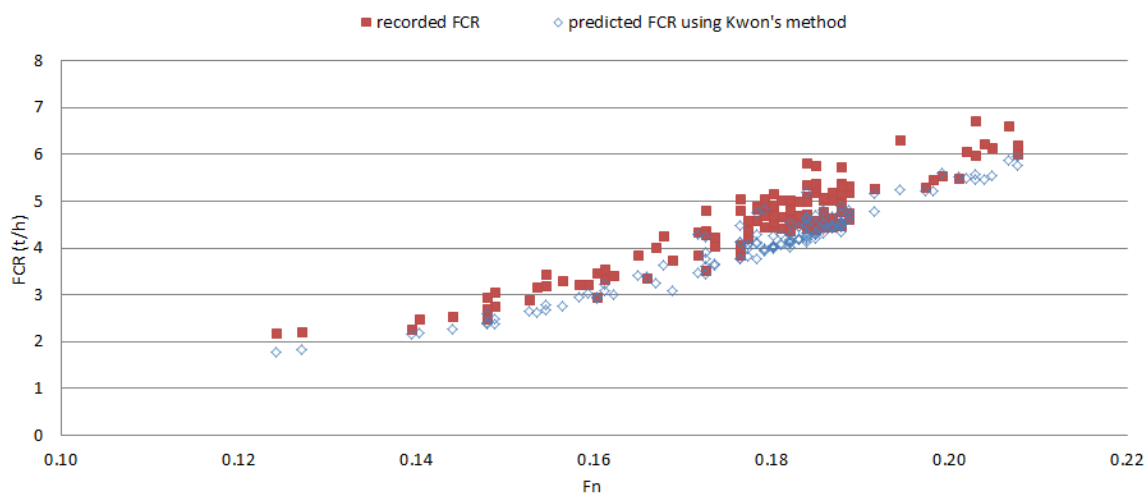


Figure 37: Overview of the comparison between the predicted FCR using original Kwon's method and recorded FCR

From Figure 37, it has been observed that the predicted FCR using original Kwon's method is commonly lower than the recorded FCR. As referred in Chapter 5.4, the shortcoming of Kwon's empirical added resistance prediction formulae and the effect of fouling are the two major sources of the error. In order to focus on the improvement of the added resistance prediction formulae for specific ship, the error caused by the effect of fouling needs to be excluded from the total error. During the first 5 months since launching, the effect of fouling is assumed to be minimum and ignorable. In order to verify this assumption, the error between recorded FCR and predicted FCR using sea trial has been studied in time manner, as



presented in Figure 38. This comparison was carried out under low BN and similar speed to exclude the error caused by weather and speed.

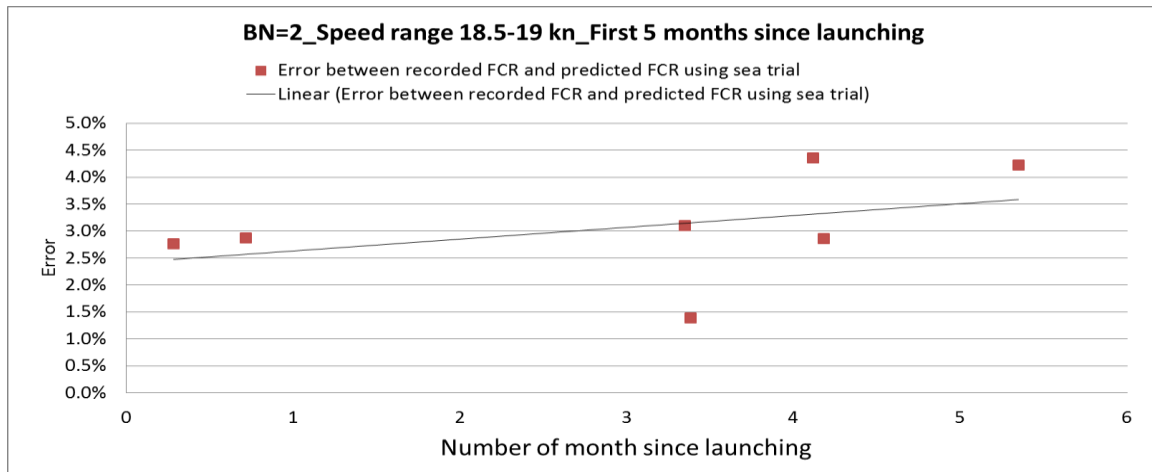


Figure 38: Time-dependent error between recorded EEO and predicted EEO using sea trial

In Figure 38, the error indicates the fouling effect on fuel consumption. It has been observed that the trend of this error is increasing with a very low rate during the first five months, which verified the assumption above: ‘During the first 5 months since launching, the effect of fouling is ignorable’.

Therefore, the predicted FCR using the empirical added resistance prediction formulae from the Kwon’s method (Kwon, 2008) was compared to the corresponding recorded FCR during the first 5 months since launching, as presented in Figure 39.

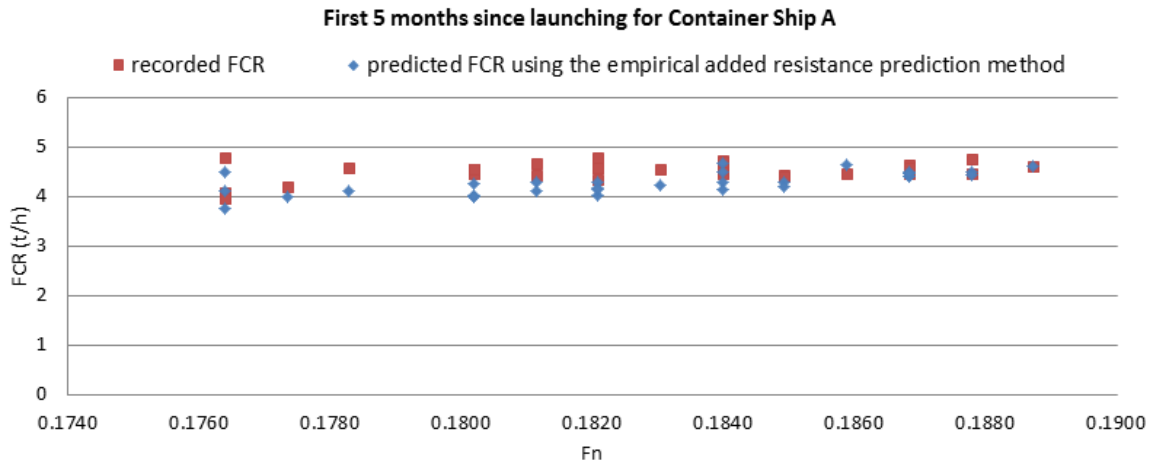


Figure 39: Comparison between the predicted FCR and recorded FCR for Container Ship A

From Figure 39, it has been observed that the predicted FCR using Kwon’s added resistance prediction method is commonly smaller than the recorded FCR. The average absolute error between the predicted FCR and recorded FCR is 6.21%. It has been also noted that the error between them is not directly related to Froude number. Thus the formula to calculate speed reduction coefficient  $C_U$  (as the speed reduction coefficient is only related to the parameter of Froude number) should not be modified. The formulae to predict direction reduction coefficient and ship form coefficient may either or both need to be modified.

Secondly, in order to determine which empirical formula (determining direction reduction coefficient and ship form coefficient in Kwon’s added resistance prediction method) needs to be adjusted for Container Ship A, the predicted FCR using Original Kwon’s method (Kwon, 2008) under each BN and each wave angle encountered has been compared to the corresponding recorded FCR. The comparison results under BN = 2, BN = 3, and BN = 4 are presented in Figure 40, Figure 41, and Figure 42 respectively. The comparison results under Head Sea, Bow Sea, Beam Sea and Following Sea are presented in Figure 43, Figure 44, Figure 45, and Figure 46 respectively.

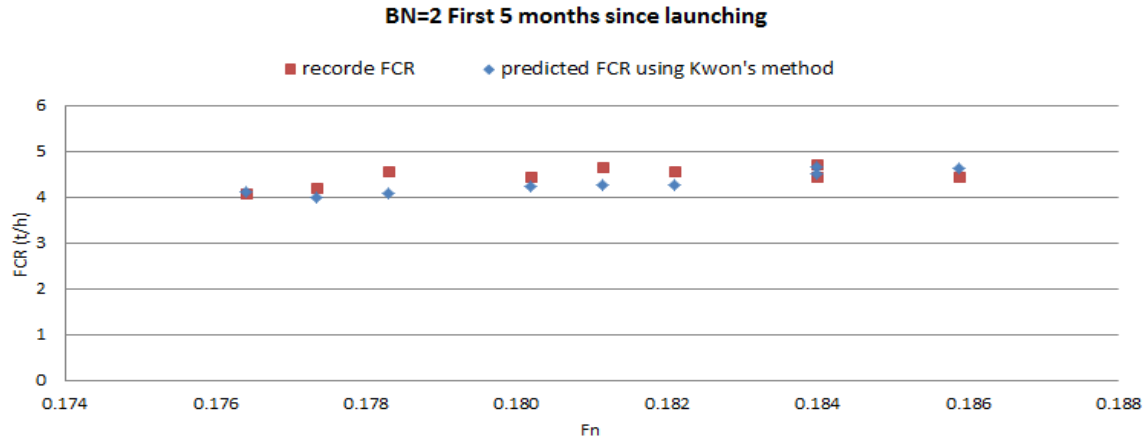


Figure 40: Comparison between the predicted FCR using original Kwon's method and recorded FCR under BN = 2

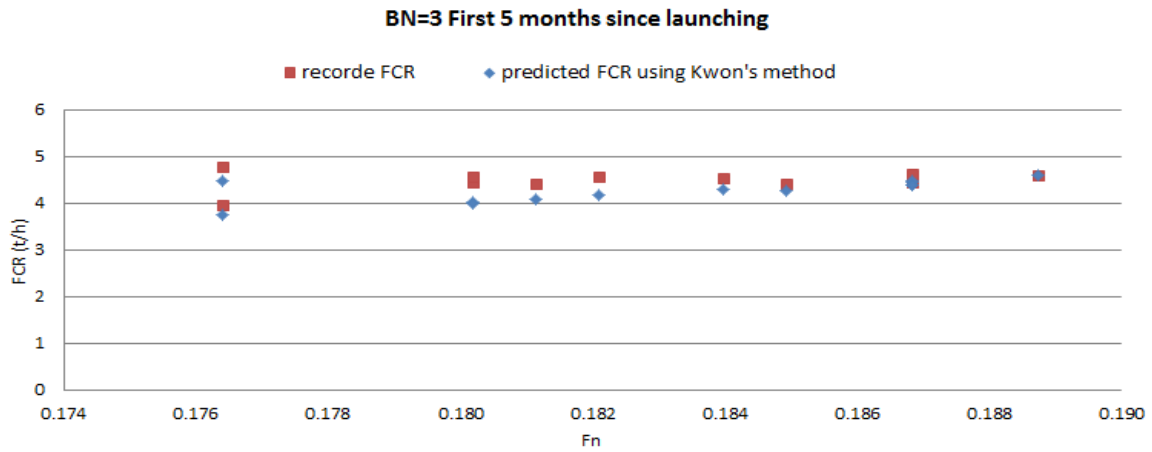


Figure 41: Comparison between the predicted FCR using original Kwon's method and recorded FCR under BN = 3

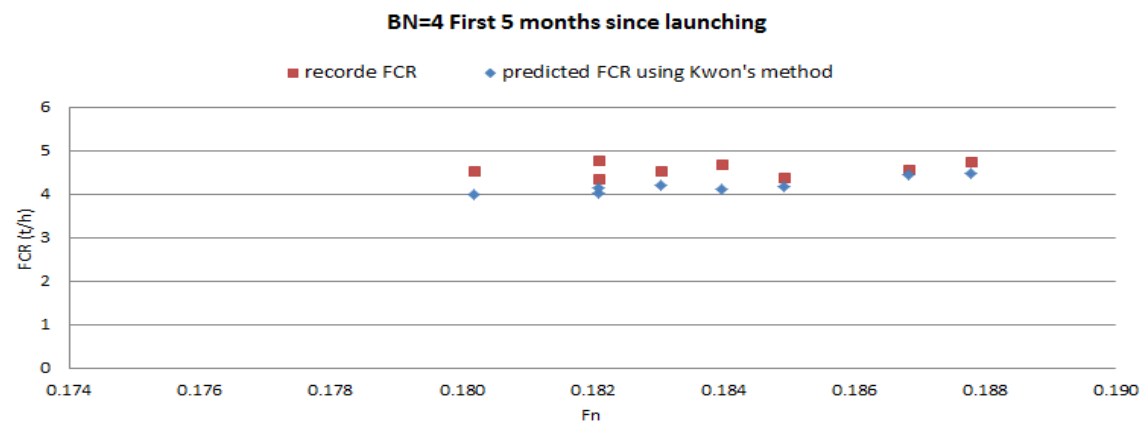


Figure 42: Comparison between the predicted FCR using original Kwon's method and recorded FCR under BN = 4

From Figure 40, Figure 41, and Figure 42, the average absolute error under BN= 2, BN=3, BN=4 are 3.92%, 5.82%, 7.43%. The results indicate that the average error increase with BN.

Under each BN, there are some points indicating that the predicted FCR is much lower than the recorded FCR. By investigating the corresponding recorded ship performance details of those points, it has been found that their strongest BN ( $BN_{Strongest}$ ) is bigger than their average BN ( $BN_{Average}$ ), while the Kwon's added resistance prediction formulae only include the average BN. As concluded in Chapter 5.6.1, both strongest BN and average BN should be included in the empirical added resistance prediction formulae for oil tanker, the BN related formulae to calculate direction reduction coefficient and ship form coefficient are both need to be improved. The conclusions also fit for container ships.

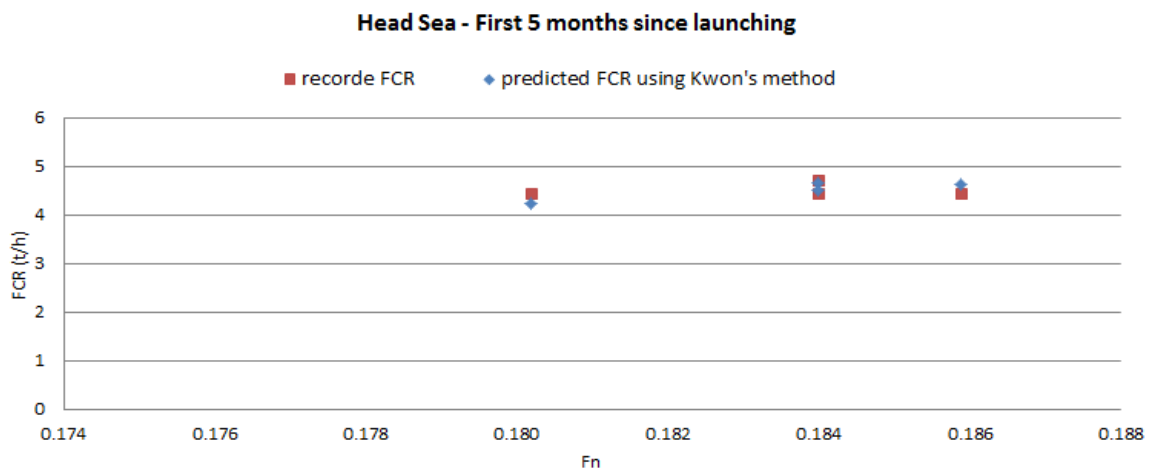


Figure 43: Comparison between the predicted FCR using original Kwon's method and recorded FCR in Head Sea

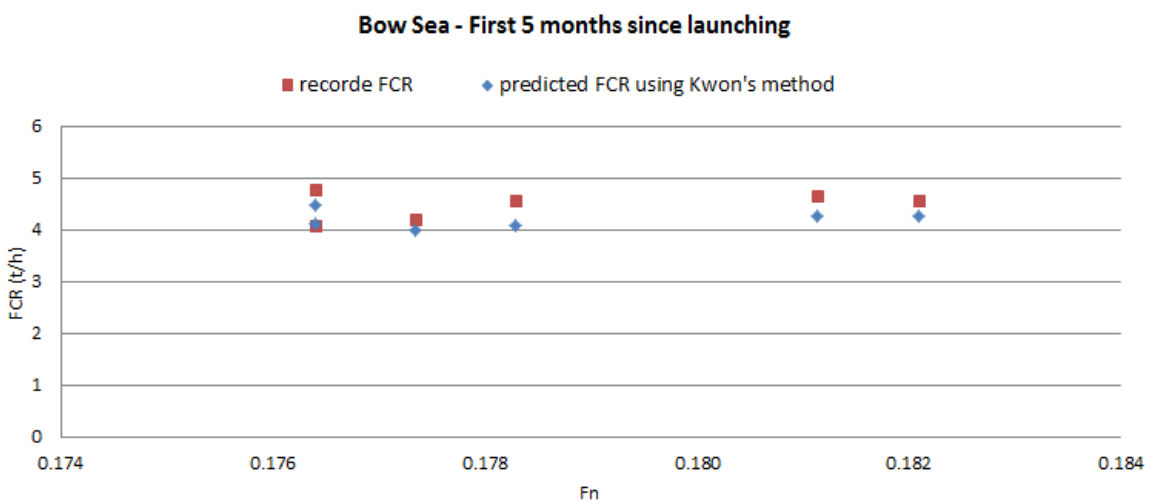


Figure 44: Comparison between the predicted FCR using original Kwon's method and recorded FCR in Bow Sea

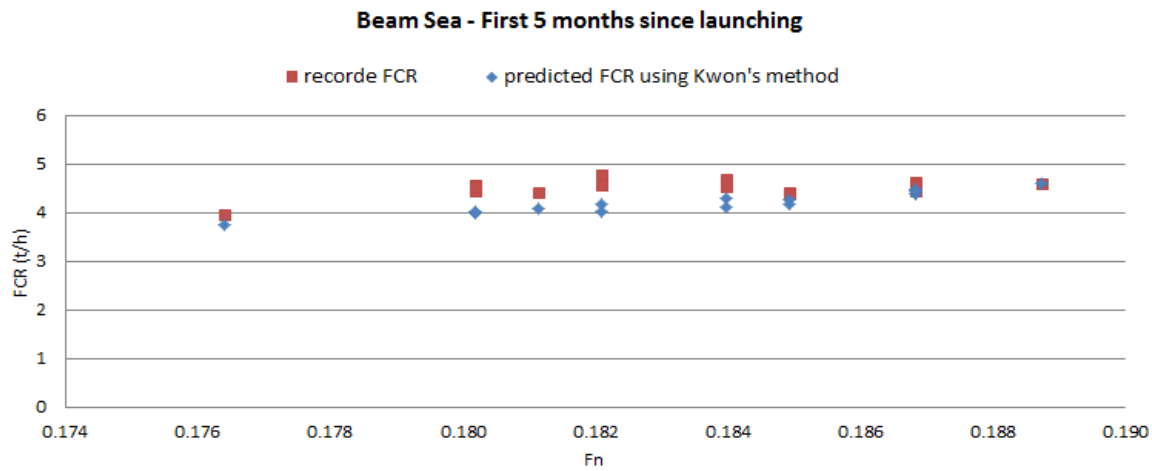


Figure 45: Comparison between the predicted FCR using original Kwon's method and recorded FCR in Beam Sea

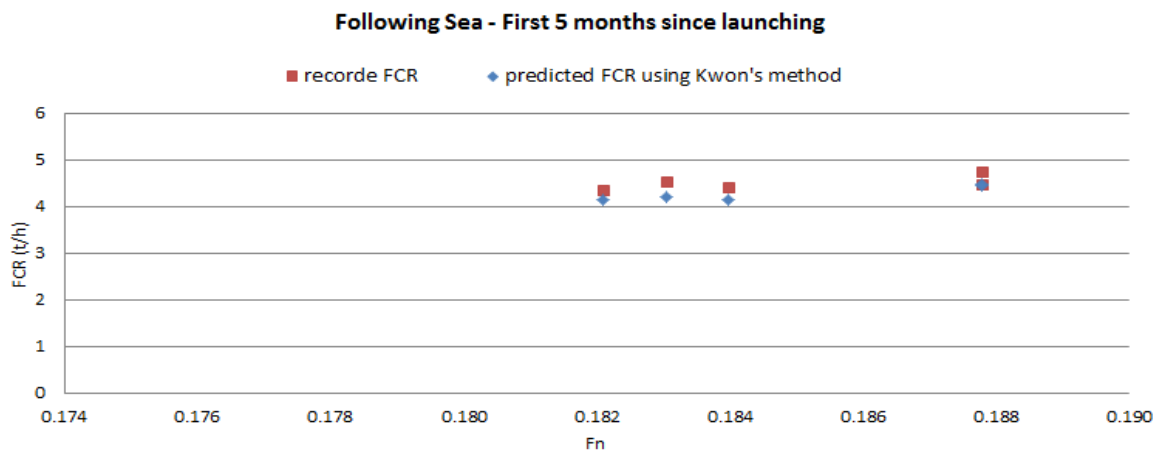


Figure 46: Comparison between the predicted FCR using original Kwon's method and recorded FCR in Following Sea

As presented in Figure 43, Figure 44, Figure 45 and Figure 46, the average absolute error under Head Sea, Bow Sea, Beam Sea and Following Sea are 1.41%, 5.83%, 9.05%, and 4.62%. It has also been observed that the predicted FCR using Kwon's method is commonly lower than that of the recorded FCR in Bow Sea, Beam Sea and Following Sea. In Head Sea, there is a good match between the predicted FCR and recorded FCR. Therefore, it can be concluded that the modifications of the formulae to calculate direction reduction coefficient should focus on Bow Sea, Beam Sea and Following Sea.

The modifications of the formulae to calculate ship form coefficient are presented in Table 16. The modifications of the formulae to calculate direction reduction coefficient are presented in Table 18. In the modification process, the variations of each coefficient have been carried out to test the sensitivity of the coefficients, and the corresponding average absolute error between the predicted FCR and the recorded FCR are compared. The modified added resistance prediction formulae providing the minimum error are proposed as the semi-empirical added resistance prediction formulae.

**Table 16: Modifications of the formula to calculate ship form coefficient for Container Ship A**

Loading condition	Name	Ship form coefficient	Average absolute error
Laden	Original	$0.7BN + BN^{6.5} / (22 * (\Delta^{2/3}))$	6.21%
	<b>Modification1</b>	$0.7 * \frac{BN_{Strongest} + BN_{Average}}{2} + (\frac{BN_{Strongest} + BN_{Average}}{2})^{6.5} / (22 * (\Delta^{2/3}))$	4.77%
	Modification2	$0.65 * \frac{BN_{Strongest} + BN_{Average}}{2} + (\frac{BN_{Strongest} + BN_{Average}}{2})^{6.5} / (22 * (\Delta^{2/3}))$	5.42%
	Modification3	$0.75 * \frac{BN_{Strongest} + BN_{Average}}{2} + (\frac{BN_{Strongest} + BN_{Average}}{2})^{6.5} / (22 * (\Delta^{2/3}))$	5.68%
	Modification4	$0.7 * \frac{BN_{Strongest} + BN_{Average}}{2} + (\frac{BN_{Strongest} + BN_{Average}}{2})^7 / (22 * (\Delta^{2/3}))$	4.96%
	Modification5	$0.7 * \frac{BN_{Strongest} + BN_{Average}}{2} + (\frac{BN_{Strongest} + BN_{Average}}{2})^6 / (22 * (\Delta^{2/3}))$	5.11%
	Modification6	$0.7 * \frac{BN_{Strongest} + BN_{Average}}{2} + (\frac{BN_{Strongest} + BN_{Average}}{2})^{6.5} / (20 * (\Delta^{2/3}))$	4.81%
	Modification7	$0.7 * \frac{BN_{Strongest} + BN_{Average}}{2} + (\frac{BN_{Strongest} + BN_{Average}}{2})^{6.5} / (24 * (\Delta^{2/3}))$	4.88%

From Table 16, it has been observed that the Modification 1 is providing the minimum average absolute error 4.77%. Compared to Modification1, the modifications of other coefficients (Modification 4-7) are not able to further reduce the average absolute error. Therefore, the semi-empirical formulae to calculate ship form coefficient for Container Ship A has been determined, as presented in Table 17.

**Table 17: Ship form coefficient  $C_{form}$  due to ship categories and loading condition for Container Ship A**

Type of ship	Ship form coefficient $C_{form}$	
	modified	original
Post-Panamax Container Ship	$0.7 * \frac{BN_{Strongest} + BN_{Average}}{2} + (\frac{BN_{Strongest} + BN_{Average}}{2})^{6.5} / (22 * (\Delta^{2/3}))$	$0.7BN + BN^{6.5} / (22 * (\Delta^{2/3}))$

According to the proposed formulae to calculate ship form coefficient as described above, the modifications of the formulae to calculate direction reduction coefficient are then carried out, the corresponding average absolute error of each combination of modifications during the first 5 months since launching is compared, as presented in Table 18.

**Table 18: Modifications of the formulae to calculate direction reduction coefficient**

Weather direction	Name	Direction reduction coefficient	Average absolute error
Head sea	<b>Original</b>	$2C_{\beta} = 2.0$	4.77%
	Modification 9	$2C_{\beta} = 1.9$	4.79%
	Modification 10	$2C_{\beta} = 2.1$	4.81%
Bow sea	<b>Original</b>	$2C_{\beta} = 1.7 - 0.03 * (BN - 4)^2$	4.77%
	Modification 11	$2C_{\beta} = 1.7 - 0.03 * (\frac{BN_{Strongest} + BN_{Average}}{2} - 4)^2$	4.32%
	<b>Modification 12</b>	$2C_{\beta} = 1.8 - 0.03 * (\frac{BN_{Strongest} + BN_{Average}}{2} - 4)^2$	4.13%
	Modification 13	$2C_{\beta} = 1.9 - 0.03 * (\frac{BN_{Strongest} + BN_{Average}}{2} - 4)^2$	4.26%
	Modification 14	$2C_{\beta} = 1.7 - 0.02 * (\frac{BN_{Strongest} + BN_{Average}}{2} - 4)^2$	4.37%
	Modification 15	$2C_{\beta} = 1.7 - 0.04 * (\frac{BN_{Strongest} + BN_{Average}}{2} - 4)^2$	4.42%
	Modification 16	$2C_{\beta} = 1.7 - 0.03 * (\frac{BN_{Strongest} + BN_{Average}}{2} - 3.5)^2$	4.40%
Modification 17	$2C_{\beta} = 1.7 - 0.03 * (\frac{BN_{Strongest} + BN_{Average}}{2} - 4.5)^2$	4.43%	
Beam sea	<b>Original</b>	$2C_{\beta} = 0.9 - 0.06 * (BN - 6)^2$	4.77%
	Modification 18	$2C_{\beta} = 0.9 - 0.06 * (\frac{BN_{Strongest} + BN_{Average}}{2} - 6)^2$	4.14%
	Modification 19	$2C_{\beta} = 1.0 - 0.06 * (\frac{BN_{Strongest} + BN_{Average}}{2} - 6)^2$	4.10%
	<b>Modification 20</b>	$2C_{\beta} = 1.1 - 0.06 * (\frac{BN_{Strongest} + BN_{Average}}{2} - 6)^2$	3.86%
	Modification 21	$2C_{\beta} = 1.2 - 0.06 * (\frac{BN_{Strongest} + BN_{Average}}{2} - 6)^2$	3.91%
	Modification 22	$2C_{\beta} = 0.9 - 0.05 * (\frac{BN_{Strongest} + BN_{Average}}{2} - 6)^2$	4.23%
	Modification 23	$2C_{\beta} = 0.9 - 0.07 * (\frac{BN_{Strongest} + BN_{Average}}{2} - 6)^2$	4.17%
	Modification 24	$2C_{\beta} = 0.9 - 0.06 * (\frac{BN_{Strongest} + BN_{Average}}{2} - 5.5)^2$	4.19%
Modification 25	$2C_{\beta} = 0.9 - 0.06 * (\frac{BN_{Strongest} + BN_{Average}}{2} - 6.5)^2$	4.18%	
Following sea	<b>Original</b>	$2C_{\beta} = 0.4 - 0.03 * (BN - 8)^2$	4.77%
	Modification 26	$2C_{\beta} = 0.4 - 0.03 * (\frac{BN_{Strongest} + BN_{Average}}{2} - 8)^2$	4.31%
	Modification 27	$2C_{\beta} = 0.5 - 0.03 * (\frac{BN_{Strongest} + BN_{Average}}{2} - 8)^2$	4.22%
	<b>Modification 28</b>	$2C_{\beta} = 0.6 - 0.03 * (\frac{BN_{Strongest} + BN_{Average}}{2} - 8)^2$	4.17%
	Modification 29	$2C_{\beta} = 0.7 - 0.03 * (\frac{BN_{Strongest} + BN_{Average}}{2} - 8)^2$	4.34%
	Modification 30	$2C_{\beta} = 0.4 - 0.02 * (\frac{BN_{Strongest} + BN_{Average}}{2} - 8)^2$	4.34%
	Modification 31	$2C_{\beta} = 0.4 - 0.04 * (\frac{BN_{Strongest} + BN_{Average}}{2} - 8)^2$	4.38%
	Modification 32	$2C_{\beta} = 0.4 - 0.03 * (\frac{BN_{Strongest} + BN_{Average}}{2} - 7.5)^2$	4.33%
Modification 33	$2C_{\beta} = 0.4 - 0.03 * (\frac{BN_{Strongest} + BN_{Average}}{2} - 8.5)^2$	4.37%	

Based on the comparison results presented in Table 18, it has been observed that the Modification 12 in Bow Sea, Modification 20 in Beam Sea, and Modification 28 in Following Sea are providing the minimum average absolute error in each weather direction. Therefore, the semi-empirical formulae to calculate direction reduction coefficient for Container Ship A have been determined, as presented in Table 19.

**Table 19: Direction reduction coefficient  $C_R$  due to weather direction for Container Ship A**

Weather direction	Encounter angle (with respect to the ship's bow) (deg)	Direction reduction coefficient	
		Proposed semi-empirical formula	Original Kwon's formula
Head Sea	0-30	$2C_\beta = 2.0$	$2C_\beta = 2.0$
Bow Sea	30-60	$2C_\beta = 1.8 - 0.03 * \left( \frac{BN_{Strongest} + BN_{Average}}{2} - 4 \right)^2$	$2C_\beta = 1.7 - 0.03 * (BN - 4)^2$
Beam Sea	60-150	$2C_\beta = 1.1 - 0.06 * \left( \frac{BN_{Strongest} + BN_{Average}}{2} - 6 \right)^2$	$2C_\beta = 0.9 - 0.06 * (BN - 6)^2$
Following Sea	150-180	$2C_\beta = 0.6 - 0.03 * \left( \frac{BN_{Strongest} + BN_{Average}}{2} - 8 \right)^2$	$2C_\beta = 0.4 - 0.03 * (BN - 8)^2$

In the second step, based on the study of error between predicted FCR using empirical Kwon's added resistance prediction method and recorded FCR from field data under each specific BN and weather direction, a semi-empirical added resistance prediction method for container ship, as presented in Table 17 and Table 19, has been proposed by adjusting the direction reduction coefficient  $C_R$  and ship form coefficient  $C_{form}$ .

Compared to the semi-empirical added resistance prediction method proposed for oil tanker, two concluding remarks have been drawn as following:

- Regarding the four weather directions, the semi-empirical direction reduction coefficient proposed for container ship is relatively larger than that of oil tanker in Head Sea and Bow Sea. As the average voyage speed of container ship is commonly larger than that of oil tanker, the 'faster' container ships have more speed loss in Head Sea and Bow Sea.



- In Beam Sea and Following Sea, the semi-empirical direction reduction coefficients proposed for container ships and oil tankers are identical, which indicate that wave caused added resistance in Beam Sea and Following Sea are relatively less affected by speed compared to that of Head Sea and Bow Sea.

By utilizing the proposed semi-empirical formulae for container ship, the predicted FCR has been compared with the recorded FCR during the first 5 months since launching, as presented in Figure 47.

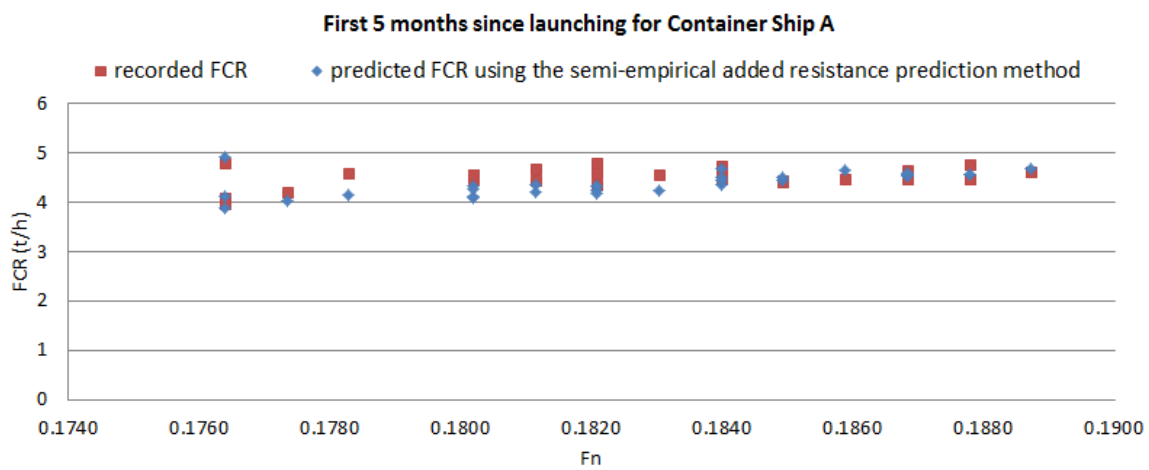
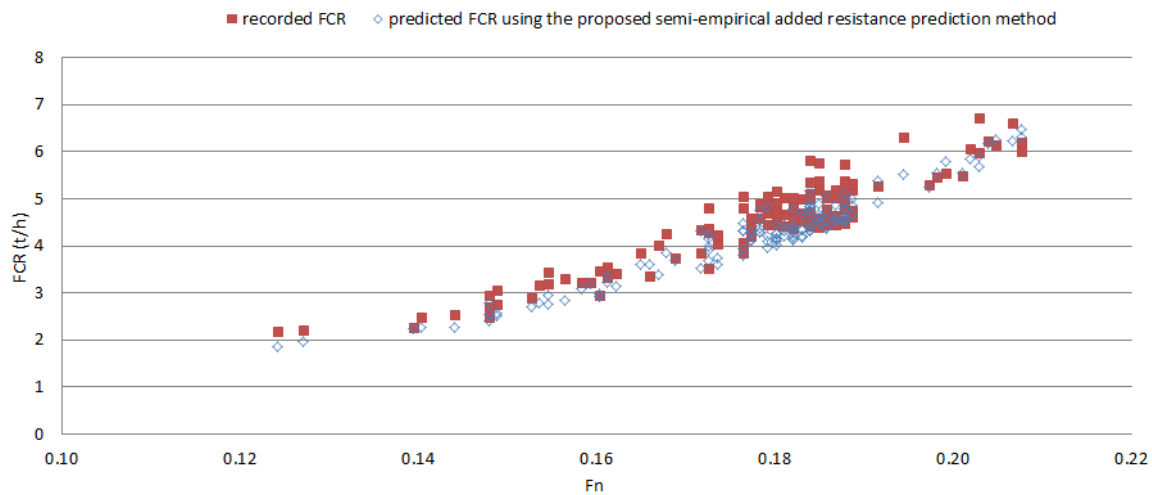


Figure 47: Comparison between the predicted FCR using the proposed semi-empirical method and recorded FCR during first 5 months since launching

The statistical analysis of the error between the predicted FCR and recorded FCR has been carried out. Compared to the Kwon's added resistance prediction method, the average absolute error reduces from 6.21% to 3.94% by utilizing the proposed semi-empirical added resistance prediction method. Considering the uncertainty of actual operational data (referred in Chapter 4.2), the error of 3.94% indicates that the proposed semi-empirical added resistance prediction formulae for container ships provides a good prediction of the added resistance caused by wave.

Thirdly, the proposed semi-empirical added resistance prediction method for container ship is applied along all available daily ship performance reports, as presented in Figure 48.



**Figure 48:** Overview of the comparison between the predicted FCR using the semi-empirical added resistance prediction method and recorded FCR

By comparing Figure 37 and Figure 48, it has also been observed that the predicted FCR using the proposed semi-empirical added resistance prediction method is better matching the corresponding recorded FCR. In order to include the fouling effect, the error between the predicted FCR using the semi-empirical method and recorded FCR is then investigated in time dependent manner, as illustrated in the following section.

### *5.8.2 Integrating the time-dependent correction for container ship*

The error between the recorded FCR and predicted FCR (using the semi-empirical added resistance prediction method) is assumed to be majorly caused by the fouling effect. In time-dependant manner, the correction factors are derived from the trend lines, as presented in Figure 49.

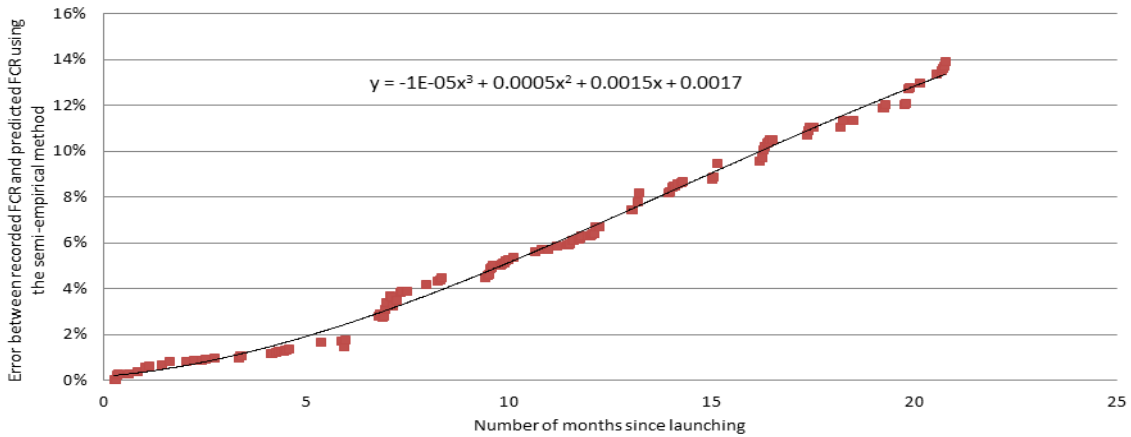


**Figure 49:** Error between predicted FCR and recorded one since launch date for Container Ship A

From Figure 49, it has been observed that the error increases with the number of months since launching. From the launching date to the 6<sup>th</sup> months, the error increases slowly with 0.33% per month. After the 7<sup>th</sup> month, the error increases sharply with 0.78% per month. In an overview of the 21 months voyage for Container Ship A, the average error increases with 0.6% per month on average.

By integrating the correction factor withdrawn from Figure 49, the updated predicted FCR using the semi-empirical added resistance prediction method for container ship has been compared with the recorded FCR, as presented in Figure 50.

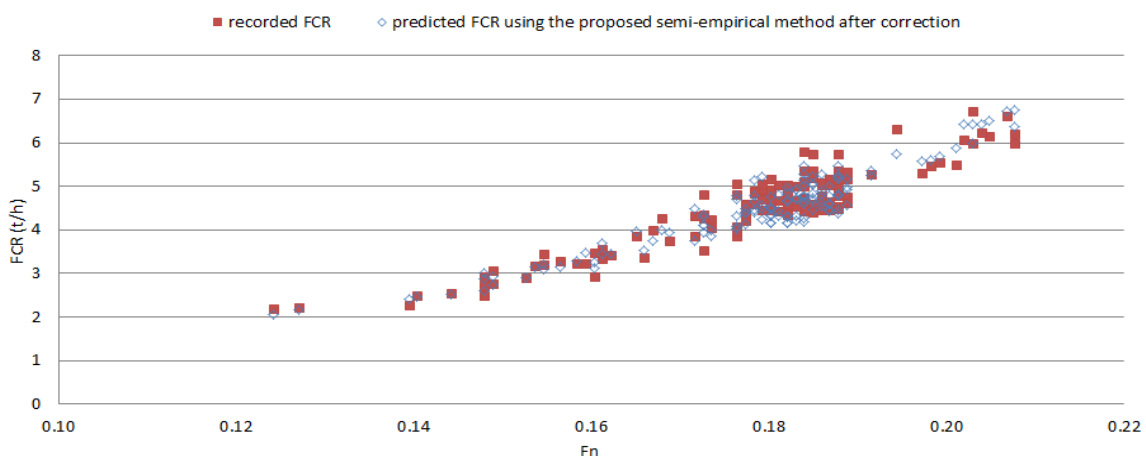


**Figure 50:** Overview of the comparison between the predicted FCR using the semi-empirical added resistance prediction method after time-dependent correction and recorded FCR

The comparison results above show great agreement between the predicted FCR using the semi-empirical added resistance prediction method after time-dependent correction and recorded FCR. Compared to Figure 47, the integration of the time-dependant correction is helpful to improve prediction accuracy.

The statistical analysis of the error between recorded FCR and the predicted FCR using empirical method, semi-empirical method and semi-empirical method with correction have been carried out, as presented in Table 20.

**Table 20:** Statistical analysis of the error between recorded FCR and predicted FCR for Container Ship A

Statistical analysis of the error between recorded FCR and predicted FCR for Container Ship A			
Modelling method for predicted FCR	Empirical method	Semi-empirical method	Semi-empirical method with correction
Sample time duration (No. of months)	21	21	21
Sample size (No. of daily reports)	138	138	138
Average absolute Error	11.85%	7.17%	4.50%
R <sup>2</sup>	88.0%	89.2%	92.8%

As observed from Table 20, compared to the empirical Kwon’s added resistance prediction method, the average absolute error has been reduced from 11.85% to 7.17%, and the coefficient of determination ( $R^2$ ) increased from 88.0% to 89.2%. by utilizing the semi-empirical added resistance prediction method. Especially after the time-dependant correction, the average absolute error further drops to 4.50% and the  $R^2$  value reaches to 92.8%.

In summary, within the development of semi-empirical ship operational performance model for container ship, the semi-empirical added resistance prediction method for container ship has been proposed. Based on the comparison results (Table 20), it has been verified that the semi-empirical added resistance prediction method for container ship can provide more accurate added resistance prediction compared to empirical Kwon’s method. By integrating the time-dependent correction, the prediction accuracy can be further improved. Therefore, the semi-empirical ship operational performance model for container ship has been developed.

As the semi-empirical ship operational performance model for container ship is developed based on Container Ship A, then a question comes out:

*‘Whether the semi-empirical ship operational performance model developed based on Container Ship A is also compatible to other container ship’*

Therefore, a validation study by applying the proposed semi-empirical model on Container Ship B has been carried out to answer this question in the following section.

## **5.9 Validation of Semi-empirical Ship Operational Performance Model for Container Ship**

As described in Chapter 5.8, the semi-empirical ship operational performance prediction model for container ship has been developed. In this section, the proposed method will be applied on another container ship – Container Ship B. The improvement of the performance prediction accuracy will be assessed to validate the suitability of the proposed semi-empirical method for container ship.

Firstly, before applying the proposed semi-empirical model on Container Ship B, the predicted Fuel Consumption Rate (FCR) using the empirical Kwon’ added resistance prediction method (Kwon, 2008) was compared to the corresponding recorded FCR. The overview of the comparison is presented in Figure 51. The statistical analysis of the error between the recorded FCR and predicted FCR using original Kwon’s method has been carried out. The results (Table 22) indicate that the average absolute error is 10.83%, and the coefficient of determination ( $R^2$ ) is 88.1%.

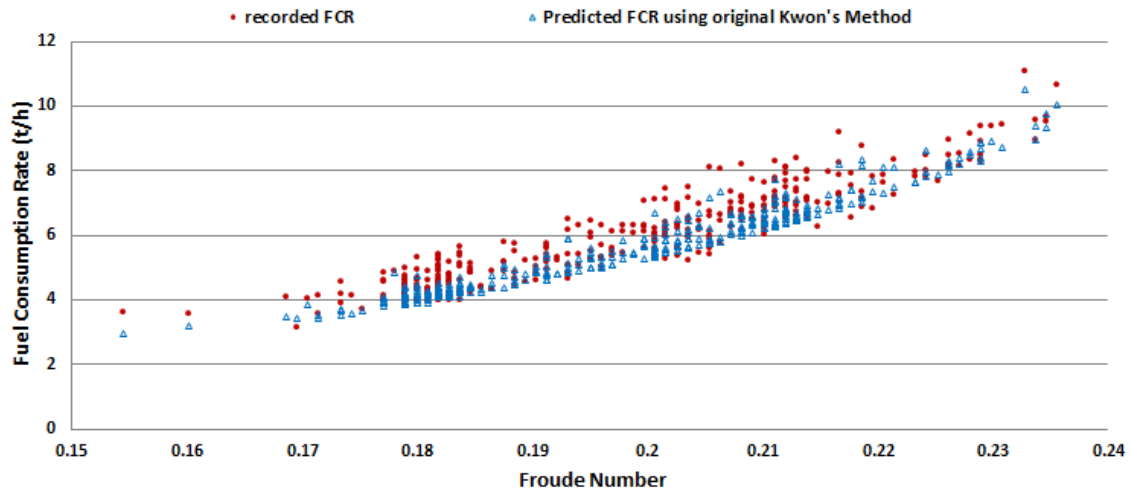


Figure 51: Overview of the comparison between the predicted FCR using original Kwon’s method and recorded FCR

Secondly, the proposed semi-empirical added resistance prediction method developed based on Container Ship A was applied to Container Ship B. The predicted FCR using the semi-empirical added resistance prediction method was compared to the corresponding recorded FCR. The overview of the comparison is presented in Figure 52.

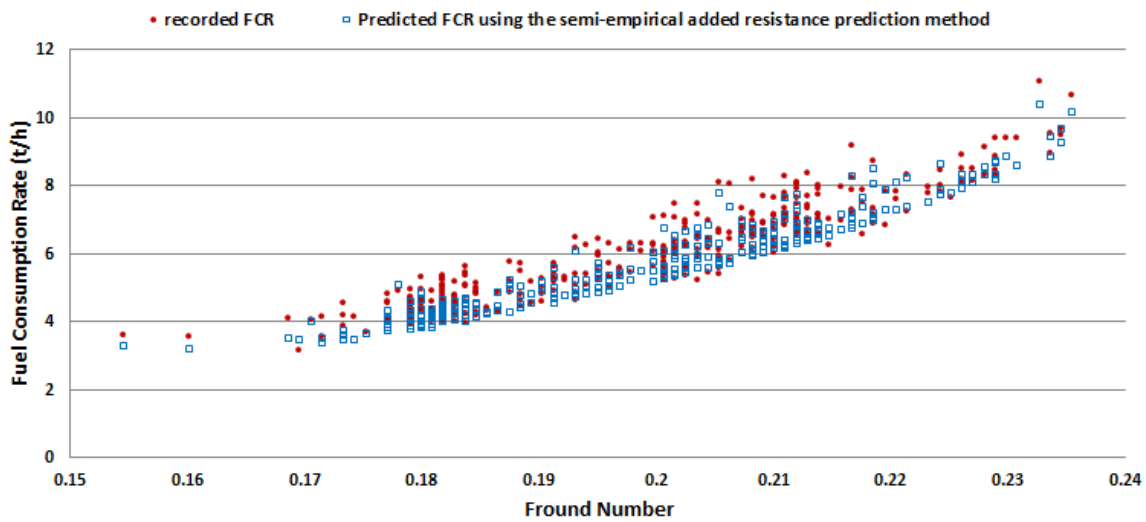


Figure 52: Overview of the comparison between the predicted FCR using the semi-empirical added resistance prediction method and recorded FCR

By comparing the Figure 51 and Figure 52, it has been observed that the predicted FCR by using the semi-empirical added resistance prediction method is better matching the recorded FCR. Based on the statistics analysis, compared to original Kwon’s method, the average absolute error between the predicted FCR and recorded FCR is reduced from 10.83% to 8.36% and the coefficient of determination ( $R^2$ ) is increased from 88.1% to 88.9%, which indicate that the proposed semi-empirical added resistance prediction method for container ship is validated for Container Ship B.

Thirdly, the error between recorded FCR and predicted FCR using the semi-empirical added resistance prediction method for Container Ship B was studied in time dependent manner. The time-dependant correction has been derived and presented in Figure 53.

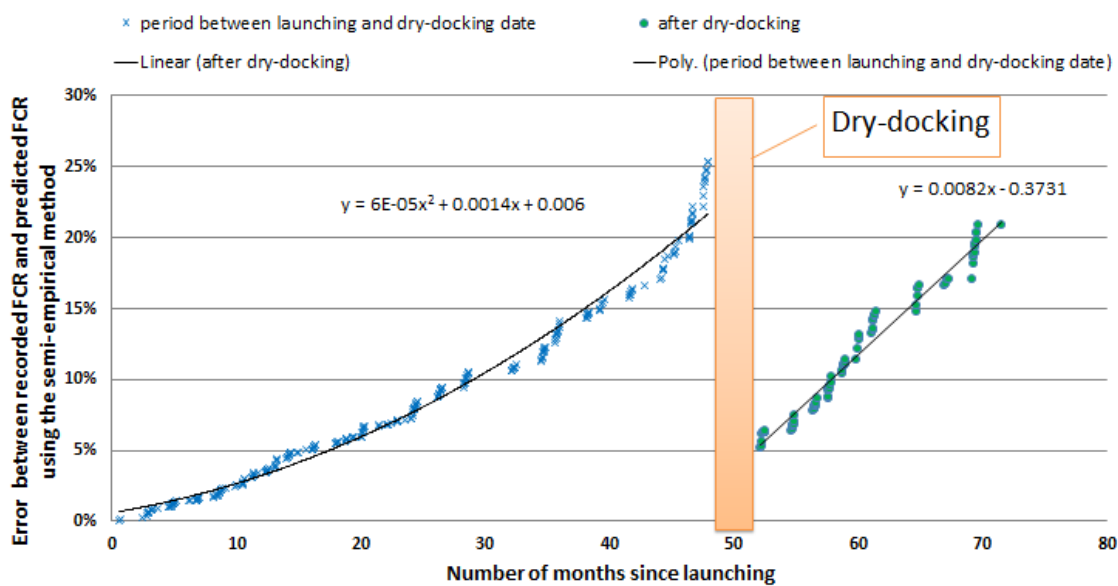


Figure 53: Error between predicted FCR and recorded one since ship launch date for Container Ship B

As presented in Figure 53, from the ship launched date to the 12<sup>th</sup> service month, the energy consumption due to fouling effect is increased relatively slowly with 0.35% per month, then the rate increases sharply afterwards and the error reaches 25% in 48<sup>th</sup> service month. On

average, from the ship launched date to the 48<sup>th</sup> month, the fuel consumption due to fouling effect is increased with 0.52% per month.

After the dry-docking, from the 52<sup>nd</sup> (dry-docking) to the 71<sup>st</sup> month, the fuel consumption due to fouling effect is increased with 0.75% per month.

For Container Ship A and Container Ship B, the increasing energy consumption rates due to fouling effect are compared in Table 21.

**Table 21:** Increasing energy consumption rate due to fouling effect for Container Ship A and Container Ship B

	Before dry-docking	After dry-docking
Container Ship A	0.6% per month	N/A
Container Ship B	0.52% per month	0.75% per month

Due to the lack of performance results for Container Ship A, its increasing energy consumption rate due to fouling effect after dry-docking is not available. From Table 21, it has been observed that the increasing energy consumption rate before dry-docking are 0.6% per month for Container Ship A and 0.52% per month for Container Ship B, which indicates better performed painting have been applied on Container Ship B. After dry-docking, the increasing energy consumption rate for Container Ship B is 0.75% per month (higher than 0.52% per month before dry-docking), which might be caused by the hull surface damage or the less effective anti-fouling painting has been applied to Container Ship B during dry-docking.

Fourthly, after the time-dependent correction, the updated predicted FCR using the semi-empirical added resistance prediction method for container ship was compared to the corresponding recorded FCR. The overview of the comparison is presented in Figure 54.



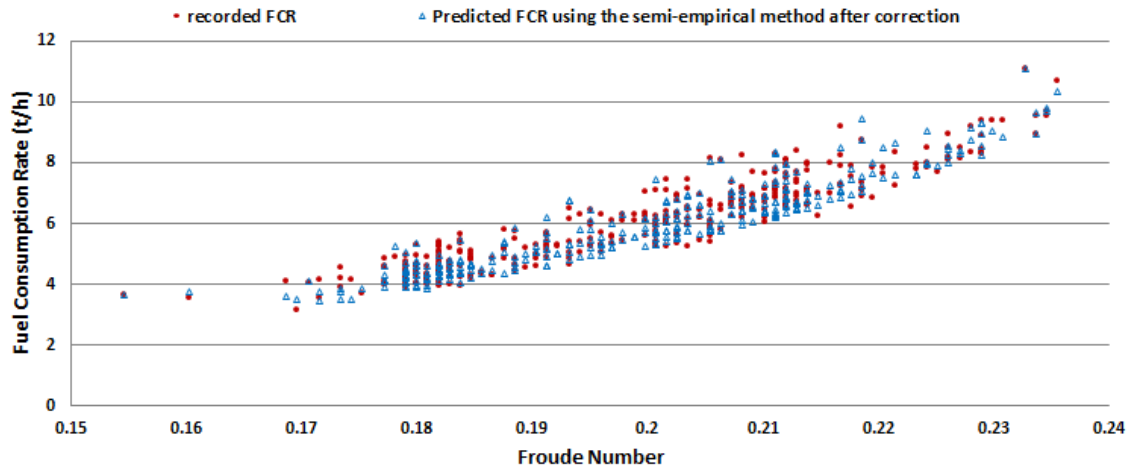


**Figure 54:** Overview of the comparison between the predicted FCR using the semi-empirical added resistance prediction method after time-dependent correction and recorded FCR

By comparing Figure 52 and Figure 54, it has been observed that there is an obvious improvement of prediction accuracy by including the time-dependent correction. The statistical analysis of the average absolute error between the predicted FCR using the semi-empirical method with correction and recorded FCR has been carried out and presented in Table 22.

**Table 22:** Statistical analysis of the error between recorded FCR and predicted FCR for Container Ship B

Statistical analysis of the error between recorded FCR and predicted FCR for Container Ship B			
Modelling method for predicted FCR	Empirical method	Semi-empirical method	Semi-empirical method with correction
Sample time duration (No. of months)	70	70	70
Sample size (No. of daily reports)	343	343	343
Average absolute Error	10.83%	8.36%	5.12%
R <sup>2</sup>	88.1%	88.9%	90.9%

In summary, based on the comparison results and the statistical analysis of the error between recorded FCR and predicted FCR for Container Ship B, it has been verified that the proposed semi-empirical added resistance prediction method developed based on Container Ship A is also suitable to Container Ship B. By integrating the time-dependent correction, the proposed semi-empirical ship operational performance prediction model for container ship can provide accurate ship operational performance prediction for specific container ship under varying speeds, sea states and wave angle encountered.

## 5.10 Discussion on Time-dependent Correction for Oil Tanker and Container Ship

As referred in Chapter 5.6 – 5.9, it has been concluded that the accuracy of ship operational performance prediction has been obviously improved by integrating the time-dependent correction. The causes of the time-dependent correction are listed as following:

- Hull fouling
- Propeller fouling
- Main engine performance degradation
- Hull surface/propeller damage

As the paintings, hull surface/propeller damage, and main engine performance applied/installed on each specific commercial ship are various, it would be the best to withdraw the time-dependent correction based on its actual performance records.

For Suezmax Oil Tanker A, Aframax Oil Tanker B, Post-Panamax Container Ship A, and Post-Panamax Container Ship B, the increasing energy consumption rates are compared in time manner, as presented in Table 23.

**Table 23: Time-dependent corrections for Suezmax Oil Tanker A, Aframax Oil Tanker B, Post-Panamax Container Ship A, and Post-Panamax Container Ship B**

	Before dry-docking	After dry-docking
Suezmax Oil Tanker A	0.53% per month	0.44% per month
Aframax Oil Tanker B	0.63% per month	0.75% per month
Post-Panamax Container Ship A	0.6% per month	N/A
Post-Panamax Container Ship B	0.52% per month	0.75% per month

However, as the actual ship operational performance reports are not always available, a general time-dependent correction for oil tankers and container ships is in need. Therefore,

the time-dependent corrections for the two oil tankers and two container ships have been investigated. As presented in Table 23, before dry-docking, the range of time-dependent correction on fuel consumption is between 0.52% per month and 0.63% per month. On average, 0.575% per month is assumed to be the fuel consumption increasing rate before dry-docking for oil tanker and container ship.

During dry-docking, there are many uncertainties affect the time-dependent correction for each specific ship:

- Painting strategy

Partially/fully removal of original paintings – high pressure water jetting or other surface preparation method

Selection of new paintings applied on hull surface, the anti-fouling effectiveness of different paintings differs.

- Treatment to the hull surface/propeller damage

After the high pressure water cleaning, the treatment of the corrosions on hull surface and propeller will affect the increasing rate of fouling.

- Main engine maintenance strategy

The main engine may/may not be overhauled during dry-docking, this needs to be identified from the dry-docking report for each specific ship

Due to the uncertainties listed above, the time-dependent correction after dry-docking varies for each specific ship. It also needs to be noted that the correction factor depends on operational zones. The accurate time-dependent correction after dry-docking requires the actual ship performance records while considering their operational zones.

## 5.11 Chapter Summary

By utilizing the actual operational data, the empirical added resistance prediction formulae have been improved to adapt for specific oil tanker and container ship. The time-dependent correction factor further improves the prediction accuracy. Within this chapter, the semi-empirical added resistance prediction method for oil tanker and container ship, and the semi-empirical ship operational performance prediction models for oil tanker and container ship have been developed.

In order to verify the prediction accuracy and suitability, the proposed semi-empirical ship operational performance prediction models have been applied on another oil tanker and container ship correspondingly. The predicted ship operational performance has been compared to the actual ship operational performance data. Based on the comparison results and statistical analysis, it has been summarized that the development of semi-empirical added resistance method and the integration of time-dependent correction are the two key factors for the improvement of prediction accuracy.

However, there are also some limitations of using the proposed semi-empirical ship operational performance prediction models. As has been highlighted in Chapter 4, the development of semi-empirical ship operational performance prediction model requires ship noon reports, sea trial documents and main engine performance reports. The uncertainties of analysed data from these three sources may cause error in ship operational performance prediction. The correction factor for fouling effect and engine performance degradation was extracted with actual ship daily reports. Without the ship dry-docking reports, and long-term ship performance reports, the extra fuel consumption caused by fouling effect and engine performance degradation cannot be identified separately.

Based on the validation study, it has been verified that the proposed semi-empirical ship operational performance prediction model for oil tanker and container ship can provide accurate performance prediction for Suezmax Oil Tanker, Aframax Oil Tanker and Post-Panamax Container Ships. More validation studies of other oil tankers and container ships are expected to test the suitability of the proposed model.

The next chapter will look into the integration of weather forecast, and the development of GRIDS system for voyage optimization.

# Chapter 6 –WEATHER FORECAST AND GRIDS SYSTEM

---

## 6.1 Chapter Overview

This chapter will introduce the access and utilization of weather forecast (§6.2), and then specify the development of GRIDS system (§6.3).





## 6.2 Weather Forecast

Weather forecast is an important module for voyage optimization. The reliability and availability of the weather forecast influence the accuracy of ship operational performance prediction in actual voyage. Based on the research of available weather forecast in market, it has been found out that the utilization of most weather forecasts provided by the meteorological organisations is limited by its high price or partial coverage of global ocean map. Nevertheless, in this research, the global ocean weather forecast provided by National Oceanic and Atmospheric Administration (NOAA) (NOAA, 2015) has been utilized to access the sea conditions for next 7 days period; the historical weather and sea conditions records provided by European Centre for Medium-Range Weather Forecasts (ECMWF) has been employed to access historical sea conditions.

The weather forecast from NOAA is derived from the WAVEWATCH III (Tolman, 2009) model, which is a widely used computer generation of ocean surface weather forecasts. The historical weather and sea conditions are recorded in ERA Interim dataset, which is the latest atmospheric reanalysis produced by ECMWF. The sources of observations assimilated in ERA-Interim (D. P. Dee et al. 2011) include:

- Surface observations from land stations, ships;
- Drifting buoys reports from radiosondes and pilot balloons
- Wind profiler data from North American sites, European sites and Japanese sites
- Hourly METAR airport weather reports

The weather forecast from NOAA is saved in ‘GRIB2’ format, which records the weather forecast information as a 3 Dimensional matrix. The 3 dimensions include Time, Latitude, and Longitude. The latitude measurements range from 78 degree North to 78 degree South, and equally divided into 156 rows. Therefore, the gap between each two adjacent rows in latitude is 1 degree. The longitude measurements range from 0 degree to 358.75 degree, and equally divided into 287 columns. Therefore, the gap between each two adjacent columns in longitude is 1.25 degree. The crossing points between the latitude rows and longitude columns represent the locations of weather forecast measurement nodes. The time steps of each daily forecast include 00:00, 06:00, 12:00 and 18:00 (Figure 55) and the update frequency of the next 7 days weather forecast is every 6 hours.

Name	Date modified	Type	Size
 nww3.t00z.grib	21/05/2013 17:21	GRIB2 File	25,744 KB
 nww3.t06z.grib	21/05/2013 17:21	GRIB2 File	25,760 KB
 nww3.t12z.grib	21/05/2013 17:21	GRIB2 File	25,785 KB
 nww3.t18z.grib	21/05/2013 17:21	GRIB2 File	25,791 KB

**Figure 55: Daily Four Updated GRIB2 Files (Corresponding to the update frequency of weather forecast)**

The historical weather and sea conditions from ECMWF are saved in ‘GRIB1’ format, and the historical sea conditions are also saved as 3-D matrix, which is identical with ‘GRIB2’. But the latitude measurements range from 90 degrees North to 90 degrees South, the longitude measurements range from 180 degrees West to 180 degrees East, the grids density

is 0.75 degrees \* 0.75 degrees. The available date ranges from 1979-01-01 to 2015-10-31(ECMWF, accessed in 2016), and the time steps are identical with that of ‘GRIB2’.

For utilizing the weather forecast from NOAA and historical sea conditions from ECMWF, two decoding program have been written by the author to read ‘GRIB1’ files and ‘GRIB2’ files. Based on the decoding program, a few screenshot of the global sea conditions have been taken as following:

- A screenshot of the global ocean wind speed (m/s) is presented in Figure 56.

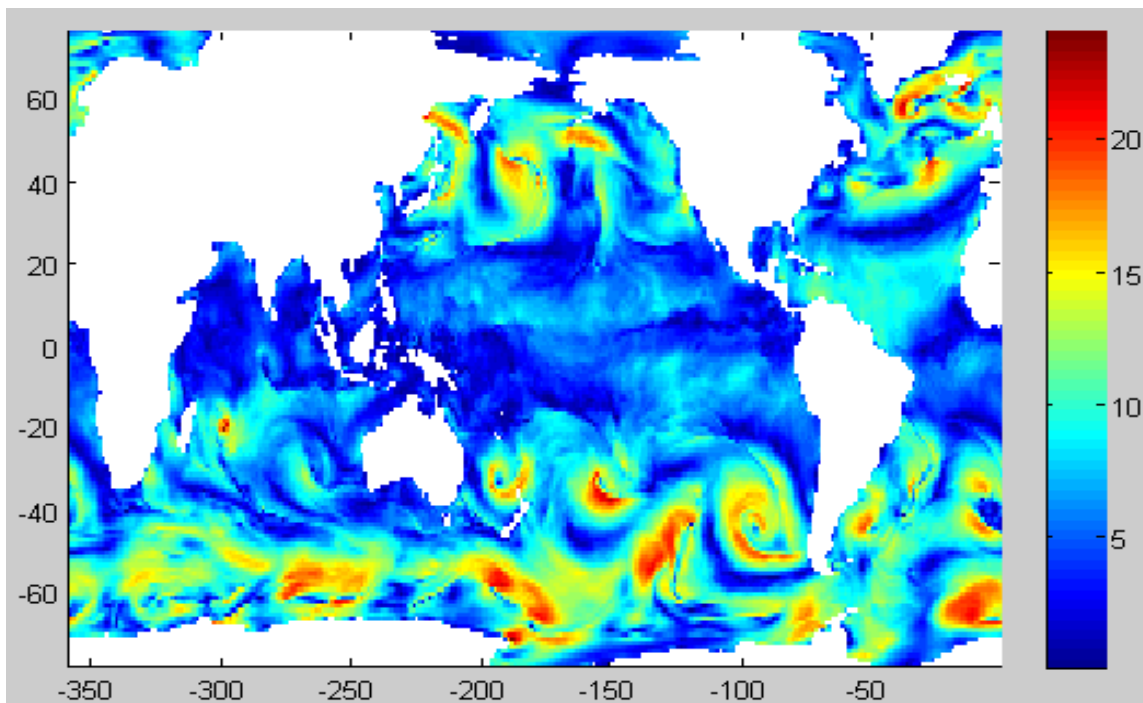


Figure 56: Screenshot of Global Ocean Wind Speed (Based on the program written in Matlab)

- A screenshot of the global sea direction (direction of wind and wave in true surface, 0 degree indicate North) is presented in Figure 57.



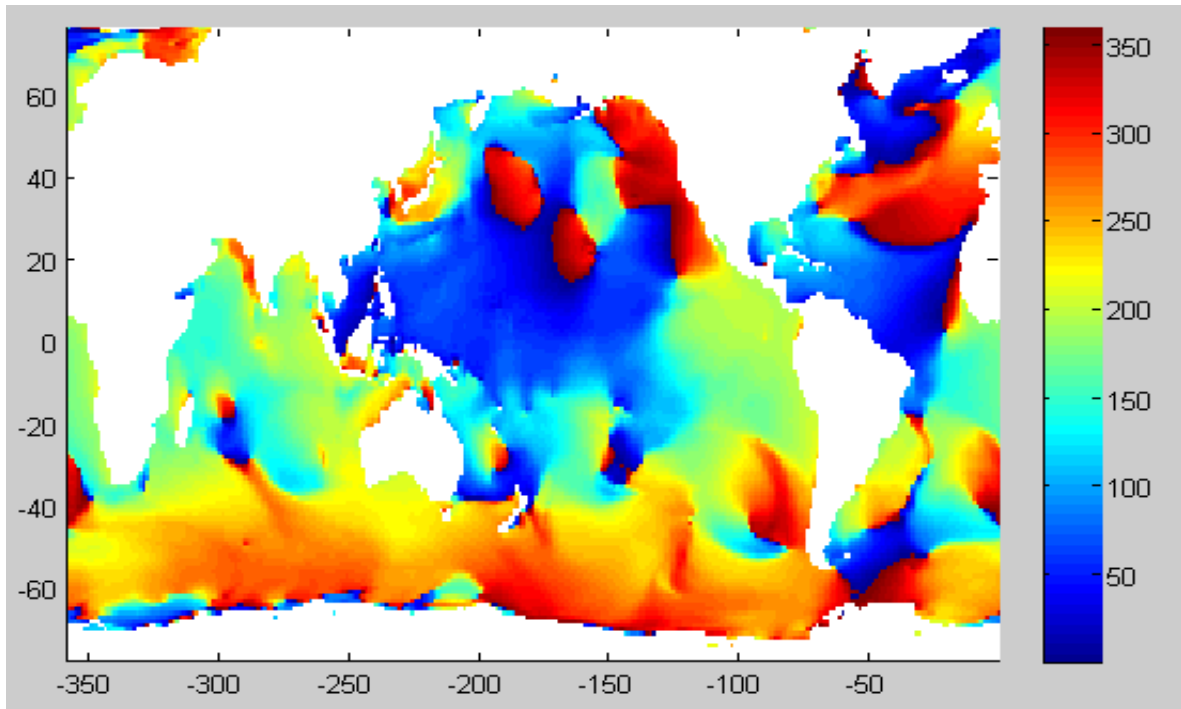


Figure 57: Screenshot of Global Sea Direction (Based on the program written in Matlab)

- A screenshot of the global significant wave height (m) is presented in Figure 58.

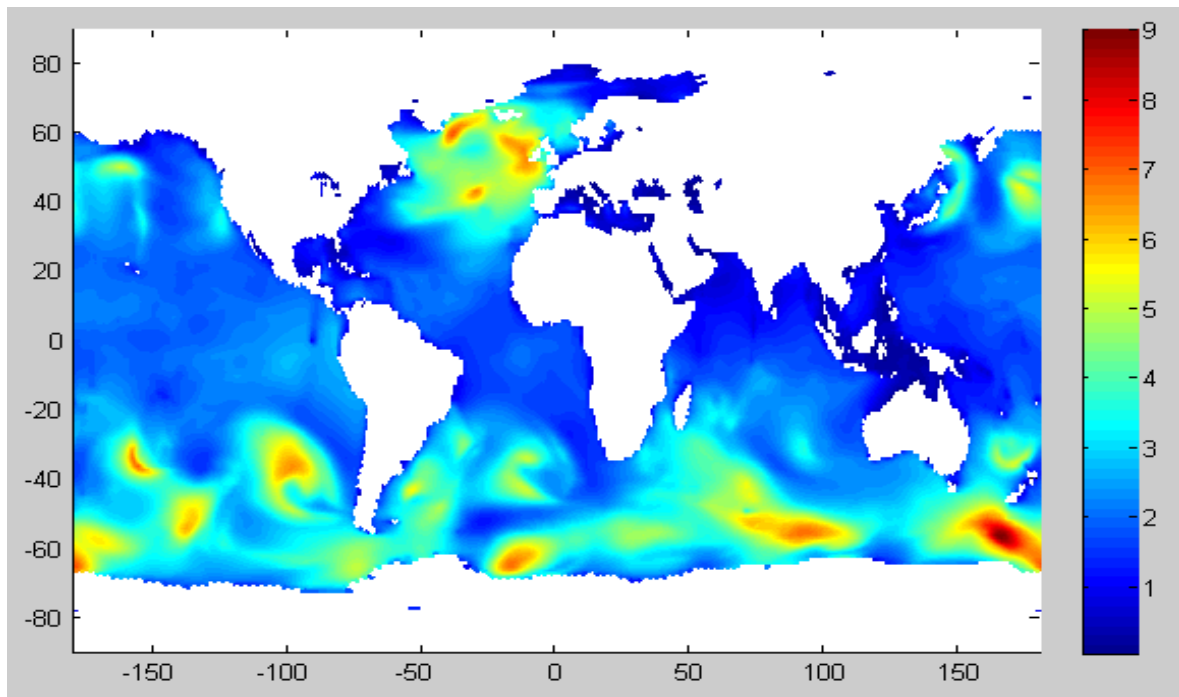


Figure 58: Screenshot of Global Significant Wave Height (Based on the program written in Matlab)

The information contained in the weather forecast from NOAA includes wind speed and directions, significant wave height, swell, and mean wave period. The information contained in the historical weather and sea conditions records from ECMWF includes 128 parameters, such as '2 metre dewpoint temperature', '10 metre U wind component' and '2 metre temperature'. These 128 parameters are listed in the website of ECMWF. (ECMWF, accessed in 2016) In this study, '10 metre U wind component', '10 metre V wind component', 'Mean wave direction', and 'Significant height of combined wind wave and swell' have been adopted to describe the historical global sea conditions.

### 6.3 GRIDS System

As an important module for voyage optimization, GRIDS system is an interface between semi-empirical ship operational performance prediction model, weather forecast, and optimum route selection model. The development of GRIDS system includes two steps:

1. Select reference route

Since the locations of the departure and arrival ports have been input into the world map, the reference route between these two ports is selected from shortest distance route or commonly used route from practical view. As the shortest distance on earth surface is great circle distance, the Great Circle Route (GCR) is normally taken as the shortest distance route. For the GRIDS system development between Los Angeles Offshore and Chiba, Japan, as presented in Figure 59, the GCR (orange dashed line) between these two ports is selected as the reference route. For the GRIDS system development between Lagos, Nigeria and Barcelona, as presented in Figure 60, the commonly used route recorded in noon reports (red dashed line) is selected as reference route.

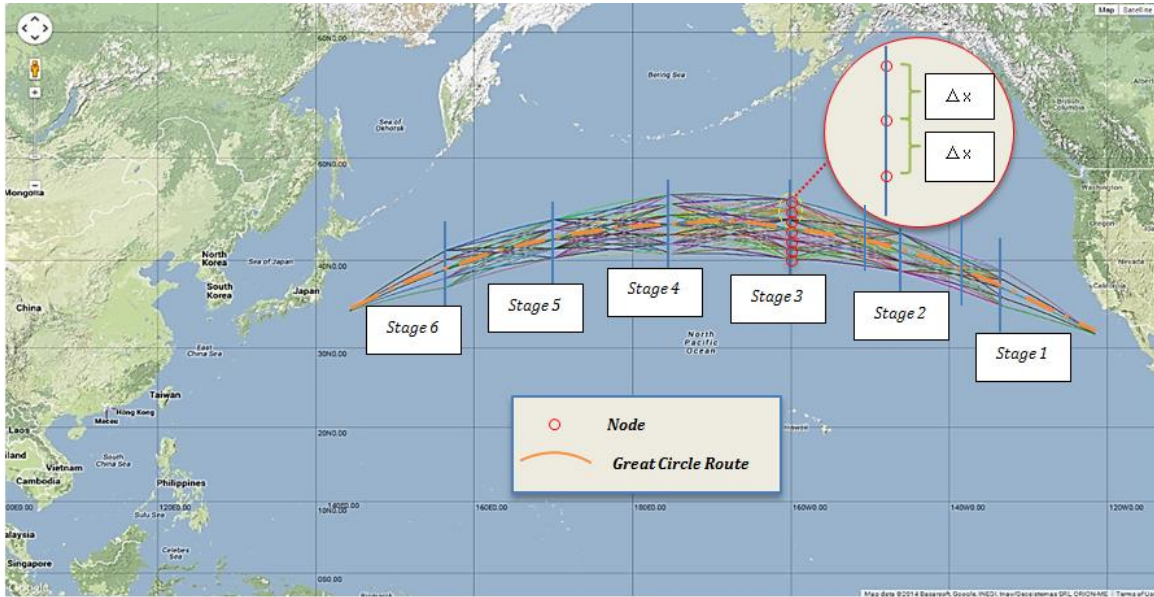


Figure 59: Grids example for the route between Los Angeles Offshore, United States and Chiba, Japan



Figure 60: Grids example for the route between Lagos, Nigeria and Barcelona, Spain

## 2. Determine stages and nodes

The amount of stages and nodes and the distribution of stages and nodes are the two elements in determining the density of the grid, the route legs distribution and then navigation district. The number of stages and quantity of nodes in each stage are determined according to the total distance of voyage and the availability of computing

capacity. Large amount of stages and nodes create high density grids, which is helpful to track the weather changes in route legs but require more computing time for voyage optimization. Small amount of stages and nodes create low density grids, which is helpful to save computing time for voyage optimization but may ignore the weather changes in some route legs. As the weather forecast is updated every 6 hours and the voyage optimization is supposed to be carried out with the weather forecast update frequency, the computing time for voyage optimization is expected to be as short as possible and no more than 6 hours. Therefore, it is flexible in determining the amount of stages and nodes, and the principle is balancing the density of grids and computing time for voyage optimization from practical view.

In general, the stages are supposed to be equally distributed along the reference route, and the nodes on each stage are expected to be distributed on both sides of reference route while keeping the identical space between adjacent nodes. As presented in Figure 59, the GCR (orange dashed line) is equally divided by 6 stages, and the nodes in each stage are equally distributed with unique longitude. From Stage 1 to Stage 6, there are 5 nodes, 5 nodes, 7 nodes, 7 nodes, 5 nodes, 5 nodes on corresponding stage. On each stage, the distance between the adjacent nodes is  $\Delta x$ . However, the distribution of stages and nodes also depends on the land/shallow water conditions of specific route. When the reference route is close to land or passing channels, the distribution of stages and nodes need to be adjusted manually. As presented in Figure 60, according to the 12 days voyage recorded in noon reports, the reference route (red dashed line) is divided unevenly by 11 stages. For land and shallow water avoidance, there is only one node on Stage 1, Stage 2 and Stage 11. For crossing the Strait of Gibraltar, there is only one node on Stage 10. There are 3 nodes on the rest stages. For land avoidance, the distance between the adjacent nodes on Stage 8 is not identical. Therefore, it is also flexible in determining the distribution of stages and nodes. As the

development of GRIDS system is the precondition of route selection for voyage optimization, the distribution of stages and nodes is able to provide the solution for land avoidance in voyage optimization.

## 6.4 Integration of Weather forecast and GRIDS System

For the integration of weather forecast and GRIDS system, 'Latitude', 'Longitude', and 'Time' are the three parameters of their links. Based on the positions of the departure port and destination, a program used for developing GRIDS system is written in Matlab. The combinations of potential routes between these two ports are developed and presented by the GRIDS system. In this study, the nodes and potential routes are plotted on the digital world map, which is developed using the google maps Application Programming Interface (Google maps API). Thus the 'Latitude' and 'Longitude' are included in GRIDS system. With the input of departure time and ETA, the average speed of each potential route is determined, which indicate that the arriving time of any position (latitude and longitude) in each potential route is fixed. Thus, the 'Time' is included in GRIDS system.

For example, in the route between Lagos, Nigeria and Barcelona, Spain (Figure 60), 2187 potential routes are computed by the GRIDS system. For each potential route, the 'Latitude', 'Longitude', and 'Time' of each node are sent to weather forecast module, and the corresponding significant wave height, wind speed and direction are read from the weather forecast provided by NOAA. As Beaufort number (BN) is the interface parameter between the semi-empirical operational performance model and GRIDS system, the significant wave height and wind speed needs to be converted into BN. The Beaufort number is also known as the Beaufort scale, which is an empirical measure describing the observed sea conditions, as presented in Table 24. Therefore, the BN and sea direction are returned to GRIDS system from weather forecast module

Table 24: Specifications of Beaufort scale (Met Office, retrieved 2015)

Beaufort wind scale	Mean Wind Speed		Limits of wind speed		Wind descriptive terms	Probable wave height	Probable maximum wave height	Seastate	Sea descriptive terms
	Knots	ms <sup>-1</sup>	Knots	ms <sup>-1</sup>					
0	0	0	<1	<1	Calm	-	-	0	Calm (glassy)
1	2	1	1-3	1-2	Light air	0.1	0.1	1	Calm (rippled)
2	5	3	4-6	2-3	Light breeze	0.2	0.3	2	Smooth (wavelets)
3	9	5	7-10	4-5	Gentle breeze	0.6	1.0	3	Slight
4	13	7	11-16	6-8	Moderate breeze	1.0	1.5	3-4	Slight - Moderate
5	19	10	17-21	9-11	Fresh breeze	2.0	2.5	4	Moderate
6	24	12	22-27	11-14	Strong breeze	3.0	4.0	5	Rough
7	30	15	28-33	14-17	Near gale	4.0	5.5	5-6	Rough-Very rough
8	37	19	34-40	17-21	Gale	5.5	7.5	6-7	Very rough - High
9	44	23	41-47	21-24	Strong gale*	7.0	10.0	7	High
10	52	27	48-55	25-28	Storm	9.0	12.5	8	Very High
11	60	31	56-63	29-32	Violent storm	11.5	16.0	8	Very High
12	-	-	64+	33+	Hurricane	14+	-	9	Phenomenal

For the long distance voyage, it also needs to be noted that the arriving time of some nodes may exceed the period of weather forecast. The route between Lagos and Barcelona is a 12 days voyage while the period of weather forecast provided by NOAA is 7 days. Under this circumstance, the sea conditions of those nodes (whose arriving time is more than 7 days) are temporarily assumed to be identical with that of the 7<sup>th</sup> day, and then updated according to the latest weather forecast and location of the ship.

## 6.4 Chapter Summary

This chapter has introduced the access and properties of weather forecast and historical sea conditions records, and the development of GRIDS system.

As the 'Latitude', 'Longitude', and 'Time' are all included the GRIDS system, the sea conditions of any point on each potential route at specific time are available to be outputted by utilizing the weather forecast module.

The next chapter will clarify the integration of the semi-empirical ship operational performance model with the GRIDS system and illustrate how to achieve weather routing and speed optimization for voyage optimization.

# **Chapter 7 – WEATHER ROUTING AND SPEED OPTIMIZATION FOR VOYAGE OPTIMIZATION**

---

## **7.1 Chapter Overview**

This chapter will introduce the integration of the proposed semi-empirical ship operational performance prediction model with GRIDS system (§7.2), clarify how to select optimum route for weather routing, (§7.3) followed by a case study of optimum route selection, present the approach of optimal speed set selection for speed optimization in given environment and route, (§7.4) followed by two case studies of speed management. The effect of weather routing and speed optimization on fuel savings will be clarified.

## **7.2 Integration of the Semi-empirical Ship Operational Performance Modelling with GRIDS system**

As the proposed semi-empirical ship operational performance model has been validated to provide accurate ship performance prediction under varying weather and sea states while the GRIDS system has been developed to provide potential routes with corresponding weather and sea states forecast, the ship operational performance modelling in potential voyage routes is achieved by integrating the semi-empirical ship operational performance model with the GRIDS system. Based on this modelling tool, weather routing and speed optimization are developed in this research for voyage optimization.



### 7.2.1 Statement of Parameters

In GRIDS system, as described in Chapter 6.3, each potential route is divided into route legs by stages and a certain quantity of nodes is located on different stages. The integration of the semi-empirical ship operational performance model with GRIDS system includes several parameters, which will be discussed in the following:

- Number of route legs:

For each potential route, the number of route legs  $N_l$  is determined by the number of stages  $N_s$

$$N_l = N_s + 1 \quad (18)$$

- Great Circle Distance:

Given the departure location  $N_0(x_0, y_0)$  and the terminal location  $N_n(x_n, y_n)$ , where  $x$  and  $y$  are latitude and longitude in degree of the node,  $n = 1, 2, 3 \dots n$ . The great circle distance ( $D_{GC}$ ) between any two nodes is calculated by

$$D_{GC} = \arccos\left(\sin\left(\frac{x_0}{180} \cdot \pi\right) \cdot \sin\left(\frac{x_n}{180} \cdot \pi\right) + \cos\left(\frac{x_0}{180} \cdot \pi\right) \cdot \cos\left(\frac{x_n}{180} \cdot \pi\right) \cdot \cos\left(\frac{y_n}{180} \cdot \pi - \frac{y_0}{180} \cdot \pi\right)\right) \cdot \frac{180}{\pi} \cdot 60 \quad (19)$$

where, the unit of distance is nautical mile.

- Step distance:

The step distance ( $D_{Step}$ ) is the distance between two adjacent nodes on the same route, which is also known as the distance of each route leg. From departure port to destination, each potential route is determined by selecting one node on each stage. Route leg is the connection line between two nodes located in adjacent stage. As the latitude and longitude of each node in the GRIDS system is known, the step distance

is calculating the geometry distance by latitude and longitude, as presented in Formula 19.

- Step relative angle:

The step relative angle ( $RA_{Step}$ ) is the relative angle between the sea direction and ship heading direction of each route leg. The ship heading direction is determined by the latitude and longitude of the nodes on specific route leg. The sea direction is read from weather forecast.

- Engine load

As the actual ship average speed ( $U_{Step}$ ) is fixed and the speed loss due to weather and sea conditions has been modelled by utilizing the semi-empirical ship operational performance model, there is a corresponding calm water speed under varying sea conditions by summing the actual ship speed and speed loss. Based on the calm water resistance modelling (Section 5.3) and propulsion efficiency modelling (Section 5.5), the relation between calm water ship speed and required main engine power has been determined. Therefore, the relation between required main engine power and actual ship speed under varying sea state is determined. The engine load is modelled by dividing the Maximum Continuous Rate (MCR) from the required main engine power.

- Step voyage time:

The step voyage time ( $T_{Step}$ ) is determined by the step distance ( $D_{Step}$ ) and step average speed ( $U_{Step}$ ), as presented in Formula 20

$$T_{Step} = \frac{D_{Step}}{U_{Step}} \quad (20)$$

- Step fuel consumption

By utilizing the main engine performance report (Section 4.4), the step specific fuel oil consumption rate ( $SFOC_{Step}$ ) is determined by the main engine load. The step fuel consumption ( $FC_{Step}$ ) is determined by step specific fuel oil consumption rate ( $SFOC_{Step}$ ) and step voyage time ( $T_{Step}$ ), as presented in Formula 21.

$$FC_{Step} = SFOC_{Step} \times T_{Step} \quad (21)$$

- Total voyage time

The total voyage time ( $T_{Total}$ ) of each potential route is determined by summing the step voyage time, as presented in Formula 22.

$$T_{Total} = \sum_{i=1}^k T_{Step_i} \quad (22)$$

where,  $k = 1, 2, 3 \dots N_i$

- Total fuel consumption

The total fuel consumption ( $FC_{Total}$ ) of each potential route is determined by summing the step fuel consumption ( $FC_{Step}$ ), as presented in Formula 23.

$$FC_{Total} = \sum_{i=1}^k FC_{Step_i} \quad (23)$$

### 7.2.2 Fuel Consumption Modelling between Two Stages

For integrating the semi-empirical ship operational performance model with GRIDS system, *Time*, *Latitude* and *Longitude* are the three interface variables. The procedures of determining the fuel consumption for a specific merchant ship between two stages are presented as the following:

1. Setting the average speed between two stages

The average speed is determined based on the total voyage distance and ETA.

2. Loading weather forecast and sea conditions

The step distance between two nodes (on adjacent two stages) is determined by their latitude and longitude. Based on the step distance and average speed, the step voyage time between two stages is determined. According to the departure time, the arrival time of these two nodes are determined and the corresponding weather forecast and sea conditions are loaded into the nodes. Therefore, the average sea conditions between these two nodes are taken as the sea conditions during this route leg.

3. Modelling the relative angle between sea direction and ship heading direction

The details of relative angle between two stages have been clarified in Chapter 7.2.1.

4. Modelling of speed loss

As the weather forecast has been integrated into GRIDS system and the relative angle between two nodes has been determined, the speed loss due to weather and sea conditions is computed based on the proposed the semi-empirical added resistance prediction method.

5. Modelling of required engine power

Different engine power is required to maintain the average speed under varying weather and sea conditions. The average speed and speed loss determine the corresponding calm water speed, which linked to the required engine power. The relation between required main engine power and ship speed under varying sea state is presented in Figure 17.

#### 6. Modelling of fuel consumption

The details of fuel consumption modelling between two stages are presented in the statement of step fuel consumption (Section 7.2.1).

### 7.3 Best Route Selection for Weather Routing

Since the departure date and time, ordered average ship speed during each route leg have been given while the GRIDS system for specific route has been developed, the encountered sea state, encountered angle, the step fuel consumption and voyage time during each route leg, and the total fuel consumption and voyage time of each potential route are simulated by a program written by the author. Then the output of predicted ship operational performance with corresponding routes is recorded in a database. Based on the database, the best route are determined by sorting the parameters of total fuel consumption, encountered sea conditions (evaluated by Beaufort Number), and relative angle between sea directions and ship heading direction. The best routes include:

- The minimum fuel consumption route
- The minimum fuel consumption route with lowest Beaufort Number;
- The minimum fuel consumption route with shortest distance,
- The minimum fuel consumption route with most Head Sea and Bow Sea.

With the positions of the nodes, the best routes are plotted on the world map. A case study of the best route selection for weather routing has been carried out, as presented in Section 7.3.2. As the best routes referred above can be quickly and easily selected from the database, the optimization algorithms are not adopted in weather routing.

As the weather is stochastic, the simulations of ship performance need to be iteratively carried out with the weather forecast update frequency, which is normally 4 times a day. Based on the up-to-date position of the ship, the position of destination port and ETA, the updated total distance and updated average ship speed is determined, which indicates that the variables of *Time*, *Latitude* and *Longitude* are updated. Therefore, the weather forecast in each node of GRIDS system is updated, and the database representing ship operational performance under different potential routes is updated. In an overview of the iterative process, minor changes of the suggested route are expected in a seaway.

### **7.3.1 Constraints for Route Selection**

In this research, Estimated Time of Arrival (ETA) and Land Avoidance are the two constraints adopted to select optimum route for weather routing. The Estimated Time of Arrival (ETA) determines the average voyage speed. The land avoidance determines the selection of reference route and the distribution of grids.

#### **7.3.1.1 Estimated Time of Arrival**

The ETA is simulated by utilizing the function of total voyage time referred in Section 7.2.1. When the arriving time is not strictly limited, the ETA is generally determined by economic ship speed or ship masters' preference. When the arriving time is strictly limited, the average ship speed is determined by dividing ETA from the total voyage distance for a specific route. As the route selection model is updated with the weather forecast updating frequency, and the

sea state might change significantly during a long-term voyage, the ship average speed needs to be iteratively adjusted along her voyage to meet the ETA.

#### 7.3.1.1 Land Avoidance

In this research, there are two solutions to achieve land avoidance:

- Weather forecast based solution

As the ship operational performance in this study is based on weather forecast of sea conditions and there is no sea states forecast on land, the routes go across land are avoided in the route selection from ship operational performance database.

- Grids distribution based solution

As referred in Section 6.3, it is quite flexible in determining the distribution of stages and nodes. For land avoidance, the stages and the nodes are able to be manually distributed. A Grids example for the route between Lagos and Barcelona is presented in Figure 60.

#### 7.3.2 Case Study of Best Route Selection

A case study of best route selection for weather routing has been carried out. With given departure date and time, loading condition, fixed average speed, specific ship noon reports and sea trial data, a set of optimum routes with minimum fuel consumption (Figure 61) can be provided to shipmaster as following,

**Route a** - The blue route is the route with lowest Beaufort Number (low risk to damage the ship and/or its deck cargo; high comfort to passengers) and minimum fuel consumption

**Route b** – The green route is the Great-Circle Route - with shortest distance between two ports on earth as well as the route with shortest time

**Route c** - The violet route is the route with most Head Sea and Bow Sea with minimum fuel consumption

**Route d** - The brown route is the route with minimum fuel consumption

**Route e** - The red route is the frequently used route as recorded in noon report

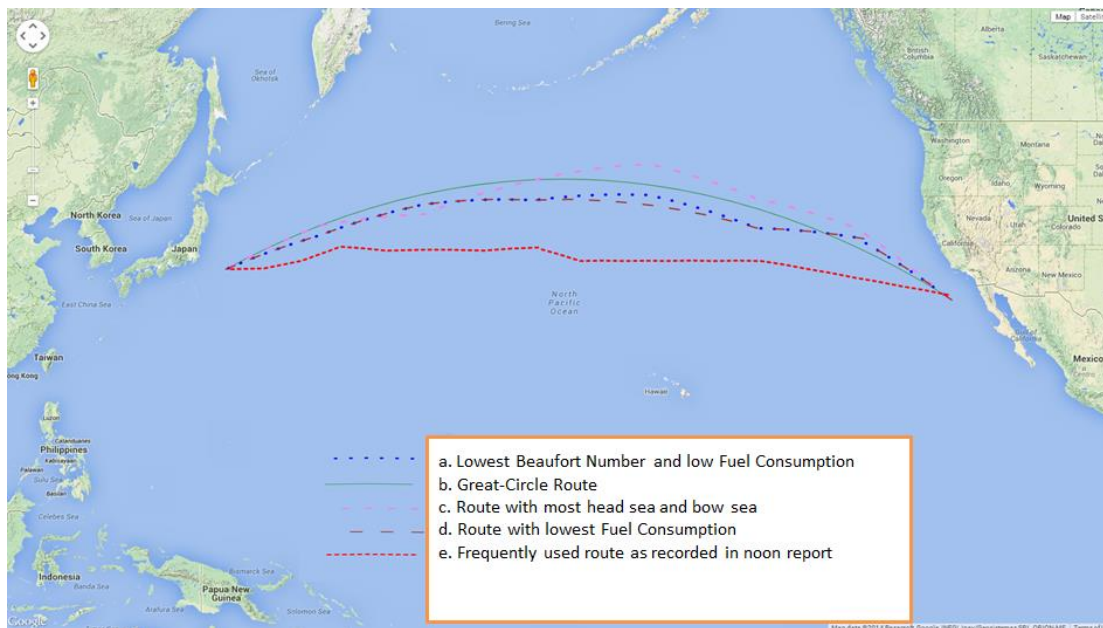


**Figure 61:** Optimum route selection for weather routing (Los Angeles Offshore, United States and Chiba, Japan)

As illustrated in Chapter 6.4 and Chapter 7.2, the weather forecast and semi-empirical ship operational performance model are both integrated with the GRIDS system. Based on the GRIDS system, a ship operational performance database including the step encountered sea state, step relative angle, the step fuel consumption and voyage time during each route leg, and the total fuel consumption and voyage time of each potential route is computed by a MATLAB programme written by the author. As presented in Figure 61, From Los Angeles Offshore to Chiba Japan, the programme is able to generate all potential routes within specific boundary. Based on the departure time and average ship speed, the expected sea conditions are automatically downloaded, and the corresponding ship operational performance along each potential voyage is simulated and output into a database. The



weather routing case in Figure 60 includes 30625 potential routes and the computing time is 6 minutes on a typical desktop PC with a 3.4 GHz Intel-i7 CPU in serial model.

Next, the best routes are selected by sorting specific parameter from the database:

**Route a** – Sorting by the sum of encountered BN, then sorting by total fuel consumption to find out the minimum fuel consumption route with lowest BN along the voyage

**Route b** – Sorting by total distance, then by sorting total fuel consumption to find out the minimum fuel consumption route with shortest voyage time

**Route c** - Sorting by the amount of Head Sea and Bow Sea, then sorting by total fuel consumption to find out the minimum fuel consumption route with most Head Sea and Bow Sea along the voyage

**Route d** - Sorting by the total fuel consumption to find out the minimum fuel consumption route

Based on the best route selection described above, the ship operational performance between the selected best routes is compared with that of recorded route in Table 25.

**Table 25:** Comparison of ship operational performance between the selected optimum routes and recorded route

The encountered Beaufort Number (BN), Heading Directions with given departure date & time, loading condition and fixed average speed	Route a			Route b			Route c			Route d			Route e		
	Average BN	Strongest BN	Relative angle	Average BN	Strongest BN	Relative angle	Average BN	Strongest BN	Relative angle	Average BN	Strongest BN	Relative angle	Average BN	Strongest BN	Relative angle
	5	6	Bow	5	5	Bow	5	6	Head	5	5	Bow	5	5	Bow
	5	5	Beam	5	6	Beam	5	5	Bow	5	5	Beam	7	7	Bow
	3	3	Bow	4	4	Bow	5	5	Bow	3	3	Bow	6	6	Head
	3	4	Beam	3	3	Beam	4	4	Beam	3	3	Beam	5	5	Head
	3	4	Beam	4	4	Beam	4	5	Beam	3	4	Beam	5	6	Head
	3	3	Beam	3	3	Beam	4	4	Bow	3	4	Beam	5	5	Head
	1	2	Head	1	2	Head	2	2	Head	1	2	Head	2	2	Bow
Voyage Duration (h)	367.7			366.1			368.5			367.3			392		
Main Engine Fuel Consumption (t)	563.5			561.8			586.4			559.9			623.5		
Fuel saving compared to Route e	9.62%			9.90%			5.95%			10.20%			0		

As presented in Table 25, the step encountered sea state, step relative angle during each route leg, and the total fuel consumption and voyage time of the four optimum routes (Route a, b, c, d) are compared with that of recorded route (Route e). The summary remarks include:

- With fixed average speed, the optimum route with lowest BN (Route a) saves 24.3 hours on total voyage duration and 9.62 % of total fuel consumption than those of the recorded route (Route e).

The comparison results indicate that developed weather routing model is able to select the minimum fuel consumption route while keeping the lowest BN along the voyage.

- With fixed average speed, the shortest distance route (Route b) saves 26.9 hours on total voyage duration and 9.90 % of total fuel consumption than those of the recorded route (Route e).

The comparison results indicate that developed weather routing model is able to select the minimum fuel consumption route while keeping the shortest voyage distance. As the average voyage speed is assumed to be fixed along each potential route, the shortest voyage time route is also represented by the shortest distance route

- With fixed average speed, the optimum route with most Head sea and Bow sea (Route c) saves 24.5 hours on total voyage duration and 5.95% of total fuel consumption than those of recorded route (Route e).

The comparison results indicate that the developed weather routing model is able to select the minimum fuel consumption route while considering specific encountered angle between ship heading direction and sea direction.

- The minimum fuel consumption route (Route d) can achieve 10.20% fuel savings and 25.7 hours on voyage duration compared to those of the recorded route (Route e).

The comparison results indicate that the developed weather routing model is able to select the minimum fuel consumption route, and the fuel savings is up to 10.20%

- In general, regarding the fuel consumption, optimum route selected by the proposed weather routing model is able to save 10% on average compared to that of the recorded route, which indicates the big contribution of weather routing for fuel savings. Besides the fuel savings, the optimum routes are also able to decrease voyage duration by shortening the voyage distance.

## **7.4 Optimal Speed Set Selection for Speed Optimization**

As described in Chapter 3, the speed optimization in this research is achieved by optimal speed set selection. The flowchart of the optimal speed set selection for speed optimization is presented in Figure 62.

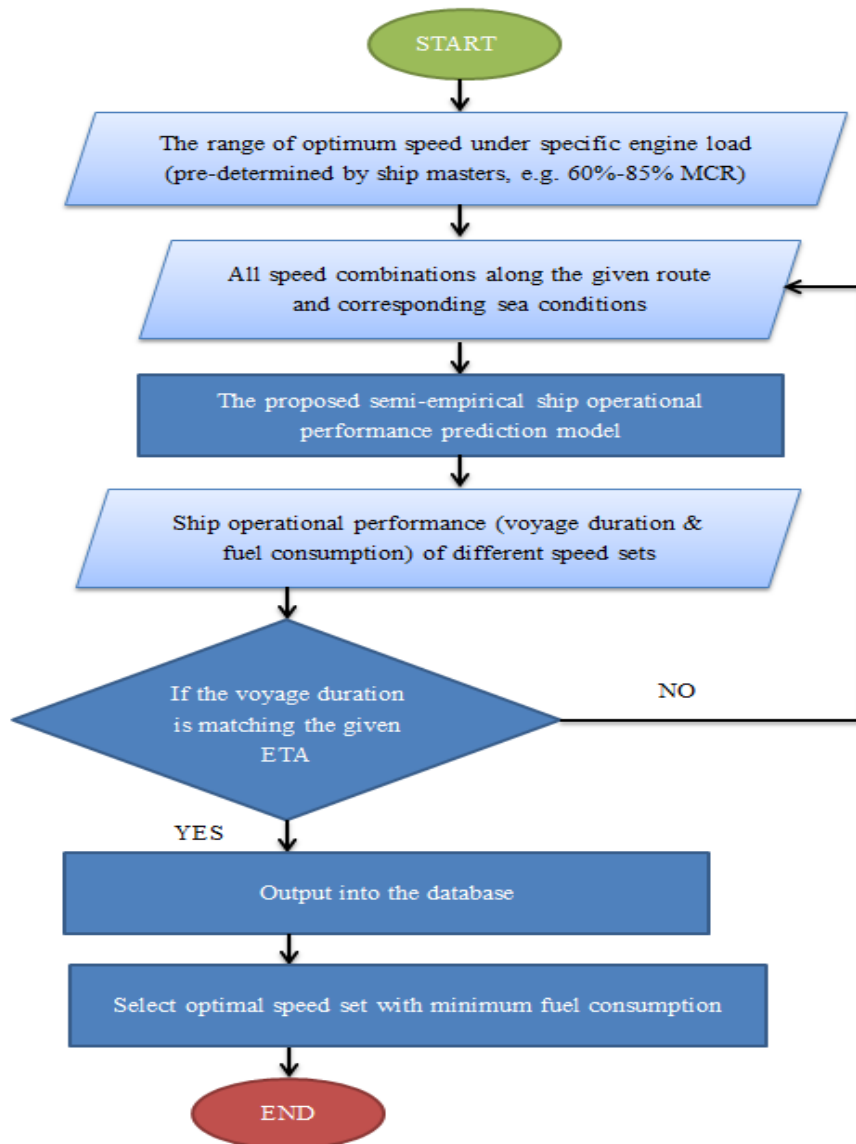


Figure 62: Flowchart of the optimal speed set selection for speed optimization

Firstly, in order to decrease the requirement of computation resources and speed up the optimization process, the main engine power output range is pre-defined by the user. Based on the relation between required main engine power and ship speed under varying sea state (Figure 17), the range of optimum speed is determined by the range of pre-defined main engine load (e.g. 60%-85% MCR), as presented in Table 26 and Table 27.

With a given route, departure date and time, and ship's loading conditions, the corresponding sea conditions with different speed sets are integrated with the GRIDS system. By integrating

the semi-empirical ship operational performance prediction model, the ship operational performance (voyage duration and total fuel consumption) with all possible speed combinations are then modelled.

A speed optimization programme has been written in Matlab. By taking the given ETA (determined by the ship owners/charterers) as constraint, the speed sets whose voyage duration is matching the ETA are identified and output into a database. Then the optimum speed set with minimum fuel consumption is determined by sorting the fuel consumption in the database.

In order to study the effect of speed optimization on fuel consumption savings, the predicted fuel consumption with optimal speed set has been compared with the recorded fuel consumption while maintaining the same ETA, as presented in Table 26 and Table 28. Besides the study of fuel savings contributed by speed optimization, it would also be interesting to study the effect of speed management on ship operational performance (voyage duration and main engine fuel consumption) when the recorded speed set is available. Therefore, the ship operational performance with the optimal speed set (Speed Set B) is compared with that of recorded speed set (Speed Set A): Speed Set A - Actual voyage speed as recorded in ship noon report

- Speed Set B - Optimum speed with identical ETA in actual voyage

#### *7.4.1 Case Study of Aframax Oil Tanker*

For an Aframax oil tanker, a case study regarding speed management has been carried out. A range of optimum speed is determined with 60% - 85% Maximum Continuous Rating (MCR) of the main engine. In this case study, the range of optimum speed under specific BN has been concluded in Table 26.

**Table 26:** The range of optimum speed under specific BN for an Aframax oil tanker

BN	Optimum speed range (knots)	
	60%MCR	85%MCR
1-3	13.9	15.6
4	13.8	15.4
5	13.2	14.8
6	11.7	13.2

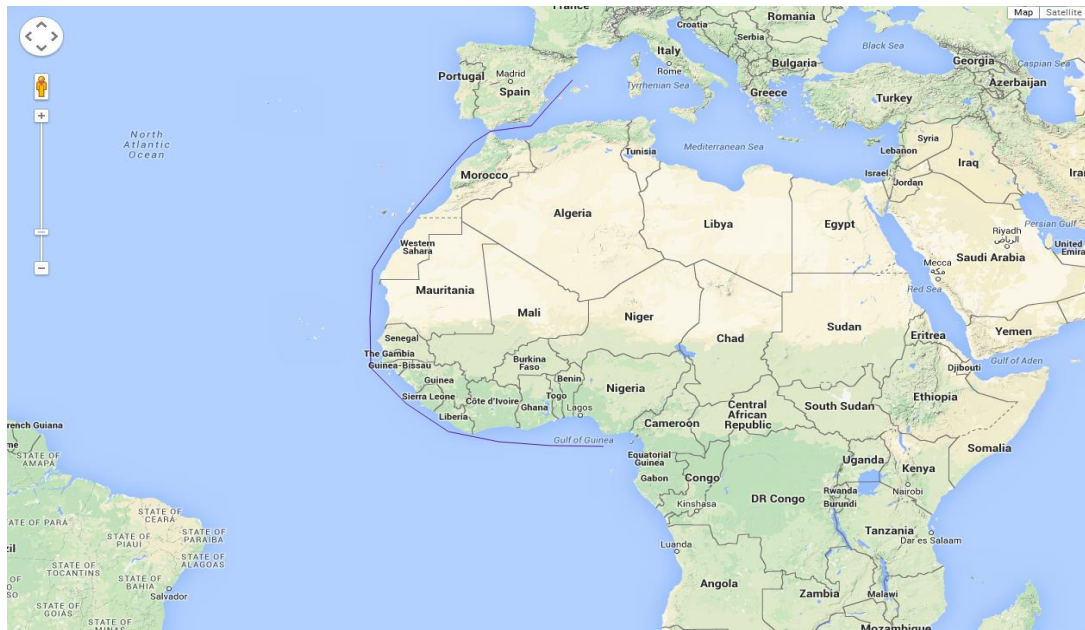


**Figure 63:** Selected commercial trade route (Lagos, Nigeria – Barcelona, Spain) for an Aframax oil tanker (Google map API, 2015)

**Table 27:** Comparison of ship operational performance with different speed sets for an Aframax oil tanker

Date	Average BN	Strongest BN	Relative Angle	Speed Set A (Recorded)	Speed Set B (Optimum)
Day 1	4	4	Bow Sea	13.5	13.8
Day 2	4	4	Bow Sea	13.2	13.8
Day 3	4	5	Bow Sea	13.4	13.8
Day 4	4	4	Bow Sea	13.5	13.8
Day 5	3	3	Head Sea	13.6	14.2
Day 6	4	5	Bow Sea	13.4	13.8
Day 7	5	5	Head Sea	13.2	12.4
Day 8	6	6	Head Sea	13.2	10.3
Day 9	5	5	Head Sea	13.1	12.4
Day 10	4	4	Head Sea	13.3	13.8
Day 11	4	5	Head Sea	13.5	13.8
Day 12	3	4	Head Sea	13.2	14.2
Voyage Duration (h)				283	283
Main Engine Fuel Consumption (t)				477	465
Fuel savings compared to Speed Set A (%)				0	2.52

For the selected 12 days voyage route, as presented in Figure 63, the ship operational performances of an Aframax oil tanker with recorded and optimum speed set have been compared, as presented in Table 27. While keeping the same sea states and ETA, 2.52% of total Heavy Fuel Oil (HFO) consumption is saved by utilizing the optimum speed set.

#### 7.4.2 Case Study of Post-panamax Container Ship

For a Post-panamax container ship, a case study regarding speed management has been carried out. A range of optimum speed is determined with 60% - 85% MCR of main engine for each BN and the results are provided in Table 28.

**Table 28:** The range of optimum speed under specific BN for a Post-panamax Container ship

BN	Optimum speed range (knots)	
	60%MCR	85%MCR
1-3	15.2	24.2
4	15	22.4
5	14.6	22.2
6	14.2	21.5

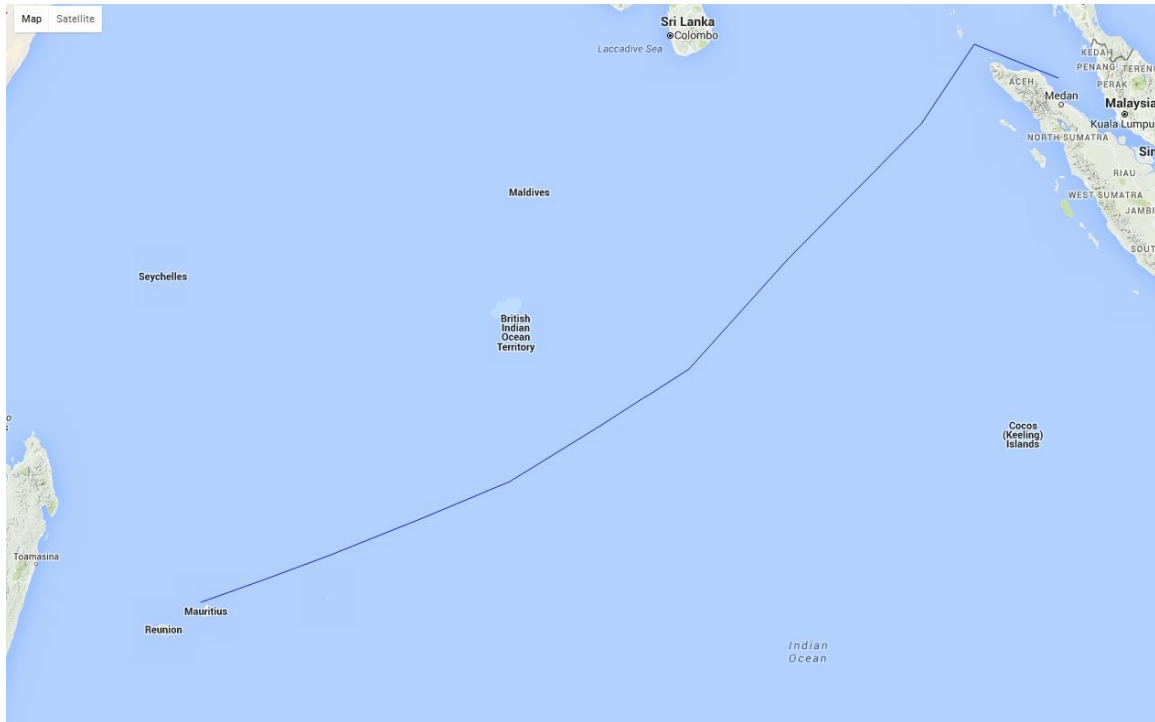


Figure 64: Selected commercial trade route (Penang, Malaysia – Port Louis, Mauritius) for a Post-panamax container ship (Google map API, 2015)

For the selected 5 day voyage, as presented in Figure. 64, the ship operational performances of the Post-panamax container ship with different speed set have been compared, as presented in Table 29. While keeping the same sea states and ETA, 1.03% of total HFO consumption is saved by utilizing the optimum speed set.

Table 29: Comparison of ship operational performance with different speed sets for a Post-panamax container ship

Date	Average BN	Strongest BN	Relative Angle	Speed Set A (Recorded)	Speed Set B (Optimum)
Day 1	5	5	Head Sea	21.2	19.8
Day 2	3	4	Beam Sea	20.9	21.9
Day 3	4	5	Beam Sea	21.3	21.7
Day 4	4	4	ollowing Se	21.4	21.7
Day 5	5	5	Beam Sea	21.4	21
Voyage Duration (h)				128	128
Main Engine Fuel Consumption (t)				681.7	674.7
Fuel savings compared to Speed Set A (%)				0	1.03



Based on the case studies of one 12 day voyage for an Aframax oil tanker and one 5 day voyage for a Post-panamax container ship, 2.52% and 1.03% of total HFO consumption can be saved respectively by utilizing optimum speed set while keeping recorded ETA and sea conditions. Between 2010 and 2012, the Aframax oil tanker sails around 263 days annually, 263.4 t HFO (820.3 t  $CO_2$  emission) is potential to be saved per year by utilizing optimum speed set. The Post-panamax container ship sails around 180 days annually, 252.8 t HFO (787.3 t  $CO_2$  emission) is potential to be saved per year by utilizing optimum speed set.

Besides the technology of speed optimization, considerable amount of fuel consumption and  $CO_2$  emission can also be saved by the ‘chartering’ of a ship. The relation between the ETA and fuel consumption provides a reference for ship charterers. Therefore, the ship owner/charterer can easily determine the ETA regarding the fuel savings and environmental issue.

## 7.5 Chapter Summary

This chapter has presented the integration of ship operational performance modelling with GRIDS system by introducing the interface parameters and the procedures of fuel consumption modelling between two stages. Constraints for route selection have been introduced and a case study of best route selection for weather routing has been carried out to illustrate the potential fuel savings. By utilizing the weather routing tool, up to 11% of fuel savings can be achieved.

The optimal speed set selection for speed optimization has been clarified. The ship operational performance with optimal speed set was compared to the actual operational performance while maintaining the same ETA. The fuel savings and the reduction of  $CO_2$  emission by utilizing speed optimization are illustrated. This speed optimization tool provides a great opportunity for ship operators to plan the voyage with minimum fuel consumption for a given route.

The next chapter will present a discussion on the finding of this study, along with the novelties and contributions to the field.

# Chapter 8 – DISCUSSION

---

## 8.1 Chapter Overview

This chapter will present the achievements of research aims and objectives of the study discussed in this thesis (§8.2), highlight the novelties and contributions to the field, especially answer the research question raised in this thesis (§8.3), and end with a discussion of the shortcomings

## 8.2 Achievement of Research Aims and Objectives

With respect to the research aims and objectives, the achievements of this research are summarized as following:

- *To develop an easy-to-use and practical model to accurately predict added resistance for specific ship type under specific speed, wave angle encountered, and sea state.*

Based on the critical review of the existing added resistance model, the research gap has been identified that an easy-to-use and practical model to accurately predict added resistance for specific ship types under specific speed, wave angle encountered and sea state is missing. Although the analytical or experimental methods can provide reasonable ship added resistance prediction. However, in actual voyage optimization application field, the ship operational performance prediction is requested to be updated every 6 hours, corresponding to weather forecast update frequency. During the 6 hours, the added resistance due to varying sea states, wave angle encountered, speeds, together with ship fouling effect is required for the ship operational performance prediction in the following ship voyage.

As the ship operational performance prediction by utilizing analytical added resistance prediction methods will demand a tremendous amount of computing; the experimental methods require model development and towing tank tests, which normally cost rather long time and are often adopted within design stage, these methods are not suitable for ship operators and managers who need to determine the voyage quickly.

The ship operational performance prediction by utilizing empirical added resistance prediction methods are simple enough for voyage management procedures, but the existing empirical methods are normally only related to a general ship type other than involving the ship particulars and ship conditions of specific merchant ship. Therefore, the semi-empirical added resistance prediction method developed based on actual operational data has been proposed in this thesis. It can accurately predict added resistance of specific oil tanker and container ship under specific speed, wave angle encountered and sea state.

- *To develop an easy-to-use and practical method to predict the specific ship operational performance under specific speed, wave angle encountered, sea state, fouling effect and engine performance degradation condition.*

Based on the critical review of ship operational performance modelling, the trend assembles method and regression method are both simple enough to be integrated with voyage management, but these two methods require huge amounts of ship performance data, and the accuracy of ship performance modelling is quite dependent on the accuracy of ship voyage records, which might be not good enough to quantify the ship performance degradation. The hydrodynamic method; system identification method; and bond graph method can provide very reasonable ship performance prediction. But the propeller open-water diagram, wake fraction, wind resistance coefficients, wave response resistance coefficients and thrust deduction fraction are the parameters partially or fully requested for utilizing these three

methods. In actual industry field, it is often infeasible for ship owner or ship charterer to access those documents/values of the parameters. Thus the prediction of ship operational performance using the referred hydrodynamics analysis method, system identification method, and bond graph method may be unavailable or not accurate enough due to lacking of necessary documents/values of the parameters. Therefore, the easy-to-use and practical semi-empirical ship operational performance prediction model has been proposed in this study. The proposed model can accurately predict the specific ship operational performance under specific speed, wave angle encountered, sea state, fouling effect and engine performance degradation condition. The fouling effect and engine performance degradation conditions are also involved in proposed model.

- *To validate the accuracy of the ship operational performance prediction for specific merchant ship types using actual ship operational data*

In order to validate the accuracy and suitability of the semi-empirical ship operational performance prediction model for oil tankers and container ships, the proposed model has been applied on another oil tanker and container ship. Under the same speed, loading condition, wave angle encountered and sea states, the predicted ship operational performance was compared to the actual ship operational performance data. The statistical analysis of the error between the predicted performance and recorded performance has been carried out as well. In summary, there is a good agreement between the predicted operational performance and the actual operational performance.

- *To select optimum routes for weather routing by evaluating encountered weather and sea state, passage time, and minimum fuel consumption*

The integration of weather forecast with GRIDS system have been introduced in Chapter 6, and the integration of the proposed semi-empirical ship operational performance prediction

model with GRIDS system has been introduced in Chapter 7. Thus the GRIDS system is able to provide the ship operational performance under different potential routes. By utilizing the optimum route selection tool, the optimum routes are selected by weighting encountered weather and sea state, passage time, and minimum fuel consumption.

- *To develop an approach to select optimum speed set for speed optimization while keeping the Estimated Time of Arrival (ETA) fixed, and illustrate the effect of speed management for energy efficient shipping in actual commercial trade routes*

A speed optimization program has been written by the author to select the optimal speed set for minimum fuel consumption while maintaining the fixed ETA. Two case studies have been carried out and indicated that 1 - 3% of fuel consumption can be saved by utilizing optimal speed set for oil tanker and container ship for a given sea state. By evaluating the ship operational performance with other optional speed sets, large amount of fuel savings can be achieved with small delay on ETA. Conversely, a large amount of extra fuel is consumed by earlier arrival compared to ETA. Based on the study of the relation between different ETA and corresponding fuel consumption for specific commercial ships, the ship charterer is able to determine the ship scheduling with higher energy efficiency and lower  $CO_2$  emissions.

### **8.3 Novelties and Contributions to the Field**

The main contribution of this PhD study is the development of an easy-to-use and practical semi-empirical added resistance prediction model and the corresponding semi-empirical ship operational performance prediction model for oil tanker and container ship in varying weather conditions. Based on the validation studies, it has been verified that the proposed model is able to provide accurate prediction of main engine fuel consumption rate under varying sea states, wave angle encountered, speeds, and ship fouling effect for specific oil

tanker and container ship. The effect of fouling conditions can be examined by using this model. According to the development procedures of the proposed model for oil tanker and container ship, the development of the semi-empirical ship operational performance prediction model for other ship types will be inspired.

Based on the proposed ship operational performance prediction model, the program for weather routing and the program for speed optimization have been written by the author. In this research, voyage optimization is achieved by weather routing and speed optimization.

Corresponding to the research question which was posed:

*“Is it possible to develop an easy-to-use and practical approach to accurately model the operational performance regarding weather conditions for specific merchant ship, and based on this good user-acceptance approach to select optimum route and optimal speed set for voyage optimization and energy efficient shipping?”*

The short answer to this question is yes. The benefits of using the semi-empirical ship operational performance prediction model to select optimum route include:

- Easy-to-use, huge amount of ship daily reports are not necessary to develop the ship operational performance model, tremendous amount of computing by using analytical added resistance prediction methods can be avoided.
- Accurate, the prediction of ship operational performance can be provided for each specific ship, currently available for oil tankers and container ships.
- Flexible, as the proposed semi-empirical ship operational performance prediction model is quite easy-to-use and has been written as an executable program, the user of the optimum route selection tool is able to test the ship operational performance of the

self-designed routes with different speed sets, which can dramatically increase the user-acceptance.

## 8.4 Shortcomings

Besides the novelties and contributions of the thesis, there are also shortcomings of the proposed model and optimum route selection tool for voyage optimization which should be addressed.

- Due to the limitations of the amount of actual ship operational performance for different oil tankers and container ships, the proposed semi-empirical added resistance model and ship operational performance model have not been validated with a lot of different ships. There is a potential to further improve the proposed semi-empirical added resistance formulae by including more ship characteristics.
- Due to the uncertainties generated from dry-docking procedures, the time-dependent correction after dry-docking varies for each specific ship. The accurate time-dependent correction after dry-docking requires the actual ship performance records.
- The ocean surface currents and safety constraints have not been included in weather routing and speed optimization.
- The best route selection for weather routing and optimal speed set for speed optimization are manually selected from the database, this process can be made faster by integrating optimization algorithm.
- There is non-filtered nature of the performance data for the co-directional wind and wave, which may potentially cause error for the container ship cases.



## 8.5 Chapter Summary

This chapter has presented a discussion of how the aims and objectives of the research have been fulfilled and answered the research question raised in the thesis.

The next chapter will present the conclusions which have been drawn from this study.

# Chapter 9 – CONCLUSIONS AND RECOMMENDATIONS FOR FUTURE RESEARCH

---

## 9.1 Chapter Overview

This chapter will present the concluding remarks (§9.2), and recommendations for future research (§9.3).

## 9.2 Concluding Remarks

As the increasing attention focused on the low carbon shipping and fuel-efficient ship operations have been brought to the attention of IMO, the SEEMP has been made mandatory by the IMO since 1<sup>st</sup> January 2013 for all ships engaged in international trade. While at the same time there is a fierce competition in shipping market, which implies that it is almost a necessity to improve the existing solutions and approaches for voyage optimization. From practical view, the development of an easy-to-use and accurate ship operational performance prediction model will dramatically increase the user-acceptance of voyage optimization.

In this study, the concluding remarks include the following:

- By utilizing the actual ship operational performance data, the empirical added resistance prediction formulae have been modified and developed for oil tankers and container ships in a semi-empirical way
- Based on the proposed semi-empirical added resistance formulae, the calm water resistance model, propulsion efficiency model, main engine performance model, and fouling effect and engine performance degradation performance corrections, the semi-

empirical ship operational performance prediction model for oil tanker and container ship has been developed. The average absolute error between the predicted fuel consumption rate and the recorded fuel consumption rate reaches 5%, the coefficient of determination reaches 85%, which indicate a very accurate ship operational performance prediction. Based on the proposed performance prediction model, it is able to develop an easy-to-use tool to plan and optimize the ship voyages to save fuel consumption and reduce GHG emissions.

- With fixed ETA, up to 10% fuel savings compared to the recorded fuel consumption can be achieved by weather routing.
- With fixed ETA, 1-3% of fuel savings compared to the recorded fuel consumption can be achieved by speed optimization.
- The voyage optimization tools can contribute to energy efficient shipping, however the user-acceptance of the voyage optimization needs to be satisfied with users as well. From practical view, a route should be created under the supervision of charterers and captains.

### **9.3 Recommendations for Future Research**

Based on the shortcomings addressed in Chapter 8, the recommendations for future work in this specific field are briefly outlined below.

- More validation studies of oil tankers and container ships size with different sizes might need to be carried out
- It would be interesting to examine the applicability of the semi-empirical model for other ship types, such as LNG and passenger ships.

- With the dry-docking reports including the information of painting strategy, treatment to the hull surface/propeller damage, and main engine maintenance strategy, it would be interesting to study the strength of different anti-fouling paintings on fuel savings
- It would be helpful to increase the accuracy of time-dependent correction for commercial ships by considering their operational zones.
- The integration of trim on ship operational performance prediction might increase the ship operational performance prediction accuracy
- The involvement of ocean surface currents and safety constraints in weather routing will increase the quality of optimum route selection
- It would be more reasonable to study the added resistance due to wave and wind respectively for container ships.
- The integration of optimization algorithm in weather routing is quite likely to save computing time dramatically, which should be studied in the future.
- The self-learning system, which will record the actual ship operational performance and the feedback from users, should be developed
- Weather routing for the commercial ship with wind-assisted technology (Kites and Rotors) is an interesting topic to be studied.

## 9.4 Chapter Summary

This chapter summarised the concluding remarks of this study. The recommendations on future research have been made.

# REFERENCE

---

Aas-Hansen, M., 2010 *Monitoring of hull condition of ships*, Norwegian University of Science and Technology, M.Sc. Thesis.

<http://www.diva-portal.org/smash/get/diva2:378149/FULLTEXT01.pdf>

Abkowitz, M. A., 1980 *Measurement of Hydrodynamic characteristics from ship maneuvering trials by system identification*, SNAME transactions, vol. 88 pp. 283-318

Abkowitz, M. A., 1988 *Measurement of ship resistance from simple trials during a regular voyage*, Report no. MA-RD-840-88019, Massachusetts institute of technology, Department of Ocean Engineering, Cambridge, Massachusetts

Abkowitz, M. A., 1989. *Use of system identification techniques to measure the ship resistance, powering and manoeuvring coefficients of the Exxon Philadelphia and a submarine from simple trials during a routine voyage*. 22<sup>nd</sup> American Towing Tank Conference 1989, pp. 363.

Aertssen, G., 1969. *Service Performance and Trials at Sea*, Report of Performance Committee 12<sup>th</sup> ITTC, Rome, 1969

Aertssen, G. and van Sluys, M. F., 1972. *Service Performance and Seakeeping Trials on a Large Containership*, RINA, October.

Alexandersson, M., 2009. *A Study of Methods to Predict Added Resistance in Waves, Performed at Seaware AB*

- Alvarez, J.F., Longva, T. and Engebretsen, E.S. (2010) 'A methodology to assess vessel berthing and speed optimization policies'. *Maritime Economics & Logistics* 12, 327–346.
- Andersen, P., Borrod, A., and Blanchot, H. (2005) "Evaluation of the service performance of ships" *Marine Technology*, Vol. 42, No. 4. October 2005 pp. 177-183
- Ballou, P., Chen, H. & Horner, J. D., 2008. *Advanced Methods of Optimizing Ship Operations to Reduce Emissions Detrimental to Climate Change*. OCEANS 2008 Conference, MTS/IEEE Proceedings.
- Bellman, R. E., 1957. *Dynamic Programming*. Princeton: Princeton University Press.
- Bijlsma, S. J., 1975. *On Minimal-Time Ship Routing*. PhD Thesis. Royal Netherlands Meteorological Institute, Delft University of Technology.
- Bijlsma, S. J., 2001. *A Computational Method for the Solutions of Optimal Control Problems in Ship Routing*. *Navigation*, 48 (3), pp. 145-154.
- Bijlsma, S. J., 2002. *On the Applications of Optimal Control Theory and Dynamic Programming in Ship Routing*. *Navigation*, 49 (2), pp. 71-80.
- Bijlsma, S. J., 2004. *A Computational Method in Ship Routing Using the Concept of Limited Manoeuvrability*. *Journal of Navigation*, 57 (3), pp. 357-369.
- Bijlsma, S. J., 2008. *Minimal Time Route Computation for Ships with Pre-Specified Voyage Fuel Consumption*. *Journal of Navigation*, 61, pp. 723-733.
- Boese, P., 1970. *Eine einfache Methode zur Berechnung der Widerstandserhöhung eines Schiffes im Seegang*. *Journal Schiffstechnik – Ship Technology Research* 17 (86).

- Broeninck, J.F. (2000). *Introduction to Physical Systems Modelling with Bond Graphs*, University of Twente, Dept EE, Control Laboratory.
- Bunker Index, IFO 380 price in Port Singapore, Rotterdam and Fujairah. Website: <http://www.bunkerindex.com/> [Accessed Aug 2014].
- Calvert, S., 1990. *Optimal weather routeing procedures for vessels on trans-oceanic voyages*. PhD thesis, University of Plymouth.
- Calvert, S., Deakins, E. and Motte, R., 1991. *A Dynamic System for Fuel Optimisation Trans-Ocean*. *Journal of Navigation*, 44 (2), pp. 233-265.
- Chen, W. Y., 1990. *Interannual variability of skill of NMC medium-range forecasts over the Pacific/North America Sector*. *Mon Wea. Rev.*, 118: 179-188.
- Christiansen, M., Fagerholt, K. & Ronen, D., 2004. *Ship Routing and Scheduling: Status and Perspectives*, *TRANSPORTATION SCIENCE*. Vol. 38, No. 1, pp. 1-18.
- Christiansen, M., Fagerholt, K., Nygreen, B. & Ronen, D., 2013. *Ship Routing and Scheduling in the new millennium*, *EUROPEAN JOURNAL OF OPERATIONAL RESEARCH*. Volume 228, Issue 3, pp. 467-483
- Corbett, J.J., Wang, H. and Winebrake, J.J. (2010) ‘*The effectiveness and costs of speed reductions on emissions from international shipping*’. *Transportation Research* 14D, 593–598.
- Corbett, J. J., Winebrake, J. J., Comer, B. & Green, E., 2011. *Energy and GHG emissions savings analysis of fluoropolymer foul release hull coating*, *Energy and Environmental Research Associates, LLC* [Online]. Available:



<http://www.theengineer.co.uk/Journals/1/Files/2011/2/21/20110215b%20International%20Paint%20Report.pdf>.

De Wit, C., 1990. *Proposal for Low Cost Ocean Weather Routeing*. Journal of Navigation, 43 (3), pp. 428-439.

Dee, D. P., 2011. *The ERA-Interim reanalysis: configuration and performance of the data assimilation system*. Quarterly journal of the royal meteorological society, Volume 137, Issue 656, Part A, Pages 553-597.

ECMWF. Note by European Centre for Medium-Range Weather Forecasts. Website: <http://apps.ecmwf.int/datasets/data/interim-full-daily/> [Accessed Jan 2016]

Fagerholt, K., Laporte, G. and Norstad, I. (2010) '*Reducing fuel emissions by optimizing speed on shipping routes*', Journal of the Operational Research Society, 61(3), 523-529.

Fagerholt, K. and Ronen, D. (2013) '*Bulk ship routing and scheduling: solving practical problems may provide better results*', Maritime Policy & Management, 40:1, 48-64.

Faltinsen, O. M., Minsaas, K. J., Liapis, N., & Skjoldal, S., 1980. *Prediction of Resistance and Propulsion of a Ship in a Seaway*. Proceedings of the 13<sup>th</sup> ONR Symposium.

Fujii, H., Takahashi, T., 1975. *Experimental Study on the Resistance Increase of a Ship in Regular Oblique Waves*. Proceeding 14<sup>th</sup> ITTC, Vol. 4, pp.351.

Gelareh, S. and Meng, Q. (2010) '*A novel modeling approach for the fleet deployment problem within a short-term planning horizon*'. Transportation Research 46E, 76-89.

- Gelareh, S., Nickel, S. and Pisinger, D. (2010) '*Liner shipping hub network design in a competitive environment*'. *Transportation Research* 46E, 991–1004
- Gerritsma, J. and Beukelman, W., 1972. *Analysis of the resistance increase in waves of a fast cargo ship Intern. Shipbuilding Progress*, 19(217):285-93.
- Google maps API. Website:  
<https://developers.google.com/maps/documentation/javascript/tutorial>  
[Accessed January 2015]
- Guo, BJ, and Steen, S., 2011. *Evaluation of added resistance of KVLCC2 in short waves*. *Journal of Hydrodynamics, Ser. B*, Volume 23, Issue 6, pp 709-722
- Hansen, S. V., 2011. *Performance Monitoring of Ships*.  
[http://orbit.dtu.dk/ws/files/77836530/Soren\\_V\\_Hansen\\_PhD\\_thesis\\_.PDF](http://orbit.dtu.dk/ws/files/77836530/Soren_V_Hansen_PhD_thesis_.PDF)
- Hagiwara, H., 1989. *Weather routeing of (sail-assisted) motor vessels*. PhD thesis, University of Delft, Netherlands.
- Hasselaar, 2010. *An investigation into the development of an advanced ship performance monitoring and analysis system*. PhD thesis.  
<https://theses.ncl.ac.uk/dspace/bitstream/10443/2367/1/Hasselaar%20rest%2012.08.14.pdf>
- Hinnenthal, J., 2008. *Robust Pareto – Optimum Routing of Ships utilizing Deterministic and Ensemble Weather Forecasts*.
- Holtrop, J., Mennen G.G. J., 1982. *An Approximate Power Prediction Method. International Shipbuilding Progress*, Vol. 29, No. 335.

Holtrop, J., 1984. *A statistical re-analysis of resistance and propulsion data*. International Shipbuilding Progress, Vol. 28, pp. 272-276.

IMO, 2009. Note by International Maritime Organization. *Second IMO GHG Study 2009*.

IMO, 2011. Note by International Maritime Organization. *Amendments to the annex of the protocol of 1997 to amend the International Convention for the Prevention Of Pollution from Ships 1972 as Modified n the protocol of 1978 relating thereto* (Inclusion of regulations on energy efficiency for ships in MARPOL Annex VI), MEPC 62/24/Add.1, Annex 19, pg.1,

IMO, 2012. Note by International Maritime Organization. *2012 Guidelines for the development of a SEEMP*, MEPC 63/23, Annex 9.

IMO, 2014. Note by International Maritime Organization. *Third IMO GHG Study 2014 – Final Report*, MEPC 67/INF, pp. 13 -161.

International Chamber of Shipping, 2009. *Shipping, World Trade and The Reduction of CO<sub>2</sub> Emissions – United Nations Framework Convention on Climate Change*  
<http://www.ics-shipping.org/docs/default-source/resources/environmental-protection/shipping-world-trade-and-the-reduction-of-co2-emissions.pdf?sfvrsn=6>

IPCC, 2014. Note by Intergovernmental Panel on Climate Change. *Climate Change 2014: Synthesis Report – Summary for Policymakers*.

[https://www.ipcc.ch/pdf/assessmentreport/ar5/syr/AR5\\_SYR\\_FINAL\\_SPM.pdf](https://www.ipcc.ch/pdf/assessmentreport/ar5/syr/AR5_SYR_FINAL_SPM.pdf)

ISO15016, 2002. *Ships and marine technology – Guidelines for the assessment of speed and power performance by analysis of speed trial data*. International Standard Organisation. 15016

ITTC, 1999. *ITTC – Recommended Procedures and Guidelines – Performance, Propulsion – 1978 ITTC Performance Prediction Method.*

ITTC, 2002. *ITTC – Recommended Procedures – Testing and Extrapolation Methods Propulsion, Performance Propulsion Test, 7.5-02-03-01.1*

ITTC, 2011a. *ITTC – Recommended Procedures - Prediction of Power Increase in Irregular Waves from Model Test, 7.5-02-07-02.2*

ITTC, 2011b. *Specialist Committee on Surface Treatment – Final report and recommendations to the 26<sup>th</sup> ITTC.* Proceedings of 26<sup>th</sup> ITTC – Volume II

ITTC, 2014. Note by International Towing Tank Conference. *Specialist Committee on Performance of Ships in Service – Final Report and Recommendations to the 27<sup>th</sup> ITTC.*

[http://itcc.info/downloads/Proceedings/27th%20Conference%20\(Copenhagen%202014\)/2-3%20Ships%20in%20Service.pdf](http://itcc.info/downloads/Proceedings/27th%20Conference%20(Copenhagen%202014)/2-3%20Ships%20in%20Service.pdf)

JEPPESEN. *Voyage Optimization Supersedes Weather Routing.* Website:  
[http://ww1.jeppesen.com/documents/marine/commercial/white-papers/Voyage\\_Optimization\\_Supersedes\\_Weather\\_Routing.pdf](http://ww1.jeppesen.com/documents/marine/commercial/white-papers/Voyage_Optimization_Supersedes_Weather_Routing.pdf)

[Accessed January 2014]

Journé, J.M.J. and Meijers, J.H.C., 1980. *Ship Routeing for Optimum Performance.* Conference on Operation of Ships in Rough Weather, Transactions IME, London

Kalnay, E., Kanamitsu, M. & Baker, W. E., 1990. *Global Numerical Weather Prediction at the National Meteorological Center.* Bull. Am. Meteorol. Soc., 71: 1410-1428.

- Kashiwagi, M., 1995. *Prediction of Surge and Its Effect on Added Resistance by Means of the Enhanced Unified Theory*, Trans. West-Japan Society of Naval Architects, No. 89, pp. 77-89
- Kashiwagi, M., Ikeda, T., Sasakawa, T., 2010. *Effects of Forward Speed of a Ship on Added Resistance in Waves*. International Journal of Offshore and Polar Engineering, Vol. 20, No. 3, pp. 196-203
- Kim, E., Yoon, H. S., Hong, S. Y., and Choi, Y., 2001. *Evaluation and computer program on the speed trial analysis method of the ongoing work in ISO/TC8*. Practical Design of Ships and Other Floating Structures: Eighth International Symposium – PRADS 2001, pp. 525.
- Klompstra, M., Olsder, G., and van Brunschot, P., 1992. *The Isopone Method in Optimal Control*. Dynamics and Control, 2 (1992), pp. 281-301
- Korving, J., 2011. *Weather routeing for cargo ships*. Master paper of Business Mathematics and informatics (BMI), Vrije Universiteit Amsterdam. Website link: [http://www.few.vu.nl/nl/Images/werkstuk-korving\\_tcm38-179762.doc](http://www.few.vu.nl/nl/Images/werkstuk-korving_tcm38-179762.doc)
- Kuroda, M., Tsujimoto, M., Fujiwara, T., Ohmatsu, S., Takagi, K., 2008. *Investigation on components of added resistance in short waves*. Journal of the Japan Society of Naval Architects and Ocean Engineers, pp. 171-176.
- Kwon, Y.J., 2008. *Speed Loss Due To Added Resistance in Wind and Waves*, the Naval Architect, Vol. 3, pp.14-16.
- Lang, N. and Veenstra, A. (2010) ‘A quantitative analysis of container vessel arrival planning strategies’. OR Spectrum 32, 477–499.

- Liu, S and Papanikolaou, A., 2013. *Added Resistance of Ships in Quartering Seas*. V International Conference on Computational Methods for Coupled Problems in Science and Engineering COUPLED PROBLEMS 2013, Spain.
- Liu, S., Papanikolaou, A. and Zaraphonitis, G., 2015. *Practical Approach to the Added Resistance of a Ship in Short Waves*. Proceeding of the 25<sup>th</sup> International Ocean and Polar Engineering Conference, USA
- MAN Diesel & Turbo, 2013. *Marine Engine IMO Tier II Programme, 2<sup>nd</sup> edition 2013*.
- MAN Diesel & Turbo, accessed 2014. *CEAS Engine Data report*. <http://marine.man.eu/two-stroke/ceas>
- Mannarini, G., Coppini, G., Oddo, P., and Pinardi, N., 2013. *A Prototype of Ship Routing Decision Support System for an Operational Oceanographic Service*. *TransNav*, the International Journal on Marine Navigation and Safety of Sea Transportation, Volume 7, Number 1.
- Marie, S and Courteille, E., 2009. *Multi-Objective Optimization of Motor Vessel Route*. *TransNav*, the International Journal on Marine Navigation and Safety of Sea Transportation, 3, 133–14.
- Maruo, H., 1957a. *Theory of the wave resistance of a ship in a regular seaway*. Bull. Fac. Eng., Yokohama Nat. University, Vol. 6.
- Maruo, H., 1957b. *On the increase of the resistance of a ship in rough sea (I)*, J.S.N.A. Japan, Vol. 101, August.
- Maruo, H., 1957c. *Advances in calculation of wave-making resistance of ships*, 60<sup>th</sup> Anniversary series, Vol. 2, Soc. Nav. Arch. Japan, pp. 1-82.

Maruo, H., 1957d. *The excess resistance of a ship in rough seas*, I.S.P., Vol. 4, July.

Matulja, D., Sportelli, M., Guedes Soares, C., PRPIĆ-ORŠIĆ, J., 2011. *Estimation of Added Resistance of a Ship in Regular Waves BRODOGRADNJA – SHIPBUILDING*

Maritime Instituut Willem Barentsz, 2014. *SPOS as key performance optimizer for Feederlines ships – An assessment of the feasibility.*  
[https://mijnmiwb.nl/kbase/uploads/39\\_rmCtWm.pdf](https://mijnmiwb.nl/kbase/uploads/39_rmCtWm.pdf)

[MAXSURF](http://www.maxsurf.net/), *Naval Architecture Software for all Types of Vessels*. Website: <http://www.maxsurf.net/> [Accessed 2014] Meng, Q., Wang, S. (2011) ‘*Optimal operating strategy for a long-haul liner service route*’. *European Journal of Operational Research* 215, 105–114.

Molland, A. A., Turnock, S. R., and Hudson, D., 2011 A. *Ship resistance and propulsion*.

Motte, R. H., Burns, R. S. and Calvert, S., 1988. *An overview of current methods used in weather routeing*. *Journal of Navigation*, 41, pp 101-114.

Motte, R. H. and Calvert, S., 1990. *On the Selection of Discrete Grid Systems for On-Board Micro-Based Weather Routing*. *The Journal of Navigation*, 43, pp. 104-117.

Motte, R. H., Fazal, R., Epshteyn, M., Calvert, S., and Wojdylak, H., 1994a. *Design and Operation of a Computerized, On-Board, Weather Routeing System*. *Journal of Navigation*, 47, pp 54-69.

Motte, R., Calvert, S., Wojdylak, H., Fazal, R. and Epshteyn, M., 1994b. *An assessment of environmental data for a computerised ship weather routeing system*. *Met. Apps*, 1: 141-154.

Munk, T., 2006. *Fuel conservation through managing hull resistance*. Motorship Propulsion Conference, 2006 Copenhagen.

NATIONAL OCEANIC AND ATMOSPHERIC ADMINISTRATION (NOAA) Website:  
[www.noaa.gov](http://www.noaa.gov) [Accessed June 2015]

Newman, J.N., 1967. *The Drift Force and Moment on Ships in Waves*. Journal of Ship Research, Vol. 11, pp. 51-60

Norstad, I., Fagerholt, K. and Laporte, G. (2011) ‘*Tramp ship routing and scheduling with speed optimization*’, Transportation Research Part C: Emerging Technologies, 19, 853-865.

Padhy, C.P., Sen, D. and Bhaskaran, P.K., 2008. *Application of wave model for weather routing of ships in the North Indian Ocean*. Nat Hazards, 44, pp. 373-385

Panigrahi, J.K. and Umesh, P.A., 2008. *Minimal Time Ship Routing Using IRS-P4 (MSMR) Analyzed Wind Fields*. Marine Geodesy, 31, pp. 39-48

Pedersen, B. P. and Larsen, J., 2009. Prediction of Full-scale Propulsion Power Using Artificial Neural Networks, 8<sup>th</sup> Int. Conf. Computer and IT Appl. Maritime Ind, Budapest, pp. 537-550.

Pedersen, B. P., Larsen, J., 2013. *Gaussian Process Regression for Vessel Performance Monitoring*. 12<sup>th</sup> International Conference on Computer and Information Science.

Péres Arribas, F., 2006. *Some methods to obtain the added resistance of a ship advancing in waves*. Ocean Engineering.



- Pontryagin, L. S., Boltyanskii, V. G., Gamkrelidze, R. V., Mishchenko, E. F. (1962). *The Mathematical Theory of Optimal Processes*. English translation. Interscience. ISBN 2-88124-077-1.
- Ronen, D., 1982. 'The effect of oil price on the optimal speed of ships'. Journal of the Operational Research Society 33, 1035–1040.
- Ronen, D., 2011 'The effect of oil price on containership speed and fleet size'. Journal of the Operational Research Society 62, 211–216.
- Salvesen, N., 1978 *Added Resistance of Ships in Waves*. Journal of Hydronautics
- Schmiechen, M., 1991. *Lecture notes of M. Schmiechen and Oral discussions*, 2<sup>nd</sup> international workshop on the rational theory of ship hull-propeller interaction and its applications, pp41, Berlin
- Schmiechen, M., 1998. *Contribution concerning a proposed ISO Standard "guidelines for the assessment of ship speed and power performance by means of speed trials,"* <http://www.m-schmiechen.homepage.t-online.de/> (accessed 17-04-2007)
- Sen, D. and Padhy, C.P., 2010. *Development of a Ship Weather-routing Algorithm for Specific Application in North Indian Ocean Region*. Proceedings of MARTEC 2010. The International Conference on Marine Technology, 11-12 December 2010.
- Seo, M., Park, D., Yang, K., Kim, Y., 2013. *Comparative study on computation of ship added resistance in waves*. Ocean Engineering, 73 (2013) 1-15

- Shao, W. and Zhou P. L., 2012. *Development of a 3D Dynamic Programming Method for Weather Routing*. International Journal of Navigation and Safety of Sea Transportation, Journal Vol. 6 No. 1 – March, 2012
- Shintani, K., Imai, A., Nishimura, E., Papadimitriou, S. (2007) ‘*The container shipping network design problem with empty container repositioning*’. Transportation Research 43E, 39–59.
- SHOPERA Project (2013-2016). *Energy Efficient Safe Ship Operation*, EU funded FP7 project, <http://www.shopera.org>
- SNAME (1988) "*Principles of Naval Architecture* (Second Revision), Vol. 2 – Resistance, Propulsion and Vibration" SNAME
- Spaans, J. A., Stoter, P., 2000. *Shipboard Weather Routing. International Symposium Information on Ships ISIS 2000*. German Institute of Navigation DGON.
- Szlapczynska, J., 2007. Multiobjective Approach to Weather Routing. TransNav – International Journal on Marine Navigation and Safety of Sea Transportation, 1, 273–278.
- Szlapczynska, J. and Smierzchalski, R., 2009. Multicriteria Optimisation in Weather Routing. TransNav – International Journal on Marine Navigation and Safety of Sea Transportation, 3, 393–400.
- Szlapczynska, J., 2013. Multicriteria Evolutionary Weather Routing Algorithm in Practice. TransNav, the International Journal on Marine Navigation and Safety of Sea Transportation, 7, 61–65.

- Toki, N., 2005. *Monitoring of Service Performance of a ROPAX Ferry*. 24<sup>th</sup> ITTC Group Discussion on Full Scale Trial, Japan.
- Takahashi, T & Tsukamoto, O (1977). *Effects of Waves on Speed Trial of Large Full Ships*, ISNAW, No 54, 1977.
- Takahashi, T (1988). *A practical prediction method of added resistance of a ship in waves and the direction of its application to hull form design*, Trans West Jpn Soc Nav Archit 75, pp 75–95.
- Taniguchi, K., and Tamura, K. (1966) *Appendix XI: On a new method of correction for wind resistance relating to the analysis of speed trial results*, 11th ITTC, pp. 144-149, Tokyo
- Townsin, R. L., and Svensen, T., 1980. Monitoring speed and power for fuel economy. Shipboard Energy Conservation Symposium, pp135-150.
- Townsin, R. L., Kwon, Y. J., 1983. *Approximate formulae for the speed loss due to added resistance in wind and waves*. R.I.N.A. Supplementary Papers, Volume 125, pp 199.
- Wang, S. and Meng, Q. (2011) ‘*Schedule design and container routing in liner shipping*’, Transportation Research Record 2222, 25–33.
- Wang, S. and Meng, Q. (2012) ‘*Liner ship fleet deployment with container transshipment operations*’, Transportation Research Part E 48, 470–484
- Wang, X., Teo, C., 2013. *Integrated hedging and network planning for container shipping’s bunker fuel management*. Maritime Economics & Logistics, pp. 172-196.

Windén, B, 2011. *The influence of surface waves on the added resistance of merchant ships.*

[https://www.southampton.ac.uk/assets/imported/transforms/content-block/UsefulDownloads\\_Download/23490F13D3464B80939603443F1704CB/Bjorn\\_winden.pdf](https://www.southampton.ac.uk/assets/imported/transforms/content-block/UsefulDownloads_Download/23490F13D3464B80939603443F1704CB/Bjorn_winden.pdf)

Yokoi, K., 2004. *On the influence of ship's bottom fouling upon speed performance.* Bulletin of Toyama National College of Maritime Technology.